

ESD-TR-72-181

ESD ACCESSION LIST

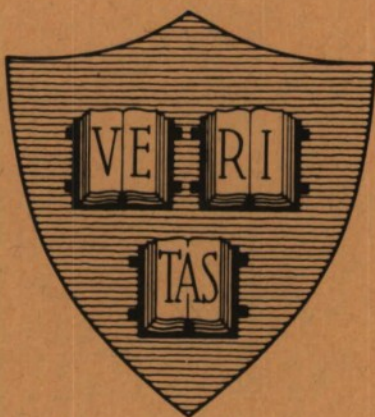
DRI Call No. 72534

July 1971

Copy No. 1 of 1 cys.

**MODIFIED DIPOLES : II
NUMERICAL SOLUTIONS**

FINAL SUMMARY REPORT



Prepared by
Harvard University
Cambridge, Massachusetts
for

Massachusetts Institute of Technology
Lincoln Laboratory

ESD RECORD COPY
RETURN TO
SCIENTIFIC & TECHNICAL INFORMATION DIVISION
(DRY), BUILDING 1433

A0745979

Approved for public release; distribution unlimited.

Scientific Report No. 13 (Vol. II)

MODIFIED DIPOLES:
II. NUMERICAL SOLUTIONS

Peter S. Kao

Prepared by
Harvard University
for

Massachusetts Institute of Technology
Lincoln Laboratory

under

Purchase Order No. C-782
Prime Contract No. F19628-70-C-0230

Approved for public release; distribution unlimited.

MODIFIED DIPOLES
II. NUMERICAL SOLUTIONS

By

Peter S. Kao

Division of Engineering and Applied Physics
Harvard University · Cambridge, Massachusetts

ABSTRACT

The 'modified dipole' has its origin in the consideration of the general properties of a satellite antenna which bears great resemblance to a dipole modified to incorporate at the center a conducting volume which is used to radiate electromagnetic waves and to house a power supply and radio frequency generators, etc. The object of this research is to pursue a theoretical and experimental exploration of the effects induced by the presence of the conducting volume on the antenna performance, i. e., input characteristics, current distribution along the surfaces of the entire radiating structure and radiation properties.

In Volume I a mathematical model consisting of a perfectly conducting sphere from which project the ends of a thin biconical antenna is chosen to simulate the actual sphere-centered thin dipole. The conical antenna is driven at its junction with the sphere by a rotationally symmetric electric field maintained across the gap by a biconical transmission line excited by the TEM mode. The attractive features of this model include the fact that it has surfaces that permit a simple specification of boundary conditions and, hence, a rigorous formulation for the electromagnetic fields and a shape such that its properties should come reasonably close to those of a modified cylindrical antenna as the cone angle becomes quite small.

The measurements of both input admittances and current distributions on modified dipoles (with either conical or cylindrical

antenna projecting from the sphere) are also presented in Volume I. Comparisons were also made between modified conical and cylindrical antennas with the same sphere radii and antenna heights. The radius of the cylindrical antenna is the same as the smaller end of the cone. The fact that the admittance curves for modified cylindrical and conical antennas involve only slight shifts suggests that by introducing an equivalent antenna length that is a little longer than the actual physical length of the conical antenna a good approximation is obtained for the cylindrical antenna.

An infinite set of algebraic equations was solved numerically in Volume II for small cone angles. Comparisons were made between the modified conical antenna and its limiting biconical antenna which provides both an extrapolatory numerical check for the modified conical antenna with shrinking central sphere and an understanding of the underlying physical phenomena. Theoretical and experimental results are in very good agreement.

**Accepted for the Air Force
Joseph R. Waterman, Lt. Col. USAF
Chief, Lincoln Laboratory Project Office**

1. INTRODUCTION

The formal solution for the b_k 's and with them the determination of the driving point admittance, the current distribution and the far-field pattern of the modified conical antenna with half cone angle θ_0 and central sphere of radius b is contained in the infinite set of linear equations, (1-57) and (1-64) which appear in Volume I of this report. No general, exact solution of this set of equations is available for cones with arbitrary angles θ_0 . Hence, a general formula for the input admittance of the modified dipole cannot be provided. Thus, although the analysis of the problem is not restricted in its formulation, mathematical limitations make an exact solution unavailable. However, if the half cone angle θ_0 is sufficiently small (i. e., $\theta_0 < 4^\circ$), which is of special interest in the present problem, a numerical solution of (1-57) and (1-64) can be carried out. In this problem an exact result can be obtained only by an infinite sequence of steps. Since the process necessarily has to be truncated after a certain finite number of steps, truncation errors are unavoidable. There are, however, three sources of truncation errors in the approach taken to this problem. First, there is the error introduced when the infinite matrix is truncated to one of finite dimensions. Secondly, error is introduced by truncating the infinite sum (over v) in the calculation of each matrix element. Thirdly, the double series representing the input admittance, current distribution and near fields is twice truncated; once over v and once over k . In addition, because of the formidable amount of computation required to solve the truncated infinite matrix, small round-off errors may cause errors in the computed solution out of all proportion to their size. Above all, the truncated system of linear equations has to be solvable (i. e., the coefficient matrix must be non-singular) before problems of accuracy and convergence of the computed solution can be considered.

An exact error analysis relating different sources of errors to the final results is very difficult, if not impossible, when many equations are involved. It cannot be made here. Hence, after all possible precautions have been taken to prevent error from growing out of proportion and to

preserve the accuracy of the final solution, the computed results are to be justified by comparison with experimental measurements.

A brief review of the major steps taken in the course of the numerical calculation and their associated theories follows:

(A) Existence of the Solution

Once the infinite set of linear equations is truncated, a set of n simultaneous linear equations in n unknown is at hand. It is

$$\sum_{j=1}^n a_{ij} x_j = b_i \quad (2-1a)$$

Equation (2-1a) is conveniently written in matrix form as follows:

$$A X = b \quad (2-1b)$$

where $A = [a_{ij}]$ is the $n \times n$ matrix of coefficients, $X^T = (x_1 \dots x_n)$ and $b^T = (b_1 \dots b_n)$ with T denoting the transpose. Let A_b denote the $n \times (n+1)$ matrix which has the column vector b appended as an $(n+1)$ st column to A . The rank of any matrix A is $r(A)$. Then the basic theory on the existence of a solution of (2-1) states that the system of linear equations has a solution if and only if

$$r(A) = r(A_b) \quad (2-2)$$

This familiar theorem may be proved by using Gaussian elimination. This will not be pursued here [1]-[2].

The theoretical proof of the existence of a unique solution for the simultaneous linear equations does not in any way guarantee the correctness of a computed solution of (2-1a, b). There is no hard-and-fast rule in carrying out a numerical solution for simultaneous linear equations. Different approaches need be employed for different matrices with different characteristics; e. g., direct methods are usually used for matrices which are filled but not large, while iteration methods are useful for matrices that are sparse and filled etc.

(B) Ill-Condition

In numerical calculations, a class of matrices of coefficients is encountered which is called ill-conditioned such that no matter how accurately it is calculated, the solution may still be grossly in error. If the matrix A is normalized so that the largest term in magnitude has the order of magnitude of unity and is such that A^{-1} contains some very large elements, the matrix and therefore, the system of equations is ill-conditioned. Conversely, if the largest element in magnitude of A^{-1} has the order of magnitude of unity, the matrix may be said to be well-conditioned. This can easily be seen by writing (2-1b) in the following form:

$$X = A^{-1}b \quad (2-3)$$

Suppose that A^{-1} has very large elements, one of which is $a_{ji}^{-1} = A_{ij}/|A|$. $|A|$ denotes the determinant of A and A_{ij} is the cofactor of a_{ij} . The assumption that a_{ji}^{-1} is large means that A_{ij} must be large relative to $|A|$. Since one of the terms in the expansion of $|A|$ about the i th row and j th column is $a_{ij}A_{ij}$, a small error in a_{ij} may cause a large relative error in $|A|$ and therefore a large relative error in a_{ji}^{-1} . This in turn can cause a large relative error in X . Similarly, a small change in an element of b could cause a large change in X .

(C) Truncation Error

The errors caused by truncating the infinite sum by finding an approximation (or an upper bound) to the remainder in each series after truncation will be examined. Having found these, an estimate could be found of the relative error in each matrix element by comparing the remainder with the corresponding truncated sum. Finally, the remainder estimate is added to the corresponding matrix element, the system is solved and its solution compared with that of the unaltered matrix. This comparison yields an estimate of the error one might expect in the field pattern, current distribution and input admittance etc.

(D) Intermediate Round-offs

One way of checking the round-off error in the course of computation is by substituting the calculated values into the left-hand members of the original equations. The presence of the deviations between the resultant members and original right-hand members serves to indicate the presence of errors due to intermediate round-offs. Again, the relationship between the magnitudes of these deviations and the magnitude of the errors in the solution column is not a simple one. Use will be made of this simply as a check if the round-off errors are too far out of proportion to afford a reasonable solution.

(E) Convergence of the Solution

Before considering the convergence of the solution of the system of linear equations, error checks were made for several cases with various combinations of the extreme sizes of antennas and inner spheres. The maximum size of matrices has been studied so that the different kinds of errors mentioned above can be kept within one per cent. It has been found that for most cases a 40 x 40 matrix is still well within the acceptable range and the solutions show rapid convergence when the matrix size exceeds 15 x 15.

The convergence of the solution of the system of linear equations will be dealt with empirically by solving the same problem with matrices of increasing size and examining the successive solutions for convergence.

2. ROOTS OF THE CHARACTERISTIC EQUATION $L_V(\theta_0) = 0$

The application of the boundary condition given by equation (1-35) in Volume I together with the property of anti-symmetry of E_R with respect to the equatorial plane (i. e., $\theta = \pi/2$ - plane) leads to the following characteristic equation [see equation (1-30) in Volume I]:

$$L_v(\theta_0) = L_v(\pi - \theta_0) = 0$$

which is independent of the presence of the conducting sphere at the center. Once the half cone angle θ_0 is fixed, an infinite sequence of discrete values of v is obtained from the above equation. The present analysis will be restricted to small half cone angles (i. e., $\theta_0 < 4$).

In the neighborhood of the point $\theta = \pi$, Legendre's functions can be expressed in the following way [3] :

$$P_v(-\cos \theta_0) = \frac{\sin v\pi}{\pi} F(-v, v+1; 1; \sin^2 \frac{\theta_0}{2}) \cdot H(v, \theta_0) + \sum_{a=1}^{\infty} \frac{(-v) \cdots (-v+a-1)(v+1) \cdots (v+a)}{(a!)^2} \phi(v, a) \left(\sin \frac{\theta_0}{2} \right)^{2a} \quad (2-4)$$

where $\theta_0 = \pi - \theta$ is in the neighborhood of zero

$$H(v, \theta) = 2 \sin \frac{\theta}{2} + \psi(v+1) + \psi(-v) + 2\gamma \quad (2-5a)$$

and

$$F(a, b; c; z) = \frac{\Gamma(c)}{\Gamma(a)\Gamma(b)} \sum_{n=0}^{\infty} \frac{\Gamma(a+n)\Gamma(b+n)}{\Gamma(c+n)} \frac{z^n}{n!} \quad (2-5b)$$

which is the Gauss hypergeometric series whose circle of convergence is the unit circle $|z| = 1$.

$$\phi(v, r) = \frac{1}{v+1} + \cdots + \frac{1}{v+r} + \frac{1}{-v} \cdots + \frac{1}{-v+r-1} - 2\left(\frac{1}{1} + \frac{1}{2} + \cdots + \frac{1}{r}\right) \quad (2-5c)$$

and $\psi(z)$ is the logarithmic derivative of the Gamma function; i. e.,

$$\psi(z) = \frac{\Gamma'(z)}{\Gamma(z)} \quad (2-5d)$$

or

$$= -\gamma + (z-1) \sum_{n=0}^{\infty} \frac{1}{(n+1)(n+z)} \quad (2-5e)$$

where γ denotes Euler's or Mascheroni's constant equal to 0.57722.

The expression (2-4) will be single-valued, on account of the cross-cut of the plane of $\mu = \cos \theta$ along the real axis from -1 to $-\infty$.

Using the reflection formula for the ψ -function, namely,

$$\psi(z+1) = \psi(-z) - \pi \cot \pi z \quad (2-6)$$

(2-4) is rearranged in the following form;

$$L_v(\cos \theta_0) = \sin v\pi G(v, \theta_0) \quad (2-7a)$$

$$= \sin v\pi [G_1(v, \theta_0) + G_2(v, \theta_0)] \quad (2-7b)$$

where

$$G_1(v, \theta_0) = F(-v, v+1; 1; \sin^2 \frac{\theta_0}{2}) \cdot F(v, \theta_0) \quad (2-8a)$$

$$F(v, \theta_0) = C(\theta_0) + \frac{2}{\pi} \psi(v+1) - \tan \frac{v\pi}{2} \quad (2-8b)$$

In (2-8b)

$$C(\theta_0) = \frac{2}{\pi} [\ln(\sin \frac{\theta_0}{2}) + \gamma] \quad (2-8c)$$

$$G_2(v, \theta_0) = \sum_{a=1}^{\infty} (-1)^a \frac{(v-a+1) \cdots v(v+1) \cdots (v+a)}{a! \cdot a!} \frac{\phi(v, \theta_0)}{\pi} \quad (2-8d)$$

Thus, finding the roots of the characteristic equation is now equivalent to setting $G(v, \theta_0) = 0$. Before actually carrying out the numerical calculation of the roots of (2-7a), it is instructive first to survey the equation qualitatively. Some general properties of these roots regardless of the cone angle θ_0 (as long as it is small) can be derived by looking at (2-7a, b) more carefully. The vanishing of (2-7a) can also be accomplished by finding the intersections of two functions, i. e., $-G_1(v, \theta_0)$ and $G_2(v, \theta_0)$ with v as a variable.

It is convenient to look into the restrictions upon v and θ_0 such that the numerical solution of $G(v, \theta_0) = 0$ is feasible and a sufficient number of roots is obtained to provide accuracy in the calculation of the matrix elements, the input admittance and the current distribution. It has been found that both the functions G_1 and G_2 are well behaved (i. e., the series converges quite rapidly) and the above-mentioned requirements were met over the range of interest so long as v is not too large in magnitude and the cone angle θ_0 is sufficiently small so that the product of these two quantities does not exceed the order of magnitude of unity [i. e., $v \sin \frac{\theta_0}{2} \leq 0(1)$].

The function $-G_1(v, \theta_0)$ behaves essentially like $\tan \frac{v\pi}{2}$ with its values continuously adjusted by first adding to it a slowly-decreasing quantity [i. e., $-C(\theta_0) - \frac{2}{\pi} \psi(v+1)$] and then multiplying it by a slowly-varying function [i. e., $F(-v, v+1; 1; \sin^2 \frac{\theta_0}{2}) \approx (1-v(v+1) \sin^2 \frac{\theta_0}{2} + \dots)$]. Therefore, $-G_1(v, \theta_0)$ is a continuous, monotonically increasing function within each equally-spaced segment which has a total length of two and the odd integers as its end points. $G_1(v, \theta_0)$ becomes singular in the neighborhood of the end points and changes sign whenever it crosses the end points. The derivative of $G_2(v, \theta_0)$ with respect to v is proportional to $(4-3v^2 \sin^2 \frac{\theta_0}{2}) \cdot (v \sin \frac{\theta_0}{2})$ which is positive as long as $v \sin \frac{\theta_0}{2} \leq 1$. So $G_2(v, \theta_0)$ is also a monotonically increasing continuous function over the range of interest. Accordingly, the functions $-G_1(v, \theta_0)$ and $G_2(v, \theta_0)$ intersect only once in each segment. Therefore, the form of the roots is an odd integer plus a small number which increases with v and θ_0 .

The simplification usually employed [4] to obtain an approximation of the roots of (2-7) is actually to take the leading term of $G_1(v, \theta_0)$ [i. e., $F(v, \theta_0)$] and retain only the two terms in F [i. e., $\tan(v\pi/2)$ and $\ln(\theta_0/2)$] under the assumption that $\ln(\sin \frac{\theta_0}{2})$ approaches infinity for sufficiently small angles θ_0 . Therefore, the approximate roots are

$$v_{\text{app.}} = k + \frac{1}{\ln(\sin \frac{\theta_0}{2})} \quad (2-9)$$

This approximation is in error due to the fact that even for half cone angle θ_0 as small as 0.1° , $|\ln(\sin \frac{\theta_0}{2})|$ (-7.044 in this case) is still of the same order of magnitude as the two neglected terms, i. e., $(v+1)$ and γ . Furthermore, $\ln(\sin \frac{\theta_0}{2})$ becomes even smaller than $\psi(v+1)$ as one proceeds to find larger v 's. In this range, the higher-order terms of G become comparable in magnitude and can no longer be neglected.

In Fig. 2-1, the results from the approximate formula (2-9) are compared with those calculated from the exact formula (2-7a) for various cone angles. Generally speaking, (2-9) provides quite a poor approximation of the accurate formula except for very thin cones for which the approximate formula gives the correct trend but the results are shifted from the accurate ones by a constant.

The numerically calculated v 's were checked by substituting them in a subroutine which generated Legendre functions of fractional orders. At $\theta = \theta_0$, the generated values of $L_v(\theta_0)$ (which are equal to zero theoretically) are of the order of 10^{-5} which indicates the accuracy of the solution.

3. COMPUTATION OF FRACTIONAL ORDER LEGENDRE FUNCTION

The computational difficulties with the fractional order Legendre functions lie in the following facts:

(a) The Legendre function, defined in the interval $(-1, 1)$, can be expressed by the hypergeometric series with various elements, i. e.,

$$P_v(\cos \theta) = F(-v, v+1; 1; \sin^2 \frac{\theta}{2}) \quad (2-10)$$

The above expansion can be employed for the calculation of values of the function $P_v(\cos \theta)$ only in a limited region of variation of the argument $\sin \frac{\theta}{2}$ and order v . With an increase in v and θ , the convergence of the series grows worse, which makes it of little use for calculation with large values of v and θ .

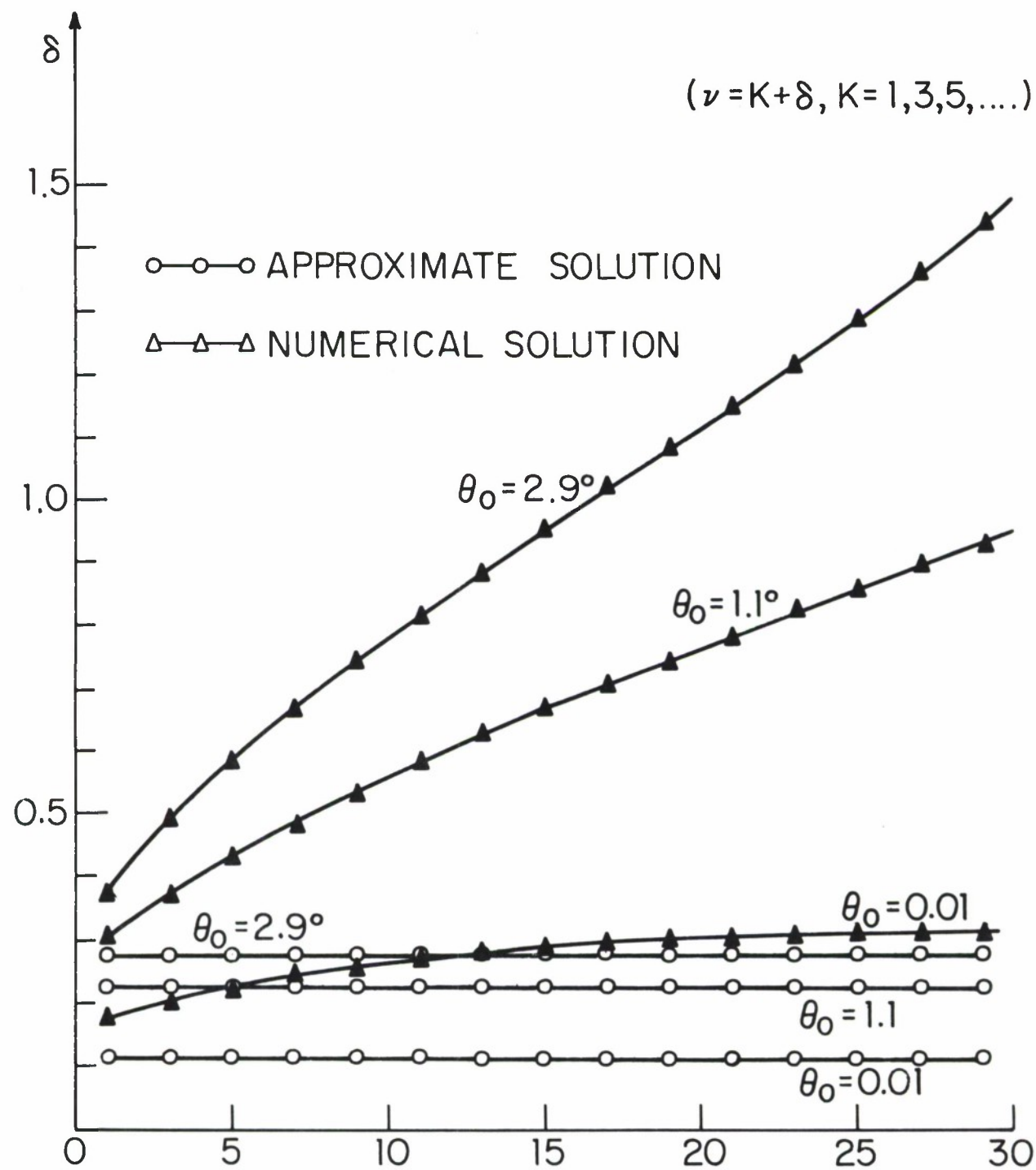


FIG. 2-1 ROOTS OF CHARACTERISTIC EQUATION $L_\nu(\theta_0) = 0$

(b) The process in generating higher-order functions by a recurrence relation is unstable, since the generation is carried out with rounded values which propagate in the recurrence process of increasing order and hence cause loss of significant figures.

The Legendre function $P_\nu(\cos \theta)$ assumes various representations suitable for numerical calculation in different ranges of ν and θ with the aid of definite and contour integrals. In this work use is made of representation of $P_\nu(\theta)$ in the form of Mehler-Fock, namely,

$$P_\nu(\cos \theta) = \frac{2}{\pi} \int_0^\theta \frac{\cos(\nu+1/2)t}{2(\cos t - \cos \theta)} dt \quad (2-11)$$

which provides (under different conditions for ν and θ) rapidly converging series for numerical calculation.

Equation (2-11) can be expanded in positive powers of $(\nu+1/2)$ by substituting in it in place of $\cos(\nu+1/2)t$ its series expansion. After changes of variables and rearrangement of terms, one obtains

$$P_\nu(\cos \theta) = \sum_{m=0}^{\infty} B_m(\nu+1/2)^{2m} \quad (2-12)$$

where

$$B_m = (-1)^m \frac{2^{(2m+1)}}{\pi (2m)!} \int_0^{\sin^{-1}(p \sin x)} \frac{1/2\pi}{(1-p^2 \sin^2 x)^{1/2}} dx \quad (2-13)$$

and

$$p = \sin(\theta/2) \quad (2-14)$$

In the last integral, the function under the integral sign becomes infinite only when $p=1$, that is for $\theta = \pi$. Consequently, outside the neighborhood of the point $\theta = \pi$, it is possible to calculate this integral by the usual numerical methods.

One limitation in using (2-12) for computing Legendre functions is its slowness in convergence as ν becomes larger.

An expansion of Legendre's function of (2-11) can be expressed in a series of Bessel's function [5], namely,

$$P_{\nu}(\cos \theta) = \sum_{m=0}^{\infty} a_m(\theta) J_m[(\nu+1/2)\theta] (\nu+1/2)^{-m} \quad (2-15)$$

where the a_m 's are elementary functions, regular in $0 \leq \theta \leq \pi$, and

$$a_0(\theta) = \frac{\theta}{\sin \theta} \quad (2-16a)$$

$$a_m(\theta) = (2m-1)!! a_0(\theta) \theta^m \psi_m(\theta) \quad (2-16b)$$

$\psi_m(\theta)$ is a combination of functions of ϕ_m which is obtained from $2(\cos t - \cos \theta)$ in terms of a series of $(\theta^2 - t^2)$, i. e.,

$$2(\cos t - \cos \theta) = (\theta^2 - t^2) \frac{\sin \theta}{\theta} \left[1 + \sum_{m=2}^{\infty} (\theta^2 - t^2)^{m-1} \phi_m(\theta) \right] \quad (2-17)$$

where

$$\phi_m(\theta) = \frac{1}{m!} \frac{1}{2^{(m-1)}} \frac{J_{m-\frac{1}{2}}(\theta)}{\theta^{(m-1)} J_{\frac{1}{2}}(\theta)} \quad (2-18)$$

Taking the inverse of the square root of (2-17), one obtains

$$\frac{1}{\sqrt{2(\cos t - \cos \theta)}} = \frac{1}{\sqrt{\theta^2 - t^2}} \frac{\theta}{\sin \theta} \sum_{m=0}^{\infty} (\theta^2 - t^2)^m \psi_m(\theta) \quad (2-19)$$

Therefore, the combination of (2-17) and (2-19) gives

$$\psi_0 = 1$$

$$\psi_1 = \frac{\phi_2}{2}$$

$$\psi_2 = -\frac{\phi_3}{2} + \frac{3\phi_2^2}{8}$$

$$\psi_3 = -\frac{\phi_4}{2} + \frac{3}{4} \phi_2 \phi_3 - \frac{1}{2} \phi_2^3$$

$$\begin{aligned} \psi_4 &= -\frac{1}{2} \phi_5 + \frac{3}{8} (\phi_3^2 + 2\phi_2\phi_3) - \frac{15}{16} \phi_3\phi_2^2 + \frac{35}{128} \phi_2^4 \\ \psi_5 &= -\frac{1}{2} \phi_6 + \frac{3}{4} (\phi_2\phi_5 + \phi_3\phi_4) - \frac{5}{16} (3\phi_2\phi_3^2 + 3\phi_4\phi_2^2) \\ &\quad + \frac{35}{32} \phi_2^3\phi_3 + \frac{63}{250} \phi_2^5 \end{aligned} \tag{2-20}$$

By using the recurrence relation for Bessel's functions of the first kind, namely,

$$J_{n-1}(z) + J_{n+1}(z) = \frac{2n}{z} J_n(z) \tag{2-21}$$

and substituting (2-21) into (2-15), we finally obtain an expression for $P_\nu(\cos \theta)$;

$$\begin{aligned} P_\nu(\cos \theta) &= J_0[(\nu+1/2)\theta] \left[a_0 - \frac{a_2}{(\nu+1/2)^2} - \frac{4a_3}{(\nu+1/2)^4} + \dots \right] \\ &\quad + J_1[(\nu+1/2)\theta] \left[\frac{a_1}{(\nu+1/2)} - \frac{(a_3\theta - 2a_2)}{(\nu+1/2)^3\theta} + \frac{8a_3}{(\nu+1/2)^5\theta^2} + \dots \right] \end{aligned} \tag{2-22}$$

At first glance, (2-22) does not assume any advantage over either of the more general expressions (2-10) and (2-11). But the asymptotic expansion for large values of ν is a convenient representation of the function $P_\nu(\cos \theta)$ from the computational point of view. It gives a good approximation to the functions themselves and can also be used for the computation of their derivatives and integrals with respect to the variable ν . Furthermore, the coefficients of the representation are associated with functions of spherical Bessel's functions and integral order Bessel's functions of the first kind J_0 and J_1 , which are available as built-in functions on the IBM 360/65 machine in use at the Harvard Computing Center. Hence, (2-22) is both a convenient and accurate formula for computation.

In summary, it is necessary to use a suitable representation for Legendre's functions of fractional order in different regions in the v - θ plane for purposes of computation with desired accuracy. Therefore, as shown in Fig. 2-2, the v - θ plane is divided into four regions. In region I, the hypergeometric expansion (2-10) is generally suitable as long as the angle is small and the order is not large; also the product of v and $\sin(\theta/2)$ must be less than one. In region II, (2-4) is a suitable expansion in generating Legendre's function with the same restrictions upon v and θ as in region I. In region III, use is made of the expansion (2-12) as long as the order is not large ($v < 10$). Finally, in region IV, (2-22) provides a good tool which is also valid in the neighborhood of $\theta = 0$ and π for large values of v . Therefore, in computing $L_v(\theta) = P_v(\theta) - P_v(\pi - \theta)$, formulae for different regions must be used simultaneously, e. g., for small θ , formulae for region I and II must be used.

The quantity Q_{rk} in the second set of linear equations is generally a small quantity for small half cone angle θ_0 . For $k \neq r$, Q_{rk} can easily be expressed in a close form, i. e.,

$$Q_{rk} = -2(1-\mu_0^2) \frac{[k(k+1)P_r'(\mu_0)P_k(\mu_0) - r(r+1)P_r(\mu_0)P_k'(\mu_0)]}{[k(k+1) - r(r+1)]} \quad (2-23)$$

and for $k=r$

$$Q_{rk} = 2[-(1-\mu_0^2)P_k'(\mu_0)P_k(\mu_0) + 2k(k+1)(1-\mu_0^2)H(k, \theta_0)] \quad (2-24)$$

where $H(k, \theta_0)$ is a polynomial of $\sin^2 \frac{\theta_0}{2}$ of order k , namely,

$$H(k, \theta_0) = \sum_{m=0}^{\infty} \frac{C_m^k}{m+1} \left(\sin^2 \frac{\theta_0}{2}\right)^m \quad (2-25)$$

where

$$C_m^k = \sum_{n=0}^m A_n^k A_{m-n}^k \quad (2-26a)$$

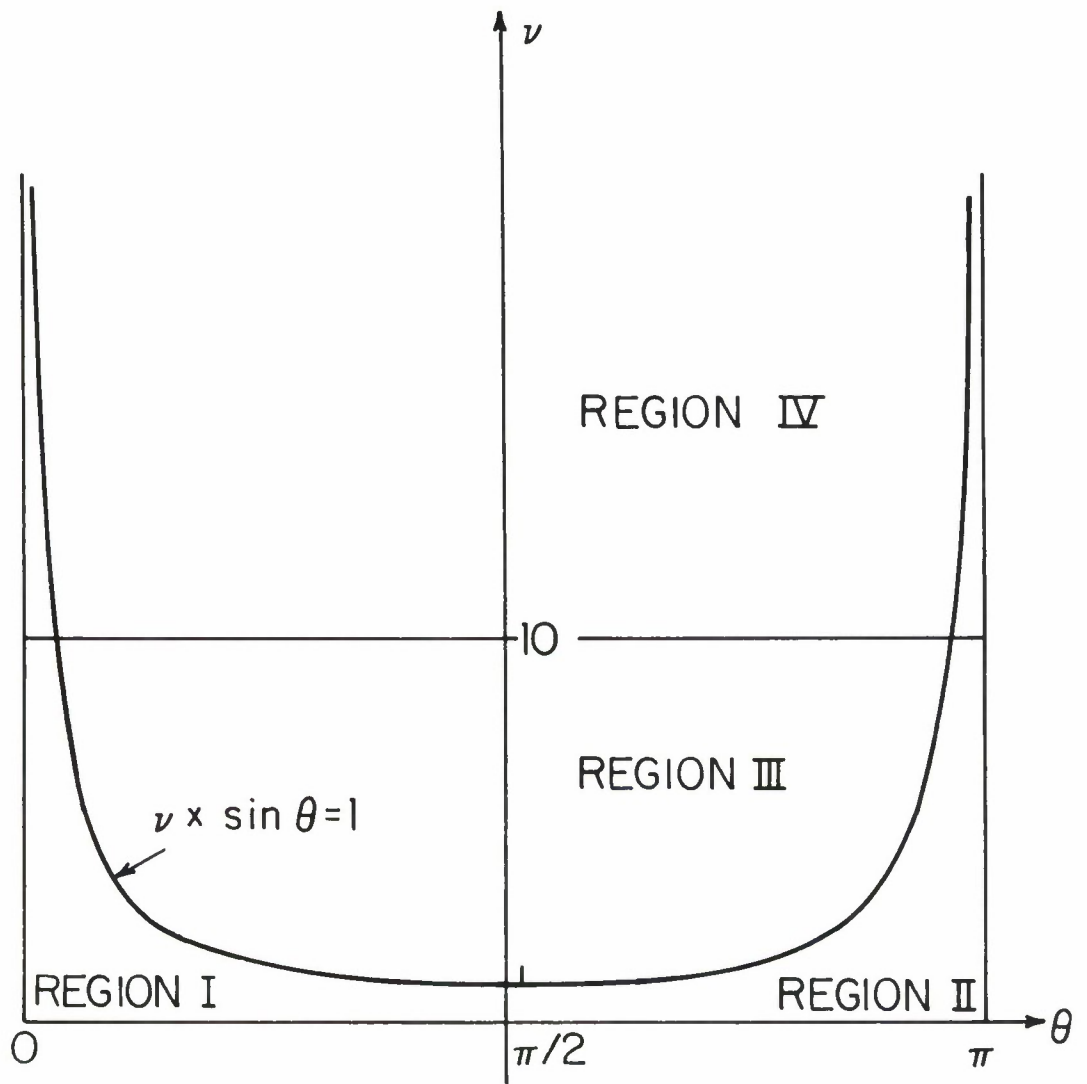


FIG. 2-2 COMPUTATION OF FRACTIONAL ORDER LEGENDRE FUNCTION

and

$$A_m^k = (-1)^m \frac{\Gamma(k+m+1)}{\Gamma(m+1)\Gamma(k-m+1)} \quad (2-26b)$$

Hence, $A_m^k = 0$ for $m > k$.

The generation of Bessel's functions of fractional order is not significantly different from that for functions of integral order. It will not be discussed here.

4. THE BICONICAL ANTENNA

As a preliminary to the later discussions of the modified dipole, the problem of the thin, center-fed biconical dipole will be treated first. Based upon equations (1-90), (1-97) and (1-99) given in Volume I, a numerical solution for the input impedance and current distribution with various cone angles and antenna heights can be obtained.

Most of the considerations here will provide an opportunity to develop the technique which will be employed later for the more complicated case of the modified dipole. Furthermore, they will also serve as a numerical extrapolatory check for the modified dipole with a shrinking central sphere.

Three sets of linear algebraic equations describing the same biconical structure will be solved numerically for various antenna lengths and cone angles with proper error estimate for the elements of the coefficient matrices and the terms with infinite summations.

The general terms of the coefficient matrix in (1-90) include the sum

$$g(r, k, v) = \sum_v \frac{(2v+1)}{v(v+1)} \frac{(1-\mu_0^2)}{[k(k+1) - v(v+1)][r(r+1) - v(v+1)]} \frac{\partial v}{\partial \mu_0} \quad (2-27)$$

To discuss this case for large v , some approximate formulae are introduced for the Legendre's functions which have been given by Schelkunoff [6] provided θ_0 is not near 0 or π ,

$$P_v(\cos \theta) \approx \frac{\cos(q - \pi/4)}{(\frac{\pi}{2} p \sin \theta)^{1/2}} \quad (2-28a)$$

and

$$P_v(-\cos \theta) \approx \frac{\cos(q\pi - q\theta_0 - \pi/4)}{(\frac{\pi}{2} p \sin \theta)^{1/2}} \quad (2-28b)$$

where

$$p = [v(v+1)]^{1/2} \quad \text{and} \quad q = [(v+1/2)^2 + 1/4]^{1/2}$$

Thus,

$$L_v(\theta) \approx \frac{\sin(q\pi/2 - \pi/4) \sin(\pi/2 - \theta)}{(\frac{\pi}{2} p \sin \theta)^{1/2}} \quad (2-29)$$

Using the fact that $L_v(\theta_0) = 0$, it follows that for v very large

$$(1-\mu_0^2) \frac{(2v+1)}{v(v+1)} \frac{\partial v}{\partial \mu_0} \approx \frac{4 \sin^2 \theta_0}{(\pi - 2\theta_0)} \quad (2-30)$$

The factor $1/[k(k+1) - v(v+1)] [r(r+1) - v(v+1)]$ tends to be quite large and sensitive to the value of v when v is near k or r . Let N be the matrix size, then the largest value that k or r may have is $(2N+1)$. Let v_m be the value of v at which the series (2-27) is terminated. An examination of (2-27) shows that the most significant values occur when $v-k$ and/or $v-r$ are small as v passes through the entire range of values obtained from $L_v(\theta_0) = 0$. Therefore, it is necessary to require that v_m be greater than $(2k+1)$ and $(2r+1)$ in all computations.

Let $R(r, k, v)$ denote the remainder such that

$$R(r, k, v_m) = \sum_{v=v_m}^{\infty} g(r, k, v) \quad (2-31)$$

From (2-27) and (2-30), one obtains for

(i) off-diagonal elements, i. e., $k \neq r$

$$g(r, k, v) \approx \frac{4 \sin^2 \theta_0}{(\pi - 2\theta_0)} A_1 \left(\frac{1}{v+k} - \frac{1}{v-k-1} \right) + A_2 \left(\frac{1}{v+r} - \frac{1}{v-r-1} \right) \quad (2-32)$$

where

$$A_1 = \frac{1}{(2k+1)(k+r+1)(r-k)} \quad (2-33a)$$

and

$$A_2 = \frac{1}{(2r+1)(k+r+1)(k-r)} \quad (2-33b)$$

From (2-30), one finds that the separation of zeros of $L_v(\theta_0)$ is approximately

$$\Delta v = \frac{2\pi}{(\pi - 2\theta_0)} \quad (2-34)$$

then

$$\begin{aligned} R(r, k, v_m) &\approx \frac{\pi - 2\theta_0}{\pi} \int_{v_m}^{\infty} g(r, k, v) dv \\ &= \frac{2 \sin^2 \theta_0}{\pi} \left[A_1 \ln \left(\frac{v_m - k - 1}{v_m + k} \right) + A_2 \ln \left(\frac{v_m - r - 1}{v_m + r} \right) \right] \end{aligned} \quad (2-35)$$

(ii) For diagonal terms, i. e., $k=r$

$$g(r, k, v) \approx \frac{4 \sin^2 \theta_0}{-2\theta_0} \frac{1}{(2k+1)^2} \left[\frac{1}{v-k-1} - \frac{1}{v+k} \right]^2 \quad (2-36)$$

thus for large v ,

$$R(k, k, v_m) \approx \frac{2 \sin^2 \theta_0}{\pi} \left[\frac{1}{(2k+1)^2} \left(\frac{1}{v_m+k} + \frac{1}{v_m-k-1} \right) - \frac{2}{k+1} \ln \left(\frac{v_m+1}{v_m-k-1} \right) \right] \quad (2-37)$$

For those terms with infinite summation over v in (1-97) and (1-99), the approximate formulae are introduced for large v and $v \gg x$, i. e., Meissel's formula [7]

$$J_v(x) \approx \left(\frac{\pi x}{2} \right)^{1/2} \frac{x^{(v+1/2)} \exp \left[\sqrt{(v+1/2)^2 - x^2} - (v+1/2) \right]}{1 - \left(\frac{x}{v+3/2} \right)^2}^{1/4} \frac{1}{1 + (1-x^2/v^2)^{1/2}}^v \quad (v-x \gg v^{-1/3}) \quad (2-38)$$

Actually, since v is much larger than x , a further approximation can be made, namely,

$$\left[(v+1/2)^2 - x^2 \right]^{1/2} - v \approx - \frac{x^2}{2v}$$

$$\left[1 - \left(\frac{x}{v+1/2} \right)^2 \right]^{1/4} \approx 1 - \frac{x^2}{4v^2}$$

$$\left[1 + \sqrt{1 - \left(\frac{x}{v} \right)^2} \right] \approx 2^v \exp \left(- \frac{x^2}{4v} \right)$$

thus,

$$J_v(x) \approx \pi^{1/2} \frac{x^{(v+1)} \exp \left[- \frac{x^2}{4(v+1/2)} \right]}{2^{(v+1)} \Gamma(v+3/2)} \quad (2-39)$$

Similarly,

$$J'_v(x) \sim \frac{v+1}{x} J_v(x) \quad (2-40)$$

Again, let $g_1(r, k, v)$ and $g_2(r, k, v)$ denote the remainders for the first and second set of linear equations, respectively; one finds for:

(i) the off-diagonal elements, i. e., $k \neq r$

$$g_1(r, k, v) = \frac{2v+1}{v(v+1)} \frac{J'_v(\beta_0 h)}{J_v(\beta_0 h)} \frac{\frac{\partial v}{\partial u_0}}{[k(k+1) - v(v+1)][r(r+1) - v(v+1)]} \quad (2-41)$$

and

$$g_2(r, k, v) = g_1(r, k, v) \frac{J_v(\beta_0 h)}{J'_v(\beta_0 h)} \quad (2-42)$$

For v large and $v \gg \beta_0 h$, one gets

$$\begin{aligned} R_1(r, k, v_m) \approx & \frac{\sin^2 \theta_0}{\pi \beta_0 h (k^2 - r^2)} \ln\left(\frac{v_m^2 - r^2}{v_m - k}\right) + \frac{1}{k} \ln\left(\frac{v_m + k}{v_m - k}\right) \\ & - \frac{1}{r} \ln\left(\frac{v_m + r}{v_m - r}\right) \end{aligned} \quad (2-43)$$

Similarly,

$$\begin{aligned} R_2(r, k, v_m) \approx & \frac{2\beta_0 h \sin^2 \theta_0}{\pi} \left[A_1 \frac{1}{k-1} \ln\left(\frac{v_m + k}{v_m + 1}\right) + \frac{1}{k+2} \ln\left(\frac{v_m - k - 1}{v_m + 1}\right) \right. \\ & \left. + A_2 \frac{1}{r-1} \ln\left(\frac{v_m + r}{v_m + 1}\right) + \frac{1}{r+2} \ln\left(\frac{v_m - k - 1}{v_m + 1}\right) \right] \end{aligned} \quad (2-44)$$

(ii) the diagonal terms, i. e., $k = r$

$$R_1(k, k, v_m) \approx \frac{\sin^2 \theta_0}{\pi \beta_0 h} \left[\frac{1}{2r^2} \ln \left(\frac{v_m - k}{v_m + k} \right) + \frac{1 - v_m/r^2}{v_m^2 - r^2} \right] \quad (2-45)$$

and

$$R_2(k, k, v_m) \approx \frac{2\beta_0 h \sin^2 \theta_0}{\pi} \left[\frac{-1}{(2k+1)^2(k-1)} \frac{1}{v_m + k} \right. \\ \left. + \frac{1}{(2k+1)^2(k+2)} \frac{1}{(v_m - k - 1)} \right] \quad (2-46)$$

Having found the error estimate due to the truncation of the infinite sum in the calculation of each matrix element, it has been possible to get the relative error introduced in each element by comparing the error estimates with the corresponding truncated matrix elements and hence keep the relative error in each element of the matrix less than a specified value (one part in 10^3 in our calculation). Furthermore, by adding the error estimates to each element of the matrix and solving the resulting equations, it is possible to determine how sensitive the solution is to the degree of uncertainty in the matrix elements.

Before solving (1-90), it is of interest to consider an approximate solution derived originally by Schelkunoff [6] by assuming a sinusoidal current distribution along the thin biconical antenna and later from a different point of view by Tai [4] by neglecting all the off-diagonal elements of the coefficient matrix of (1-90) under the assumption that the half cone angle θ_0 is small so that the diagonal elements are dominant. The fact that the same formula was obtained by both for d_k in (1-90) signifies nothing more than that the approximations involved in the two approaches are essentially the same. In other words, a sinusoidal current distribution in itself implies sufficiently severe restrictions on the magnitude of the cone angle. As in the thin cylindrical antenna [4], a sinusoidal current distribution can only be accomplished with a line of ideal generators distributed along the length of the antenna which, in practice, does not exist and thus the assumed distribution is acceptable only for determining certain properties of very thin antennas over a very

limited range of length.

The approximate formula for the input impedance of a thin biconical antenna is [4],

$$Z_0 = Z_c \left(\frac{Z_{mc}^e \sin \beta_0 h - j Z_c \cos \beta_0 h}{Z_c \sin \beta_0 h - j Z_{mc}^e \cos \beta_0 h} \right) \quad (2-47)$$

where

$$Z_{mc}^e = R_{mc}^e + j X_{mc}^e \quad (2-48)$$

$$R_{mc}^e = 30 [2\text{Cin } 2\beta_0 h + (\text{Si } 4\beta_0 h - 2\text{Si } 2\beta_0 h) \sin 2\beta_0 h \\ + (2\text{Cin } 2\beta_0 h - \text{Cin } 4\beta_0 h) \cos 2\beta_0 h] \quad (2-49a)$$

$$X_{mc}^e = 30 [2\text{Si } 2\beta_0 h + (\ln 4 - \text{Cin } 4\beta_0 h) \sin 2\beta_0 h \\ - \text{Si } 4\beta_0 h \cdot \cos 2\beta_0 h] \quad (2-49b)$$

where $\text{Si } x = \int_0^x \frac{\sin u}{u} du$ is the integral sine and $\text{Cin } x = \int_0^x \frac{1 - \cos u}{u} du$.

Generally speaking, the coefficient matrix of (1-90) has symmetric elements with its dominant part lying on and near the main diagonal. For each row in the upper triangular matrix of coefficients, the diagonal element is always the dominant quantity with the other matrix elements rapidly decreasing in value as the distance from the diagonal is increased. The size of the diagonal elements, however, also decreases in the direction of larger row numbers, but with a much smaller rate than that of the off-diagonal ones.

It is instructive to look into the elements of the coefficient matrix of (1-90) for the case of a quarter wave conical dipole. Note that, while all the off-diagonal elements are decreasing with shrinking cone angles, the diagonal elements continue to increase substantially. Therefore, in

the limit, this justifies the approximation made by Tai in deriving (2-47) for extremely small cone angles ($\theta_0 < 0.01$). Whereas, on the other hand, when the angle becomes larger, the opposite trend occurs and the dominance in value seems to spread from the diagonal elements to the ones near them. Hence, the neglect of off-diagonal terms will cause great errors in the final solution. A typical example of a 5 x 5 matrix, normalized by its maximum element for the cone angles 1° and 0.1° , is shown below

$$[C]_{\theta_0 = 1^\circ} = \begin{bmatrix} 1.000 & 0.040 & 0.020 & 0.010 & 0.007 \\ & 0.230 & 0.070 & 0.005 & 0.003 \\ & & 0.096 & 0.003 & 0.002 \\ & & & 0.056 & 0.0013 \\ & & & & 0.034 \end{bmatrix}$$

$$[C]_{\theta_0 = 0.1^\circ} = \begin{bmatrix} 1.000 & 0.010 & 0.005 & 0.003 & 0.002 \\ & 0.160 & 0.018 & 0.001 & 0.0008 \\ & & 0.083 & 0.0006 & 0.0004 \\ & & & 0.050 & 0.0003 \\ & & & & 0.0320 \end{bmatrix}$$

A concentration of the dominant values is readily observed from the above examples. But even for angles as small as 0.1° , element C_{31} which is small compared to C_{11} is still of comparable magnitude with respect to element C_{33} . Hence, the neglect of C_{31} will cause at least 10% error in the final solution for b_3 . For large cone angles, elements in the first row, and hence first column, become quite comparable to the corresponding diagonal elements, which implies that a greater error is introduced by neglecting the off-diagonal terms.

The results presented in Fig. 2-3 are the calculated input impedance from (1-90) for the biconical antenna with cone angles $\theta_0 = 1.5^\circ, 1.1^\circ$ and 0.1° . The impedance variation is given as a function of the electric length of the antenna (i. e., $\beta_0 h$) with particular points where the electric

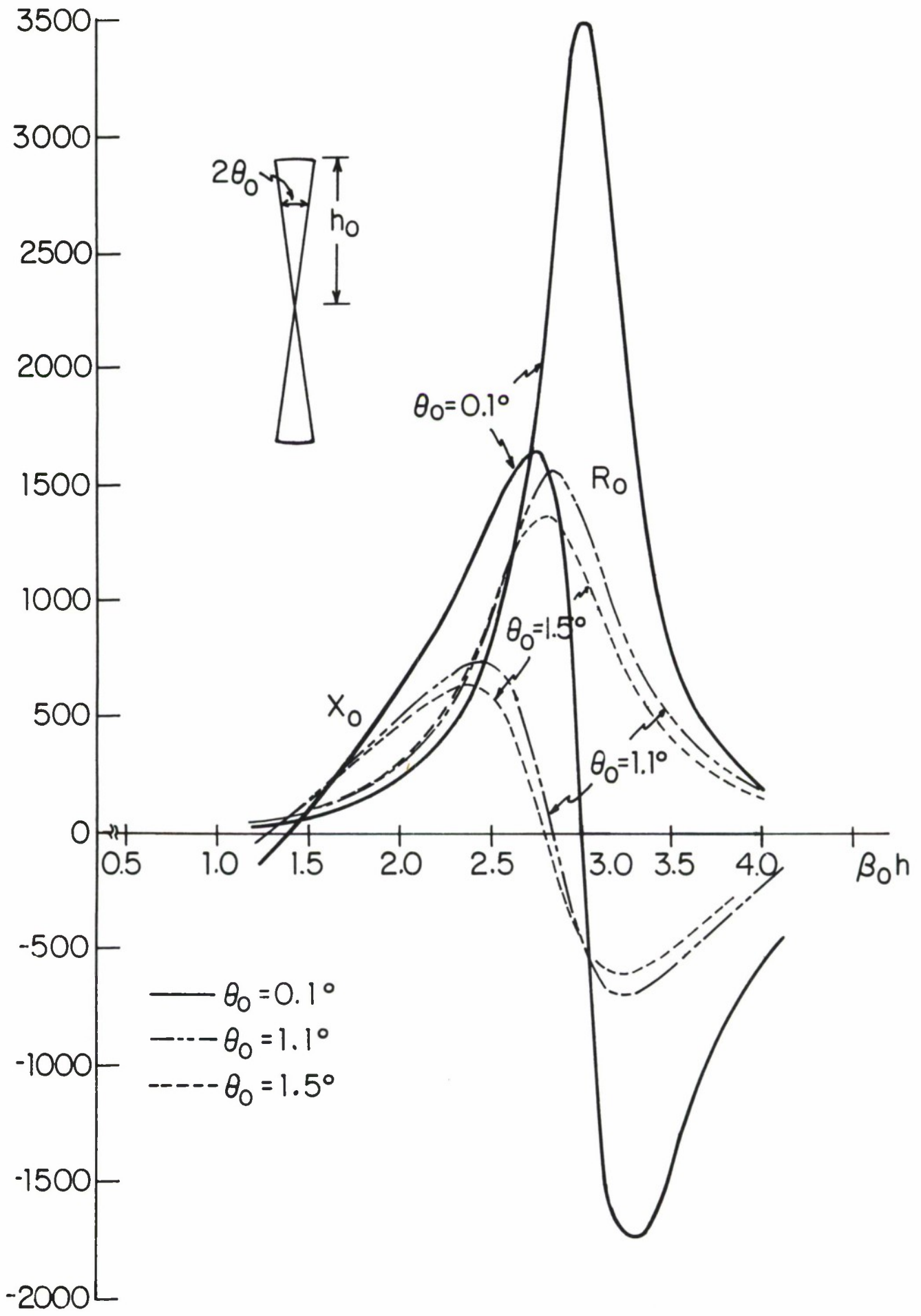


FIG. 2-3 INPUT IMPEDANCES OF THIN BICONICAL ANTENNA

length attains the values $\lambda/4$ and $\lambda/2$ specially noted. Larger cone angles tend to flatten the impedance curve and shorten both the resonant and antiresonant lengths of the antenna. A discussion of the characteristics of the curves for the impedance $Z_0 = R_0 + jX_0$ may be centered about certain critical points. Of these, the most important are the values of $\beta_0 h$ for which the reactance vanishes and which involve some interesting points which have counterparts in the cylindrical antenna.

Input resonance is characterized by

$$X_0 = 0, \quad R_0 = (R_0)_{\text{res.}} \quad \text{and} \quad X_0 = (X_0)_{\text{res.}} \quad (2-50)$$

The condition of input resonance occurs first when $\beta_0 h$ is somewhat smaller than $\pi/2$. It is seen that the resonant length of a biconical antenna moves toward $\pi/2$ as $1/\theta_0$ (and hence Z_c) increases. It is significant to note that when $\beta_0 h = \pi/2$ the input impedance given by the approximate formula (2-47) is

$$Z_0 = 73.13 + j 153.7 \text{ ohms} \quad (2-51)$$

Thus the input impedance of the thin biconical antenna as given by (2-47) is a constant independent of the cone angle θ_0 when h is a quarter wave in length and θ_0 is sufficiently small.

For the cylindrical antenna, such constancy obtains in the modified zeroth order approximation when for $\beta_0 h = \pi/2$, i. e. ,

$$(Z_0)_{\text{cylindrical}} = 73.13 + j 42.5 \text{ ohms} \quad (2.52)$$

It was observed by King [1] that the curve of Z_0 at $\beta_0 h = \pi/2$ approaches the value of $73.13 + j 42.5$ ohms as $\Omega = 2 \ln(2h/a)$ increases. The same phenomenon is observed for the biconical antenna as the corresponding characteristic impedance Z_c increases. This is shown in Fig. 2-4 in which the impedance curves tend to converge to the value of $73.13 + j 153.7$ ohms as the cone angle becomes vanishingly small. This suggests that the formula (2-47) may be no better than a modified zeroth-order approximation.

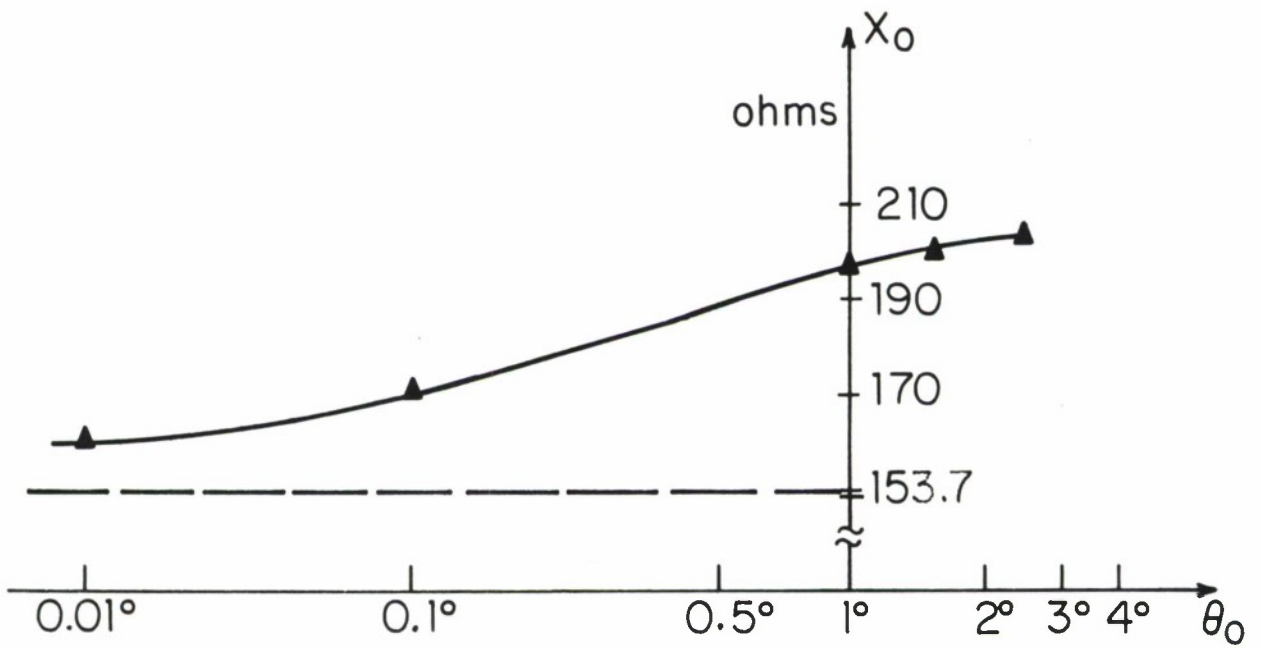
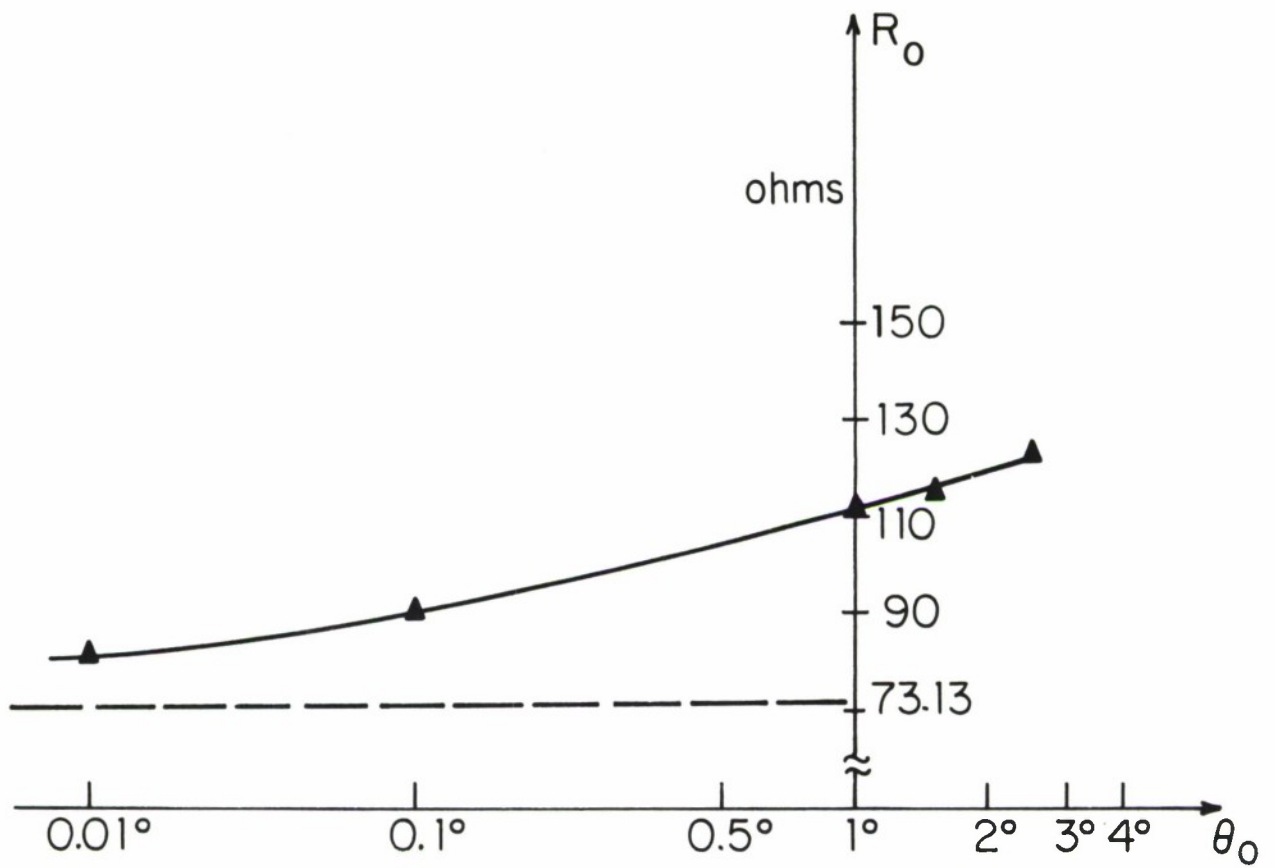


FIG. 2-4. INPUT IMPEDANCE OF $\lambda/4$ THIN CONICAL ANTENNA VS. CONE ANGLE θ_0

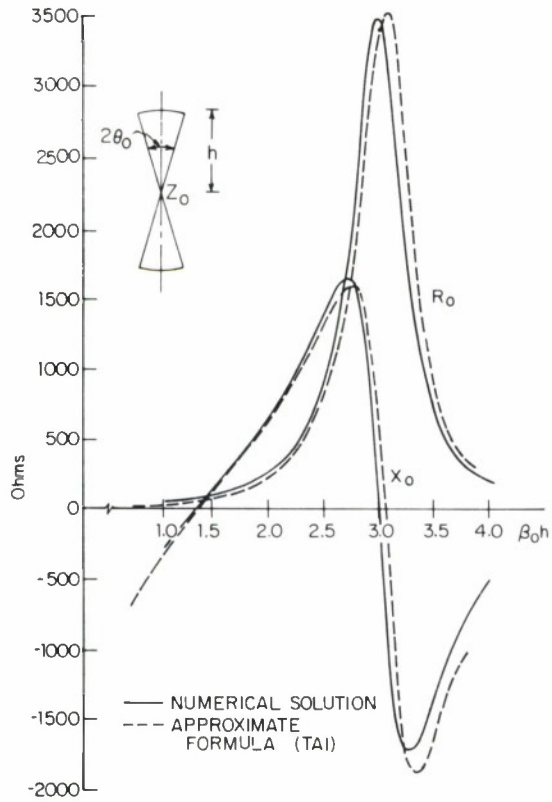
Input antiresonance is characterized by

$$X_0 = 0, \quad R_0 = (R_0)_{\text{antires.}} \quad \text{and} \quad \beta_0 h = (\beta_0 h)_{\text{antires.}} \quad (2-53)$$

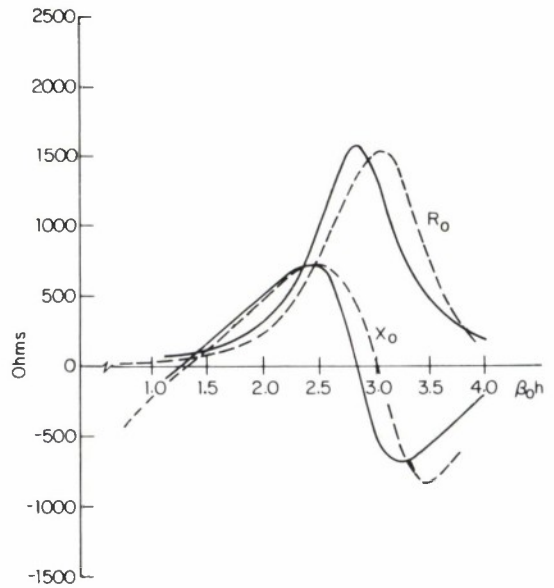
It occurs at values of $\beta_0 h$ that are less than π by an amount that increases with decreasing Z_c in a manner resembling the occurrence of resonance near $\pi/2$. The reactance X_0 has a maximum for $\beta_0 h$ slightly less than $(\beta_0 h)_{\text{antires.}}$. The resistance has its maximum very near to anti-resonance. The fact that the ratio $|X_{\min}|/|X_{\max}|$ characterizing the behavior of the reactance near antiresonance is always greater than one for the cylindrical antenna is not necessarily true of the biconical antenna. The ratio $|X_{\min}|/|X_{\max}|$ for the biconical antenna is quite different; in fact, $|X_{\min}|/|X_{\max}|$ is greater than one only for small cone angles ($\theta_0 < 1^\circ$) and becomes less than one with increasing θ_0 . This implies that the capacitive lobe of the reactance curve increases with θ_0 and becomes larger than the associated inductive lobe. In other words, the capacitive loading effect of the upper and lower conical surfaces which act more or less as a capacitor with electric lines E_θ between them to the point generator are much larger in the biconical case than in the cylindrical one.

The difference in the behavior of the reactance curves might be ascribed to the quite different driving condition in these two types of antenna; for the biconical antenna, there exists a point generator at the center while for the cylindrical dipole, the excitation is actually over a circular surface with vanishing separation between them. This suggestion is later justified in the experimental comparison between modified conical and cylindrical dipoles in which both are driven by a circular radial electric field at some distance away from the origin. Both real and imaginary parts of the impedance curves are more comparable than observed here.

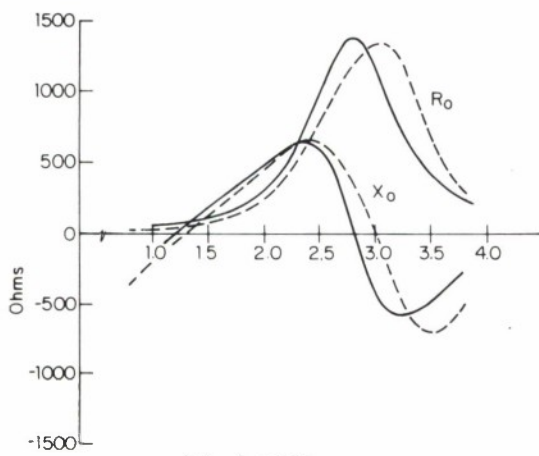
A comparison of the input impedance of the thin biconical antenna as computed from (1-90) with the corresponding approximate results using (2-47) is shown in Fig. 2-5. It is seen that the approximate results lead to lower resistance near anti-resonance and resonance and larger



(a) $\theta_0 = 0.1^\circ$



(b) $\theta_0 = 1.1^\circ$



(c) $\theta_0 = 1.5^\circ$

FIG. 2-5 INPUT IMPEDANCE FOR THIN CONICAL ANTENNA

resonant and anti-resonant length than the computed results. The reactance behaves in an analogous manner. In general, the approximate formula leads to results comparable to those with (1-90) only at very small cone angles. This suggests that for cone angles greater than 0.1° , (1-90) must be used for studying the behavior at resonance and anti-resonance.

In Fig. 2-6, is shown the variation of the cylindrical antenna impedance as a function of antenna length with various values of the parameter Ω and a comparison with a biconical antenna with half angle $\theta_0 = 1.1^\circ$. The comparison is interesting since by judicious adjustment of the radius of the cylindrical antenna, a measure of correspondence can be achieved. It is obvious from Fig. 2-6 that for the cylindrical antenna with radius equal to or greater than the maximum radius of the biconical antenna a_θ , the impedance behavior is quite different from that of the biconical antenna, whereas the impedance curves tend to be comparable as the radius of cylindrical antenna remains within the range of $1/4$ or $1/5$ of a_θ . Again the resistance curves seem to match each other better than the reactance curves. One way of measuring the comparability is by defining the average of the antenna as follows [6], i. e. ,

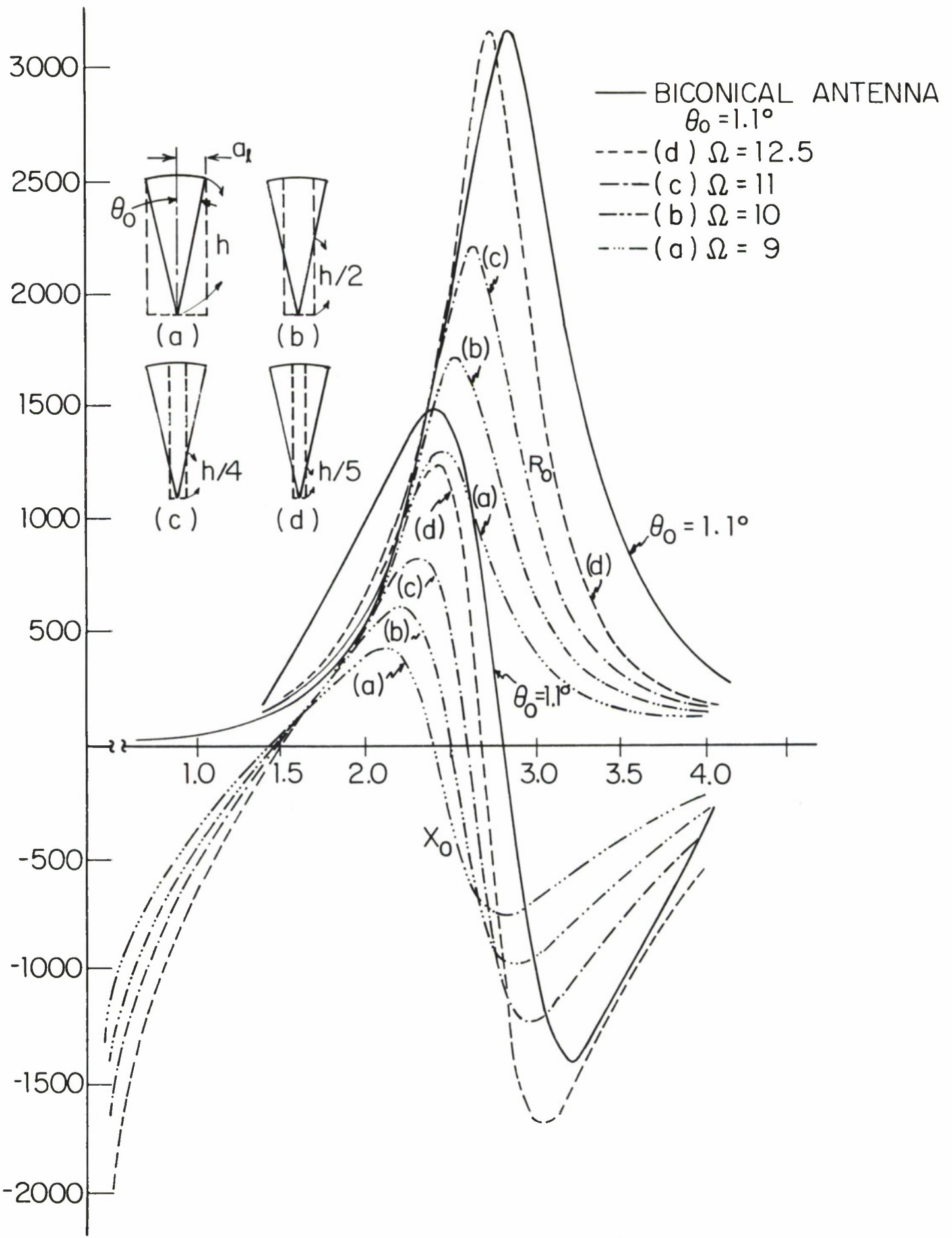
$$\langle \Omega \rangle_{\text{ave.}} = \frac{2}{h} \int_0^h \ln\left(\frac{2R}{r}\right) dR \quad (2-54)$$

where r is the radius of the section at radial distance R from the driving point at the origin. Accordingly, the average Ω for the cylindrical antenna with radius a is

$$\langle \Omega \rangle_{\text{ave.}} = 2 \left[\ln\left(\frac{2R}{a}\right) - 1 \right] \quad (2-55)$$

and that for the conical antenna with angle θ_0 is

$$\langle \Omega \rangle_{\text{ave.}} = 2 \ln(2 \cot \theta_0) \quad (2-56)$$



G. 2-6 INPUT IMPEDANCE OF CONICAL AND CYLINDRICAL DIPOLE

It is seen in Fig. 2-6 that the impedances of the biconical and cylindrical antennas are comparable when both have approximately the same $\langle \Omega \rangle$ (for curve (d) $\langle \Omega \rangle = 12.5$ and $\langle \Omega \rangle_{\text{conical}} = 14.1$). This means that for purpose of comparison, one must choose a cylindrical antenna with a radius at least smaller than half the maximum radius of the cone antenna. No attempt has been made here to pursue further a theoretical study of the relation between these two radiating structures. The general properties provide a qualitative guide of the extent to which these two radiating antennas behave reasonably alike, so that information obtained from one can be generally applied to predict the behavior of the other. This is essential later in interpreting the experimental comparison between modified cylindrical and conical antennas in which both the cone angle and antenna radius are fixed by the measuring set-up.

Numerical values for (1-97) and (1-99) for a corresponding biconical structure are also obtained along much the same lines as for (1-90). All three sets of equations give the same results with differences less than 1 per cent among them. For each equation, matrices of order $N-2$, $N-1$, N etc. are solved separately and the solution inspected for convergence. It was found if $v_m > \max. (2k+1, 2r+1)$ that the solutions converge both rapidly and monotonically. However, if $v_m < \max. (2k+1, 2r+1)$, the solutions tend to oscillate widely and show little tendency to converge.

The choice of the size of the matrices depends upon the accuracy required for the solution on the one hand and the computation time on the other. As a compromise, a less elegant method was adopted. That is, the extreme cases are examined with great care (i. e., the longest antenna). In addition to checking among themselves for convergence in the course of a numerical solution, solutions from a truncated matrix were continuously checked with those of the modified matrix in which each element was corrected by adding the error estimates. To proceed one step further, solutions from a matrix of size N (which is the number when solutions show convergence of 1 per cent) are compared with solutions from a matrix of size $(N+10)$. It is required that their difference lie within 1 per cent. Although it is not known exactly how this truncated solution converges to the true solution, at least a self-consistent one is obtained

in this manner. The number N is then used for antennas of shorter lengths without repeating the same test for convergence.

As a double check for convergence, observations were made particularly at $\beta_0 h = 1.6$ and $\theta_0 = 1.1^\circ$. Numerical results from (1-90) and (1-99) for a series of matrix sizes are shown in Fig. 2-7. It is observed that values of (1-90) tend to converge toward the final value in a monotonically increasing way with an increasing size of the matrices while the solutions from (1-99) also approach the same value in much the same but monotonically decreasing way.

The mutual checking among these three sets of linear equations suggests that the procedures used in the derivation of (1-97) and (1-99) for the biconical antenna and hence, in quite a similar manner for (1-57) and (1-64) for the modified dipole are justified.

5. THE MODIFIED CONICAL DIPOLE

Based upon (1-57), (1-64), (1-73) and (1-76), a numerical solution for the current distributions along both antenna and sphere with various sizes can be obtained. Also the input conductance and susceptance of the antenna are readily known as the real and imaginary parts of the total current at the driving point. In the process of the numerical computation, much of the analysis and many of the results from the preceding section can readily be utilized with some necessary modifications.

The general terms of the coefficient matrix of (1-57) and (1-64) are the following forms:

$$g_1(r, k, v) = \frac{(2v+1)}{v(v+1)} \frac{M'_v(\beta_0 a)}{M_v(\beta_0 a)} \frac{1}{[k(k+1) - v(v+1)]} \cdot \frac{1}{[r(r+1) - v(v+1)]} \frac{\partial v}{\partial \mu_0} \quad (2-57)$$

and

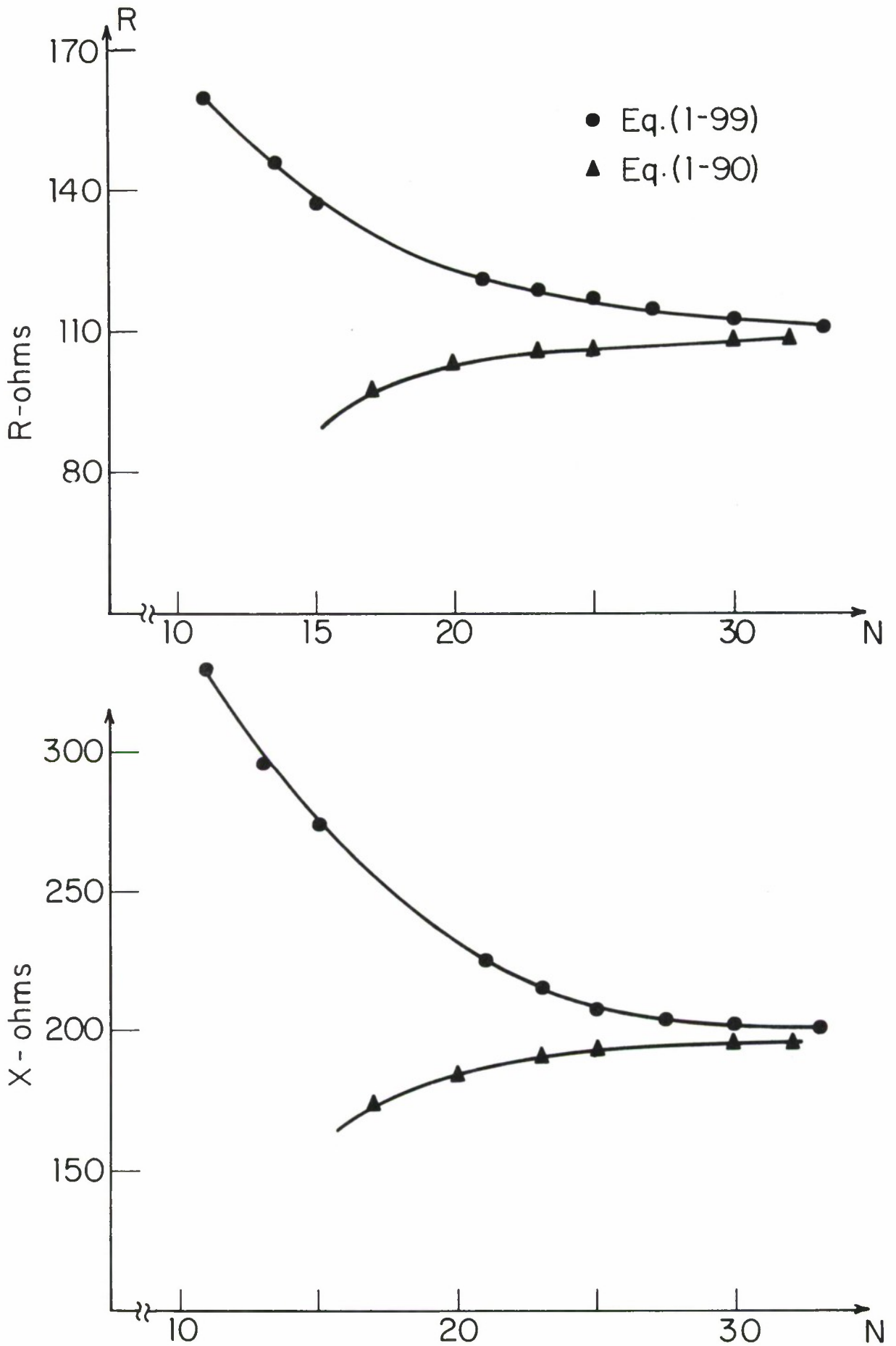


FIG. 2-7 CONVERGENCE OF NUMERICAL SOLUTION FOR $\lambda/4$ BICONICAL ANTENNA ($\theta_0=1.1^\circ$)

$$g_2(r, k, v) = g_1(r, k, v) \frac{M_v(\beta_0 a)^2}{M'_v(\beta_0 a)} \quad (2-58)$$

where subscripts 1 and 2 denote the first and second sets of linear equations respectively.

The above equations differ from those for the corresponding biconical antenna only in the ratio $M'_v(\beta_0 a)/M_v(\beta_0 a)$.

By applying the approximate formulae for the Bessel's function of the second kind for large v , i. e.,

$$N_v(x) \approx (\pi)^{1/2} 2^v \Gamma(v + 1/2) x^{-v} \exp \frac{x^2}{4(v+1/2)} \quad (2-59a)$$

and

$$N'_v(x) \approx -\frac{v}{x} N_v(x) \quad (2-59b)$$

and by using the fact that $v \gg x$, one obtains

$$\frac{M'_v(x)}{M_v(x)} \approx \frac{(v+1)}{x} = \frac{J'_v(x)}{J_v(x)} \quad (2-60)$$

The fact that $M'_v(x)/M_v(x)$ and $J'_v(x)/J_v(x)$ have the same asymptotic behavior for large v implies that all of the formulae for error estimates in the preceding section [(2-35) - (2-46)] can be used directly for the modified conical antenna with $\beta_0 h$ replaced by $\beta_0 a$. Furthermore, the same error bound obtained for the two cases suggests that the coefficient matrix associated with the modified dipole should have essentially the same convergence properties as that for the biconical one; especially for a small central sphere in which D_{r2} and D'_{r2} are small relative to D_{r1} and D_{r2} [(1-57) and (1-64)].

Additional terms (i. e., D_{r2} and D'_{r2}) which characterize the presence of the central sphere for the modified dipole are also present in the form of an infinite summation in the driving terms of (1-57) and (1-64).

For a small central sphere, these terms are of the order $(\beta_0 b)^{v_1}$ [where v_1 is the first root of the characteristic equation $L_v(\theta_0) = 0$] and vanish in the limiting case of the biconical antenna. On the other hand, D_{r2} and D'_{r2} become more important as the central sphere becomes larger.

The error estimates for D_{r2} and D'_{r2} will be examined first. Thus,

$$D_{r2} = \frac{-j V_0^e}{60} P_r(\theta_0)(1-\mu_0^2) \sum_v C_v \frac{(2v+1)}{v(v+1)} \frac{1}{[r(r+1) - v(v+1)]} \cdot \frac{1}{M_v(\beta_0 a) J'_v(\beta_0 b)} \frac{\partial v}{\partial \mu_0} \quad (2-61)$$

again, for large v , one gets

$$C_v \approx \frac{-\sin(v\theta_0)}{v \operatorname{fn}(\theta_0, \theta_1) \sin\theta_0 \cdot \sin(\theta_0 + \theta_1)^{1/2}} \quad (2-62a)$$

$$M_v(\beta_0 a) J'_v(\beta_0 b) \approx \frac{v}{2v+1} \left(\frac{a}{b}\right)^v \quad (2-62b)$$

Therefore, the upper bound of the remainder of D_{r2} is R_{1D} ,

$$R_{1D}(r, v_m) \sim \frac{4}{\pi} \frac{1}{\operatorname{fn}(\theta_0, \theta_1)} \frac{(b/a)^{v_m}}{a} \frac{1}{[\sin\theta_0 \cdot \sin(\theta_0 + \theta_1)]^{1/2}} \cdot \left[\frac{1}{r(2r+1)} \ln\left(\frac{v_m}{v_m+r}\right) + \frac{1}{(2r+1)(r+1)} \ln\left(\frac{v_m}{v_m-2r-1}\right) \right] \quad (2-63)$$

Similarly for D'_{r2} ,

$$R_{2D}(r, v_m) \approx \frac{4a}{\pi} \left(\frac{b}{a}\right)^{v_m} \frac{1}{\text{fn}(\theta_0, \theta_1) [\sin \theta_0 \cdot \sin(\theta_0 + \theta_1)]^{1/2}} \cdot$$

$$\left[\frac{1}{(r+1)v_m} + \frac{1}{(r+1)^2} \ln\left(\frac{v_m - r - 1}{v_m}\right) - \frac{1}{r^2} \ln\left(\frac{v_m + r}{v_m}\right) \right]$$

(2-64)

The errors caused by the double truncation which occurs in the computation of the fields [i. e., $(B_\Phi)_{1C}$ and $(E_\theta)_{1C}$] and the input admittance (i. e., Y_{1C}) can be estimated in the following way. A comparison of the real part of the complex power radiated as seen from the driving point with the far-field radiated power computed from (1-89) gives:

$$G_0 = 240 \sum_k \frac{|b_k|^2}{(2k+1)(k+1)k} \frac{1}{|R_k(\beta_0 a)|^2} \quad (2-65)$$

The right-hand side converges extremely fast. It was found that less than ten terms were needed to achieve accuracy of one out of 10^5 . It is reassuring to note that in the calculation, the left-hand side of (2-65) agrees within the range of relative error one part out of 10^3 with the right-hand side.

It is interesting to note that the computation on the right-hand side of (2-65) involves only the radiation field coefficients (i. e., b_k 's) which is the solution of an infinite set of linear equations while the left-hand side is a result involving all the fields inside antenna region. The excellent agreement between these two demonstrates the internal consistency and accuracy of the computation.

(A) Input Admittance

The input admittances of modified conical antennas with half cone angle $\theta_0 = 1.1^\circ$ and driving gap $\theta_1 = 1.5^\circ$ and antenna heights ranging from

$\beta_0 h = 0.6$ to 4.0 and spherical radius ranging from $\beta_0 b = 0.15$ to 1.5 have been obtained (numerical data are listed in Appendix A).

In Fig. 2-8, are shown graphs of the input admittance of a modified conical antenna as a function of $\beta_0 h$ with the sphere radius as a parameter. This is convenient theoretically and also for a later experimental check in conjunction with a partially fixed installation for which the frequency is varied (i. e., in the experimental set-up, the physical size of the central sphere, center conductor and hence the cone angle are fixed while the antenna length varies in discrete steps).

Because the input admittance of the modified conical antenna is defined as that seen at one driving terminal, the admittance curves in Fig. 2-8 have to be rescaled by a factor $1/2$ in order to compare them with that for a corresponding biconical antenna.

In general, the admittance curves are broadened and flattened as the center sphere is enlarged. More specifically, the magnitude of the maximum values of $|G_{\max}|$ and $|B_{\max}|$ and the minimum $|B_{\min}|$ decrease as the radius of the central sphere increases until approximately at $\beta_0 b = 1$ where the circumference of the sphere equals one wavelength, and the magnitudes of $|G_{\max}|$, $|B_{\max}|$, and $|B_{\min}|$ start growing again with increases in the size of the sphere.

The behavior of the susceptance near resonance and anti-resonance is also of interest with a change in the radius b . In Fig. 2-9, are shown the resonant and anti-resonant lengths as a function of $\beta_0 b$. It is seen that $(\beta_0 h)_{\text{antires.}}$ first decreases with increases in $\beta_0 b$ until $\beta_0 b$ approximately equals one, when $(\beta_0 h)_{\text{antires.}}$ begins to increase again. On the other hand, $(\beta_0 h)_{\text{res.}}$ remains at much the same value for $\beta_0 b < 0.5$, after which $(\beta_0 h)_{\text{res.}}$ increases rapidly. The increasing trend of $(\beta_0 h)_{\text{res.}}$ is stopped and reserved also at approximately $\beta_0 b = 1$. The relative constancy of $(\beta_0 h)_{\text{res.}}$ for $\beta_0 b < 0.5$ might be the result of simultaneous capacity loading due to a central modification which tends to shift $(\beta_0 h)_{\text{res.}}$ toward the right and a thickening on the average of the protruding portion which tends to pull $(\beta_0 h)_{\text{res.}}$ back toward smaller values.

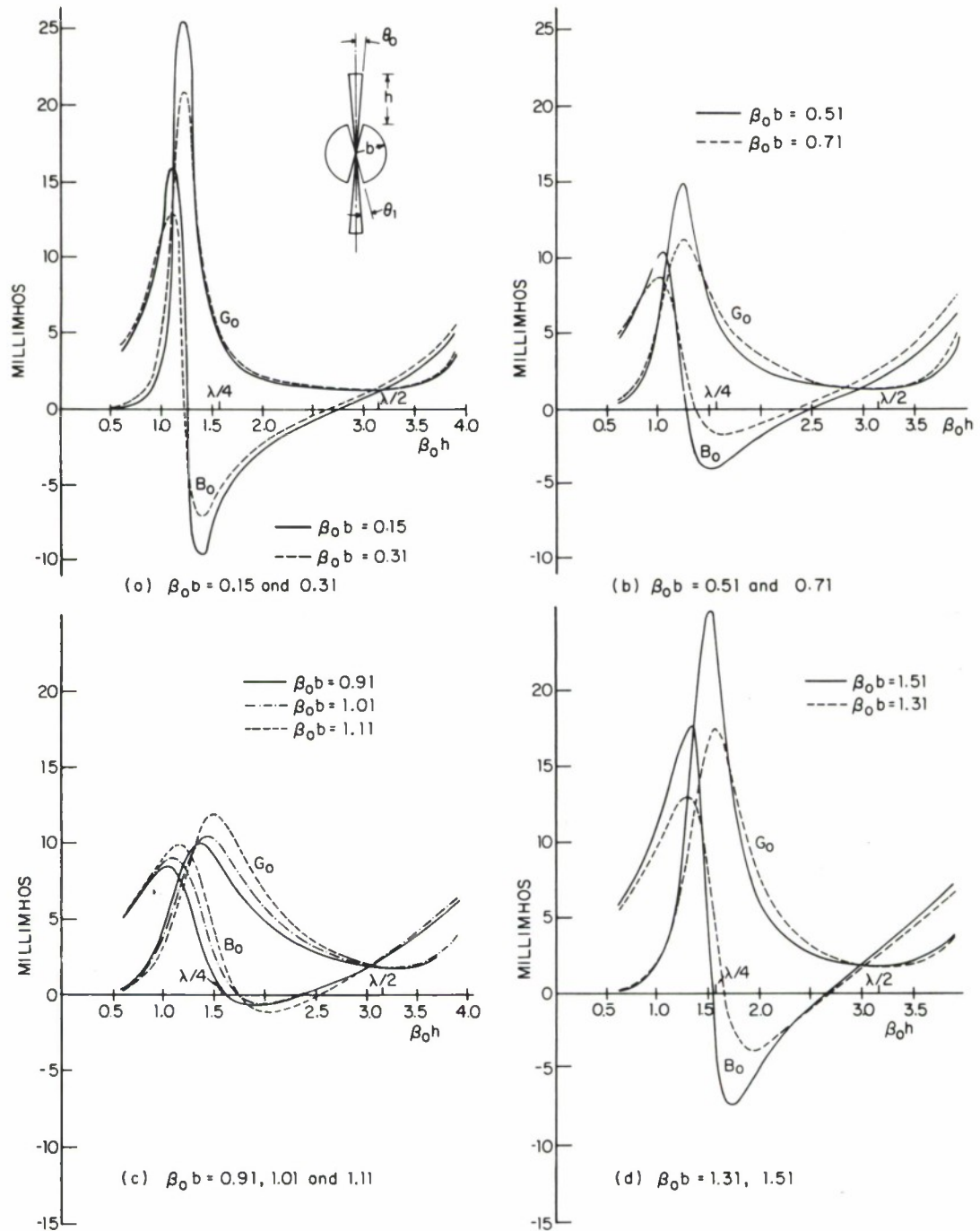


FIG. 2-8 INPUT ADMITTANCE OF MODIFIED CONICAL DIPOLE

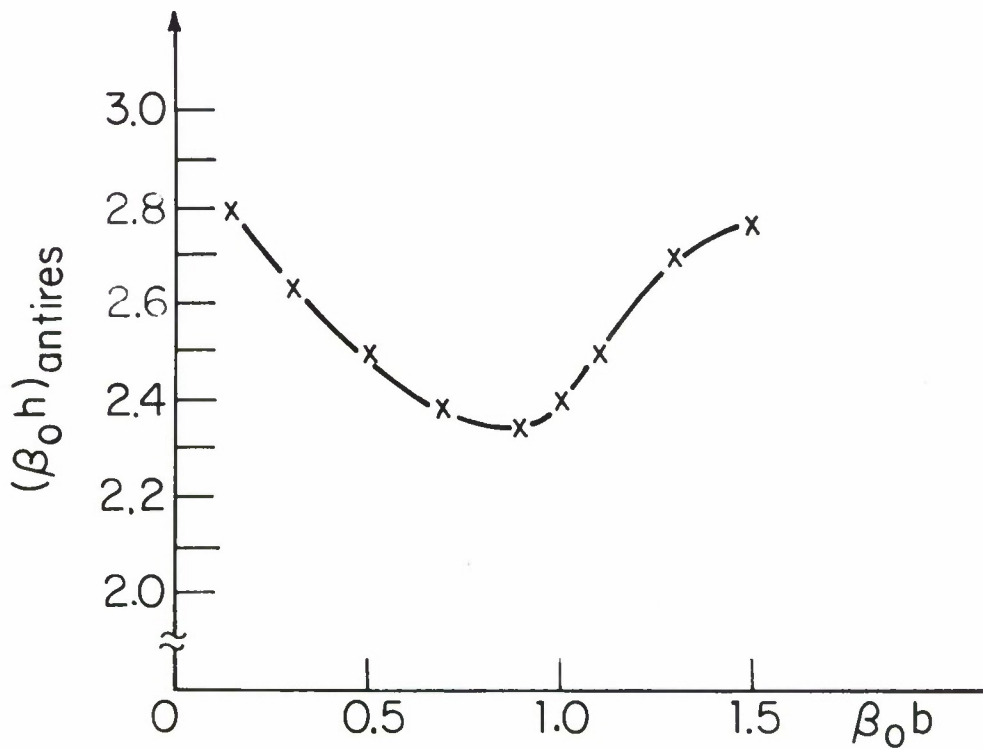
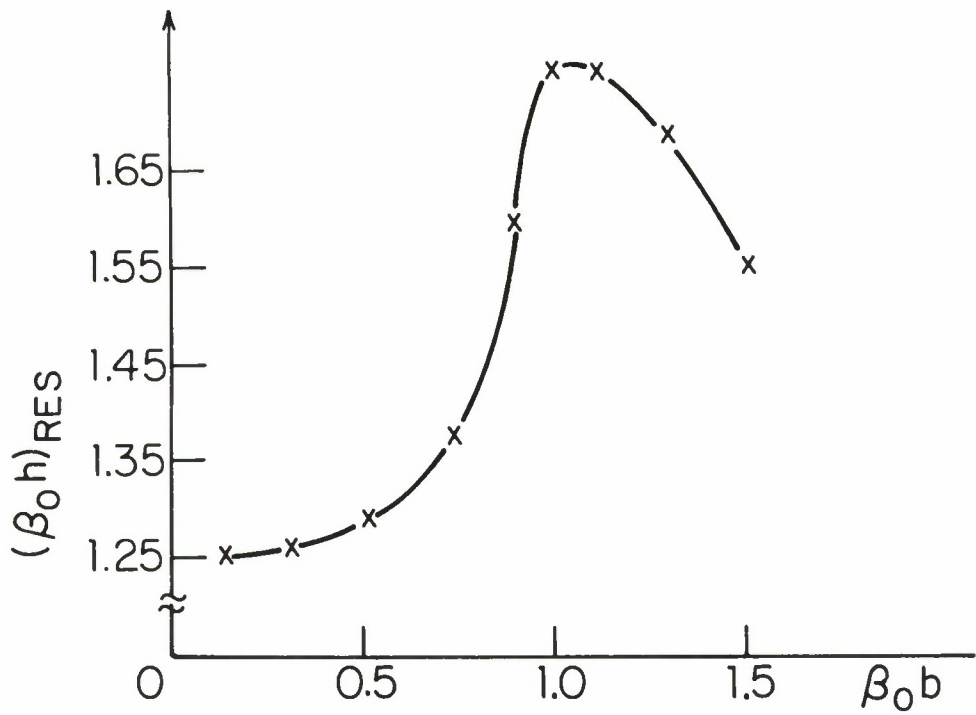


FIG. 2-9 VARIATION OF $(\beta_0 h)_{res.}$ AND $(\beta_0 h)_{antires}$ VS. $\beta_0 b$

In the neighborhood of $(\beta_0 h)_{res.}$ the slope of the susceptance curves decreases with increases in $\beta_0 b$. The flattening of the curve is accompanied by a shift of the point of zero susceptance ($\beta_0 b > 0.5$) from smaller values toward $\pi/2$. The fact that $(\beta_0 h)_{res.}$ becomes even larger than $\pi/2$ as $(\beta_0 b)$ becomes greater than 0.8 suggests that the central modification itself becomes such a substantial part of the whole radiating structure that the performance of the antenna protruding out from the sphere is changed beyond any resemblance with the corresponding dipole.

In the neighborhood of $\beta_0 b = 1$, the susceptance stays fairly constant over the range of $\beta_0 h$ from $\pi/2$ to π even though the associated conductances differ significantly (e. g., at $\beta_0 h = 0.91$, the susceptance varies within 0.7 millimhos of a mean value near 0.2 millimhos, whereas the conductance ranges between 2 and 8 millimhos). This observation confirms the experimental results for the modified cylindrical antenna reported by Iizuka [8].

Consider specifically the effect on the input characteristics of a sudden change from a point generator in the biconical case to a radial ring driving a modified conical antenna. In Fig. 2-10, the input impedance is shown near $(\beta_0 h)_{antires.}$ for both the biconical and the modified conical antenna with a small central modification ($\beta_0 b = 0.15$). Although the real parts are still comparable with each other, one remarkable change in the imaginary parts is the ratio $|X_{min}|/|X_{max}|$ which is larger than one in the biconical case but is now less than one. This means that with a small central modification which provides the modified conical antenna with a driving condition quite similar to that of the cylindrical antenna, the input characteristics of the two become more comparable.

In Fig. 2-11, is shown the variation of antenna admittance with a fixed length of protrusion as a function of the radius of the central sphere. Again, the driving point admittance of the antenna is seen to change significantly with the size of the sphere. Generally speaking, for $\beta_0 b < 1$, the change in susceptance with respect to $\beta_0 b$ is larger than that of the conductance. Specifically, for $\beta_0 b < 0.2$, there are practically no

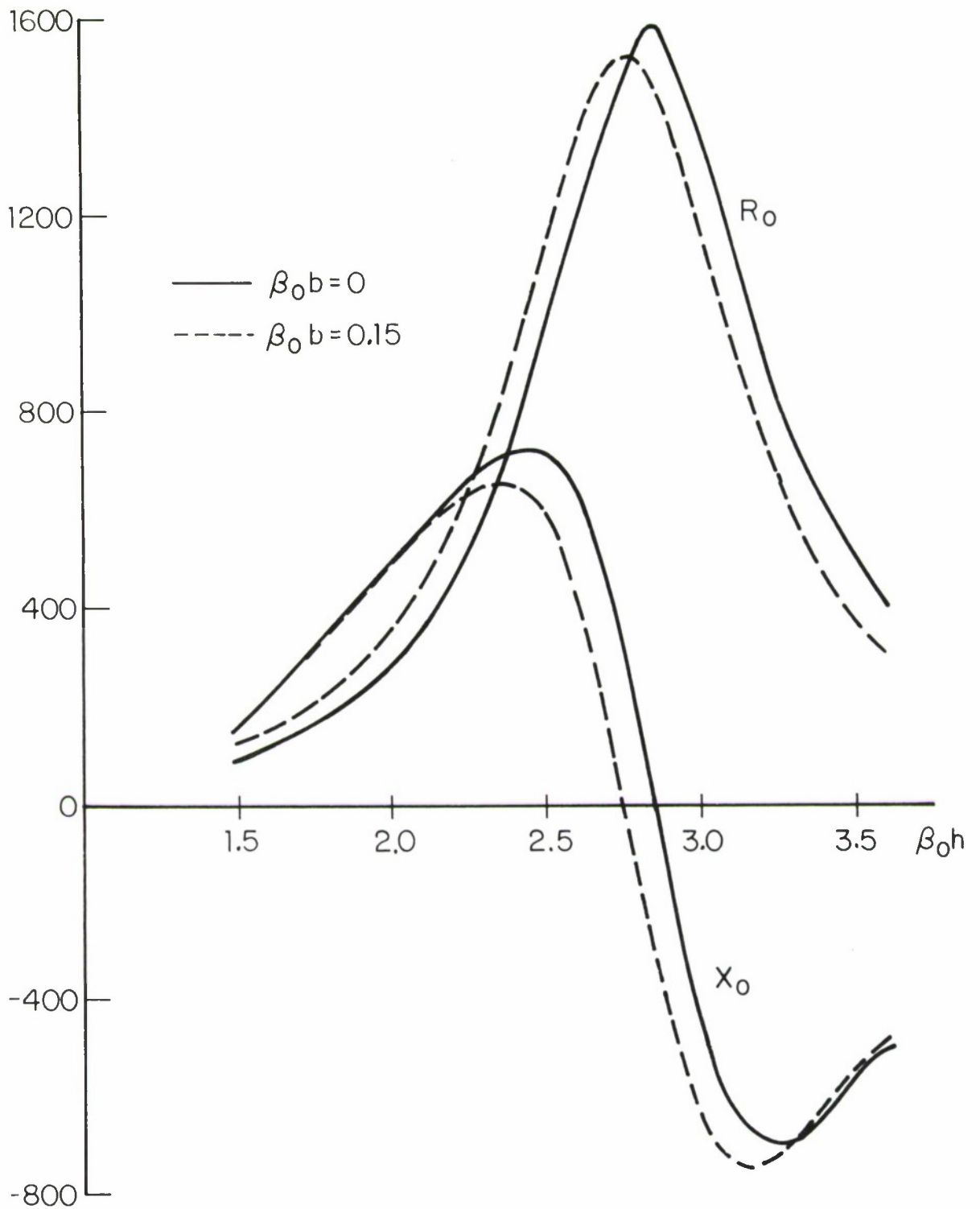


FIG. 2-10 INPUT IMPEDANCE NEAR ANTIRESONANCE OF CONICAL ANTENNA WITH SMALL CENTRAL SPHERE

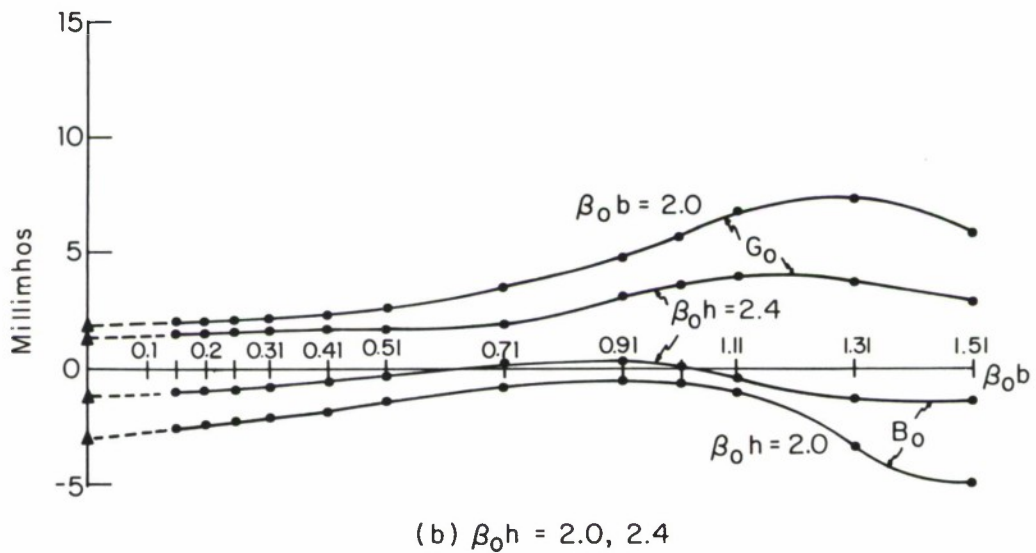
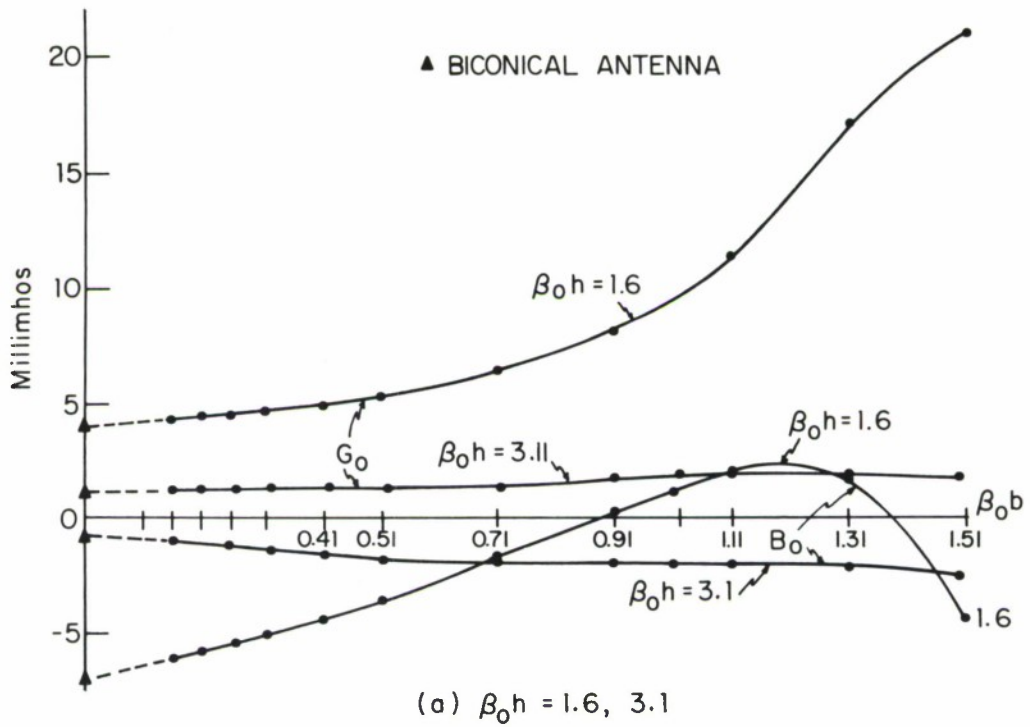


FIG. 2-11 VARIATION OF INPUT ADMITTANCE FOR MODIFIED CONICAL ANTENNA WITH FIXED LENGTH

changes in the conductance but relatively large changes in the susceptance. It is also significant to note that all admittance curves can be extrapolated toward smaller $\beta_0 b$ and that they coincide with the values of the corresponding biconical antenna.

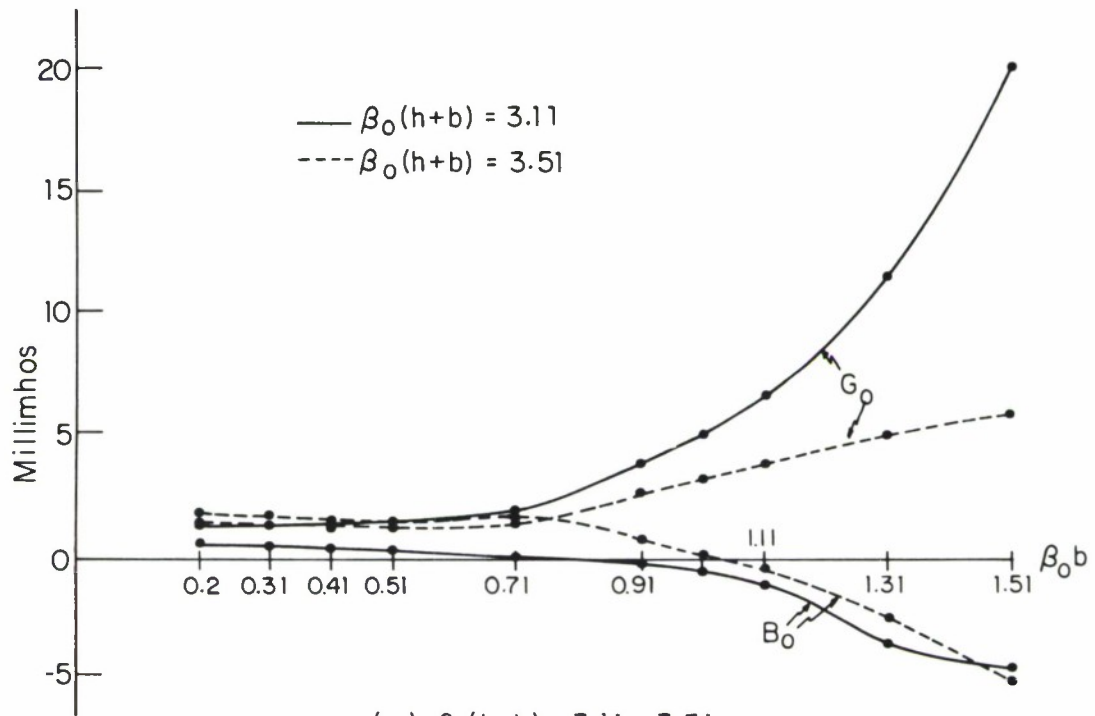
In Fig. 2-12, are shown the changes in antenna admittance with fixed total length (i. e., $\beta_0 a$ is fixed) of the radiating structure with the radius of the central sphere $\beta_0 b$ as the parameter. It is seen that drastic changes in performance are introduced by the central sphere. Again, as was observed in Fig. 2-11, the modified dipole with a small central sphere behaves essentially as the corresponding dipole with the same length.

With its driving point situated symmetrically at a distance from the center and an enlarged central volume, the modified dipole bears some resemblances to the sleeve dipole. One of the important properties of the sleeve dipole is its broad-band behavior. One would expect the same behavior from the modified dipole. This subject will not be pursued extensively here, since it is not involved in a fundamental check of the validity of the theoretical formulae. Furthermore, the broad-band properties cannot be investigated in general without extensive numerical computations of the input impedance for a range of antenna lengths and sphere radii. However, the fact that the modified conical dipole does possess broad-band properties can easily be seen by using the available tabulation of theoretical input impedance (Appendix A). Suppose the frequency for which $\beta_0 h = 1.6$, $\beta_0 (h+2b) = 3.42$ and $\beta_0 b = 0.91$ is f_0 and the associated angular frequency is ω_0 . For a variation in frequency from $\omega_0 - \Delta\omega_0$ to $\omega_0 + \Delta\omega_0$, where $\Delta\omega_0 = \omega_0/4$, the electrical lengths have the following ranges:

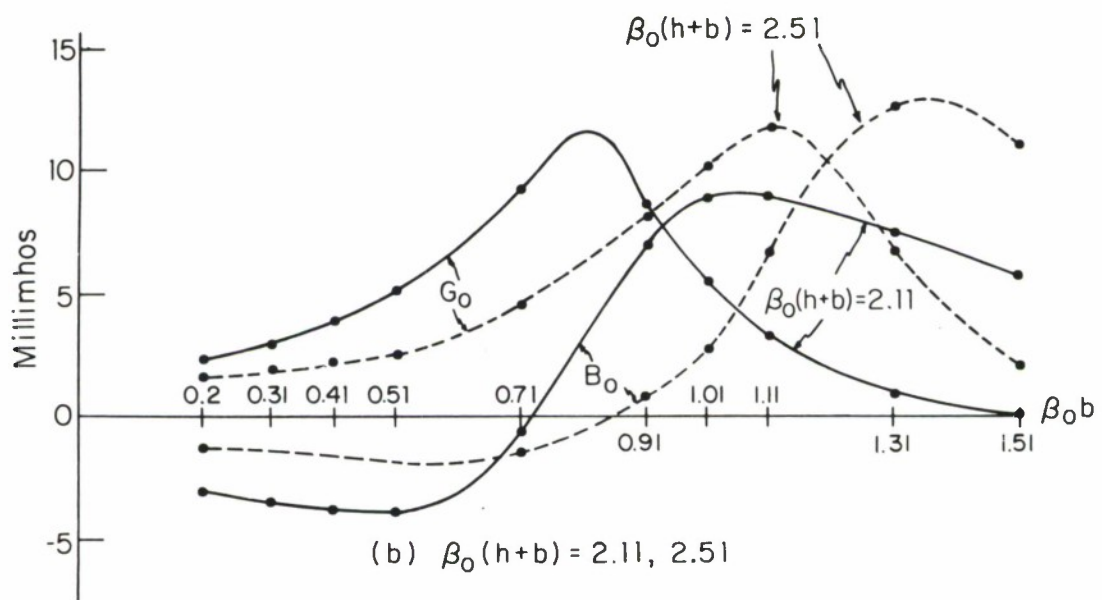
$$1.2 \leq \beta_0 h \leq 2.0$$

$$\frac{3}{4} \omega_0 \leq \omega \leq \frac{5}{4} \omega_0 \quad 2.6 \leq \beta_0 (h+2b) \leq 4.2$$

$$0.7 \leq \beta_0 b \leq 1.1$$



(a) $\beta_0(h+b) = 3.11, 3.51$



(b) $\beta_0(h+b) = 2.11, 2.51$

FIG. 2-12 VARIATION OF INPUT ADMITTANCE FOR MODIFIED CONICAL ANTENNA WITH FIXED TOTAL LENGTH.

Let the frequency response of the modified conical dipole be compared with corresponding biconical dipole with half lengths $\beta_0 h_1 = \beta_0 h$ or $\beta_0 h_2 = \beta_0 (h+2b)$. Let Z_1 and Z_2 denote the input impedance for antennas with half lengths $\beta_0 h_1$ and $\beta_0 h_2$ respectively. Tables (A-1) through (A-12) show the input impedance of the modified dipole and Fig. 2-3 shows the input impedance of the biconical antenna. It is seen that the reactance of the modified conical dipole is fairly constant near a mean value of -4 ohms over the range (i. e., from 25.3 ohms at $\beta_0 h = 2.0$ to -38.82 ohms at $\beta_0 h = 1.6$), whereas the corresponding reactance of the center-driven conical dipole (Fig. 2-3) varies widely over positive and negative values ($20 < X_1 < 480$, $-675 < X_2 < 650$). The resistance for the modified dipole varies within 30 per cent of a mean value near 111 ohms ($77 < R_0 < 145$) whereas R_1 ranges between 50 ohms and 475 ohms and R_2 varies over a range between 175 ohms and 1550 ohms. Clearly the frequency response of the modified conical dipole is very much better from the point of view of broad-band operation than the response of an unmodified dipole.

(B) Current Distribution

Due to the continuous change in the cross section of the conical antenna, the current density along the conical surface is proportional to the total current crossing the corresponding circular cross section with a constant whose value changes with the antenna length, i. e., $I_{tc} = 2\pi R \sin \theta \times I_{dc}$ where $b \leq R \leq a$. Correspondingly, for the central sphere one can also define $I_{ts}(\theta) = 2\pi b \sin \theta I_{ds}(\theta)$ where $\theta_0 + \theta_1 \leq \theta \leq \pi - \theta_0 - \theta_1$. The current density can be compared directly with experimental data while the total current along the antenna has the advantage of being readily compared with its corresponding cylindrical dipole as long as the cone angle is small.

Numerical results for the current distribution of antennas with the half cone angle $\theta_0 = 1.1^\circ$, antenna lengths $\beta_0 h = 1.6$ and 3.1 and central sphere with $\beta_0 b = 0, 0.31, 0.51, 0.91$ and 1.31 have been obtained and shown in Fig. 2-13 and Fig. 2-14.

(a) $\beta_0 h = 1.6$

Both total current distributions and the corresponding current density for $\beta_0 h = 1.6$ with various central spheres are shown in Fig. 2-13. The curves show components I'_{ct}/V_0^e , I''_{ct}/V_0^e as a function of $X_h [= \beta_0(R-b)]$ and I'_{st}/V_0^e , I''_{st}/V_0^e as a function of $X_b (= \beta_0 b \theta)$ with corresponding angle variations marked. It is to be noted that the current densities presented here are in milliamperes per volt per electrical length, so they differ from actual current density by a constant $\beta = \omega \mu \epsilon$.

Both the real and imaginary part of the total current I_{tc} remain finite at the end and change their direction as the current passes around the edge of the conical antenna to the cap. The real part of the total current seems less affected by the size of the central sphere and remains much the same in shape except for a continuous increase in magnitude with an increase in the size of the central sphere. The real current behaves very much like a combination of terms made up of cosines and shifted cosines with half-angle arguments. The imaginary part of the current I'_{tc} is capacitive along the antenna for $\beta_0 b < 0.91$ but the magnitude continues to decrease with an increase in the size of central sphere. The range over which the I'_{tc} is capacitive is reduced and inductive currents begin to appear near the driving point. Although the total current on the surface of the sphere remains quite comparable in magnitude with that on the antenna, the magnitude of the corresponding current density decreases sharply with distance from the driving point. This is due to the fact that on the hemisphere, the surface of an incremental belt $(2\pi b \sin \theta) \Delta \theta$ increases with an increase in θ and current spreads out over a widening area with distance away from the driving point.

The real current I''_{ts} , which has the same value as I''_{tc} at the driving point, remains essentially constant for a small sphere (i. e., $\beta_0 b < 0.31$). As the sphere becomes larger, it can be approximated by trigonometric functions. The imaginary part I'_{ts} , like its counterpart I'_{tc} , changes significantly with variations in sphere radius. I'_{ts} becomes larger in magnitude and more capacitive with an increase in sphere radius.

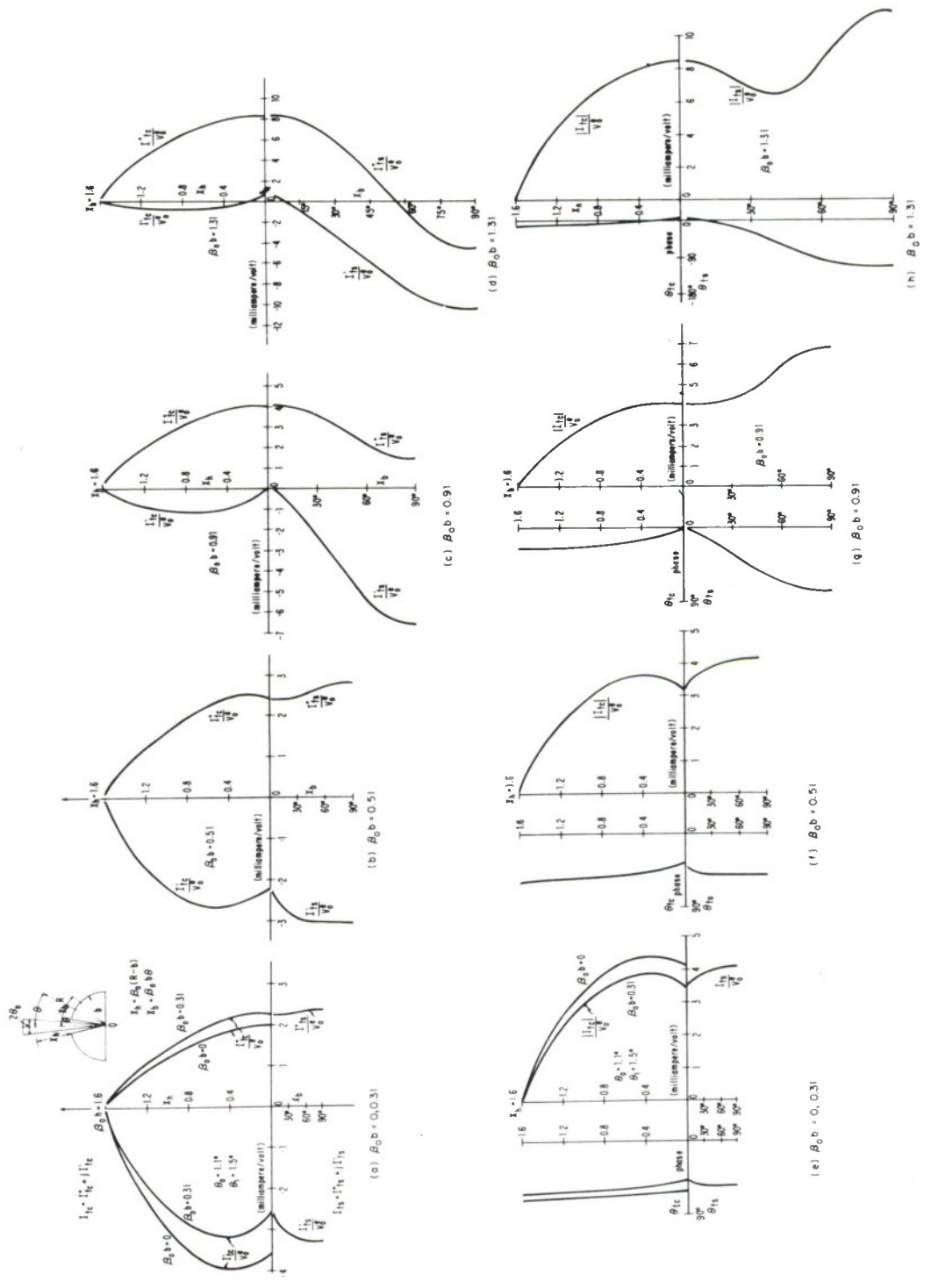


FIG. 2-13 CURRENT DISTRIBUTIONS OF MODIFIED CONICAL ANTENNA. $\beta_0 h = 1.6$

(b) $\beta_0 h = 3.1$

The distributions of total current for the antenna with $\beta_0 h = 3.1$ are shown in Fig. 2-14. The general shapes of the current distribution along the conical antenna seem less affected by the presence of the central sphere than when $\beta_0 h = 1.6$. In general, the real current I'_{tc} can still be approximated by a shifted cosine and a shifted cosine with half-angle argument, while the imaginary current I'_{tc} can still be approximated by trigonometric functions. Near the end of the antenna, the real part of the current is negative for small spheres. As b increases, this region with a small negative value decreases and the real current becomes more and more positive. The imaginary current I'_{tc} remains essentially capacitive over most of its range except near the driving point. The range over which the current is capacitive remains fairly constant except for a continuous increase in magnitude as the central sphere is made larger.

The current distribution on the sphere seems to have undergone a drastic change when compared with that for $\beta_0 h = 1.6$. Again, the behavior of I'_{ts} bears great resemblance to that with $\beta_0 h = 1.6$ but the rate of change with respect to the sphere radius seems to be approximately doubled (e. g., I'_{ts} begins to have a negative part for $\beta_0 b > 0.91$ at $\beta_0 h = 1.6$, whereas I'_{ts} has a negative part for a much smaller central sphere). The most affected part is the imaginary current I'_{ts} which has a small range of inductive current near the driving point and becomes capacitive rapidly over the rest of its range with an increase in the size of the central sphere. At $\beta_0 b = 1$, I'_{ts} begins to become less capacitive near the equatorial region of the sphere (i. e., $\theta = \pi/2$). As can be seen in Fig. 2-14c, I'_{tc} becomes inductive again near the $\theta = \pi/2$.

In general, the distribution of current along the thin conical antenna has much the same shape as along a simple dipole with enlarging central sphere. Yet, the current on the sphere is quite sensitive to the antenna lengths especially for larger spheres.

(C) Far-Field Pattern

Far-field patterns with a fixed central sphere and various antenna length are shown in Fig. 2-15. The size of the central sphere ranges from

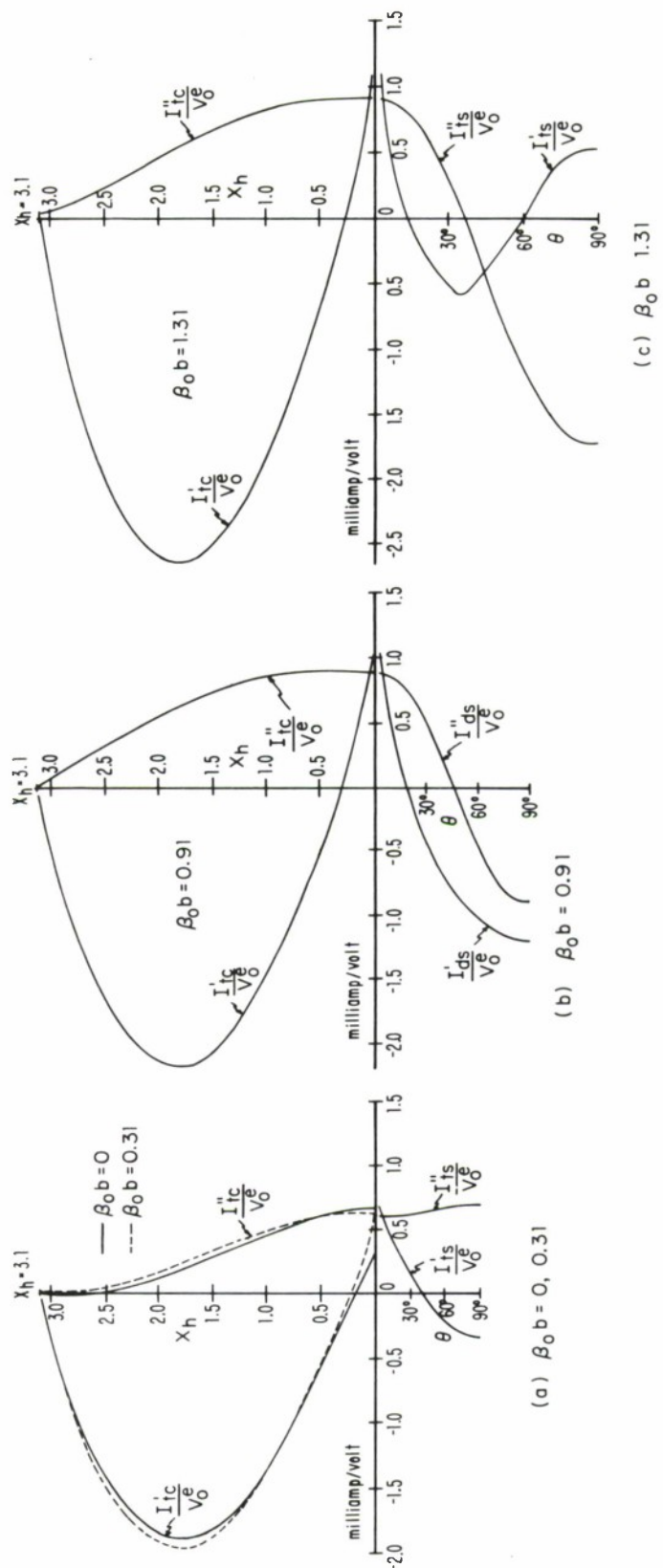
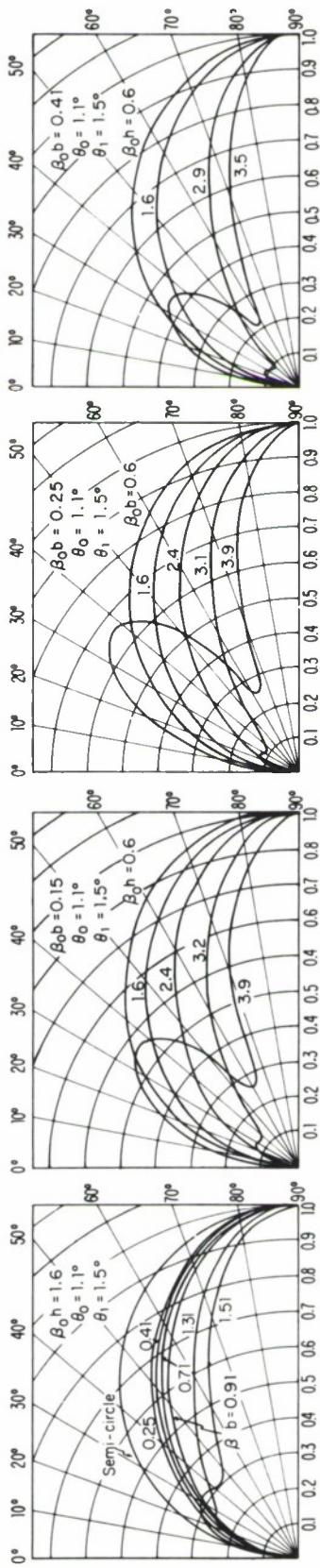


FIG. 2-14 CURRENT DISTRIBUTIONS MODIFIED CONICAL ANTENNA $\beta_0 h = 3.1$.

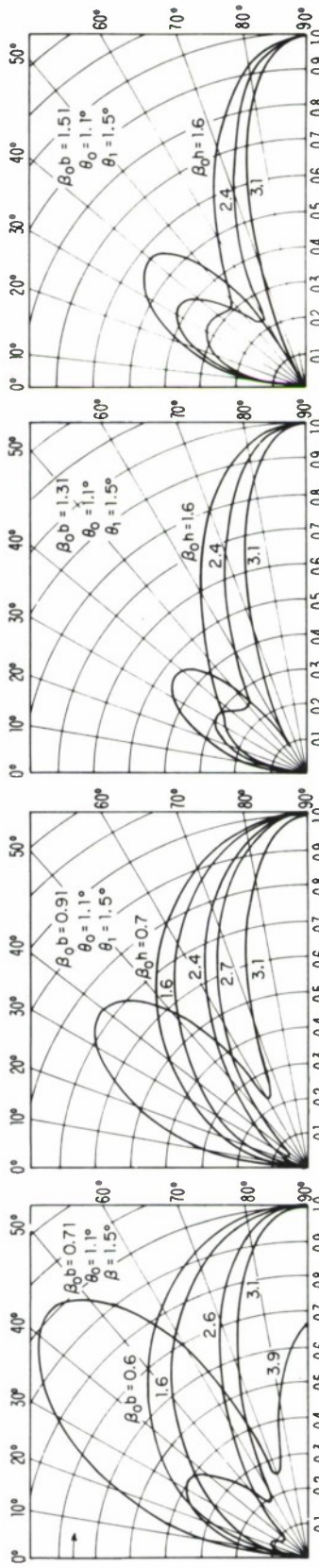


(a) $\beta_0 b = 1.6$

(b) $\beta_0 b = 0.15$

(c) $\beta_0 b = 0.25$

(d) $\beta_0 b = 0.41$



(e) $\beta_0 b = 0.71$

(f) $\beta_0 b = 0.91$

(g) $\beta_0 b = 1.31$

(h) $\beta_0 b = 1.51$

FIG. 2-15 FAR-FIELD PATTERN OF MODIFIED CONICAL ANTENNA

$\beta_0 b = 0.15$ to 1.51 and the antenna lengths range from $\beta_0 h = 1.6$ to 3.9 .

Because of the properties of symmetry of this radiating structure (i. e. , rotational symmetry and symmetry with respect to $\theta = \pi/2$ plane), it is necessary only to know the field patterns in the range $0^\circ \leq \theta \leq 90^\circ$. In order to facilitate the observation of the effect of the central sphere, all curves are normalized to have a maximum value one.

In general, the far-field pattern of the modified conical antenna behaves quite like a simple dipole for small central spheres. The presence of the central sphere effectively lengthens the antenna as compared to a simple dipole of length equal to the portion that protrudes from the sphere.

Note that the far-field patterns are more sensitive to the total length of the radiating structure than to the size of the central sphere.

In Fig. 2-15a, are drawn the field patterns of a quarter wave antenna with various central spheres. The effect of the central sphere can readily be seen in the continuous flattening of the field patterns which correspond in effect to those of a dipole with half length longer than quarter wavelength.

APPENDIX A

TABULATION OF THEORETICAL INPUT IMPEDANCES
AND ADMITTANCES

The driving point characteristics (i. e. , input impedances and admittances) have been computed for modified conical antennas with half cone angle $\theta_0 = 1.1^\circ$ and driving gap $\theta_1 = 1.5^\circ$. It covers the following ranges:

$$\beta_0 b = 0.15 \text{ to } 1.51$$

and

$$\beta_0 h = 0.6 \text{ to } 3.9$$

Table A-1 Theoretical data for the input admittance of modified dipole;

$\beta_0 h$	$\beta_0 a$	Y_0		Z_0	
0.60	0.75	0.126	+j 3.850	8.48	-j259.33
0.70	0.85	0.254	+j 4.833	10.86	-j206.34
0.80	0.95	0.574	+j 6.313	14.28	-j157.00
0.90	1.05	1.303	+j 8.394	18.05	-j116.00
1.00	1.15	3.298	+j11.637	22.54	-j 79.54
1.10	1.25	9.806	+j15.980	27.90	-j 45.50
1.20	1.35	25.410	+j 9.732	34.30	-j 13.14
1.30	1.45	20.490	-j 8.294	41.93	+j 16.97
1.40	1.55	10.210	-j 9.713	51.40	+j 48.92
1.50	1.65	6.103	-j 7.740	62.82	+j 79.67
1.60	1.75	4.228	-j 6.097	76.80	+j110.75
1.70	1.85	3.228	-j 4.884	94.19	+j142.50
1.80	1.95	2.630	-j 3.971	115.90	+j175.00
1.90	2.05	2.270	-j 3.277	142.85	+j206.23
2.00	2.15	1.976	-j 2.675	178.70	+j241.80
2.10	2.25	1.805	-j 2.205	222.32	+j271.60
2.20	2.35	1.644	-j 1.764	282.70	+j303.00
2.30	2.45	1.553	-j 1.407	353.73	+j320.30
2.40	2.55	1.457	-j 1.050	452.20	+j325.30
2.50	2.65	1.409	-j 0.750	553.19	+j294.38
2.60	2.75	1.350	-j 0.431	672.10	+j214.60
2.70	2.85	1.318	-j 0.141	750.00	+j 80.10
2.80	2.95	1.298	+j 0.145	760.80	-j 85.20
2.90	3.05	1.290	+j 0.433	696.80	-j233.70
3.00	3.15	1.294	+j 0.727	587.50	-j329.70
3.10	3.25	1.313	+j 1.033	470.40	-j370.00
3.20	3.35	1.350	+j 1.359	367.90	-j370.40
3.30	3.45	1.410	+j 1.713	286.50	-j348.00
3.40	3.55	1.500	+j 2.061	230.81	-j317.24
3.50	3.65	1.642	+j 2.549	178.60	-j277.30
3.60	3.75	1.837	+j 2.999	148.56	-j242.48
3.70	3.85	2.186	+j 3.660	120.30	-j201.40
3.80	3.95	2.658	+j 4.274	104.92	-j168.74
3.90	4.05	3.605	+j 5.153	91.03	-j130.25

Table A-2 Theoretical data for the input admittance of modified dipole;

$\beta_0 h$	$\beta_0 a$	Y_0	Z_0
0.60	0.80	0.148 +j 3.972	9.36 -j251.40
0.70	0.90	0.310 +j 5.010	12.31 -j198.85
0.80	1.00	0.705 +j 6.555	16.20 -j150.80
0.90	1.10	1.577 +j 8.671	20.30 -j111.60
1.00	1.20	3.920 +j11.850	25.15 -j 76.00
1.10	1.30	11.056 +j15.340	30.92 -j 42.90
1.20	1.40	24.280 +j 7.262	37.81 -j 11.31
1.30	1.50	18.440 -j 7.750	46.09 +j 19.38
1.40	1.60	9.990 -j 8.849	56.92 +j 49.68
1.50	1.70	6.169 -j 7.232	68.27 +j 80.03
1.60	1.80	4.336 -j 5.773	83.19 +j110.75
1.70	1.90	3.331 -j 4.653	101.70 +j142.10
1.80	2.00	2.719 -j 3.792	124.90 +j174.16
1.90	2.10	2.356 -j 3.117	154.30 +j204.19
2.00	2.20	2.039 -j 2.546	191.60 +j239.30
2.10	2.30	1.867 -j 2.082	238.73 +j266.19
2.20	2.40	1.687 -j 1.657	301.70 +j296.30
2.30	2.50	1.598 -j 1.302	376.19 +j306.33
2.40	2.60	1.485 -j 0.951	477.60 +j305.60
2.50	2.70	1.440 -j 0.653	575.85 +j261.34
2.60	2.80	1.367 -j 0.338	689.70 +j170.40
2.70	2.90	1.329 -j 0.048	751.40 +j 26.96
2.80	3.00	1.304 +j 0.239	741.90 -j135.85
2.90	3.10	1.292 +j 0.527	663.60 -j270.95
3.00	3.20	1.292 +j 0.823	550.50 -j350.80
3.10	3.30	1.307 +j 1.133	436.80 -j378.70
3.20	3.40	1.340 +j 1.463	340.34 -j371.60
3.30	3.50	1.398 +j 1.823	264.85 -j345.40
3.40	3.60	1.493 +j 2.170	215.16 -j312.76
3.50	3.70	1.631 +j 2.676	166.03 -j272.50
3.70	3.90	2.195 +j 3.815	113.30 -j197.00
3.90	4.10	3.694 +j 5.332	87.79 -j126.70

Table A-3 Theoretical data for the input admittance of modified dipole;

$\beta_0 h$	$\beta_0 a$	Y_0		Z_0	
0.60	0.85	0.180	+j 4.115	10.58	-j242.50
0.80	1.05	0.856	+j 6.784	18.30	-j145.10
0.90	1.15	1.884	+j 8.912	22.70	-j107.40
1.00	1.25	4.573	+j11.950	27.92	-j 72.98
1.10	1.35	12.870	+j14.430	34.10	-j 40.73
1.20	1.45	22.820	+j 5.433	41.48	-j 9.86
1.30	1.55	17.360	-j 6.465	50.58	+j 18.83
1.40	1.65	9.802	-j 8.037	61.00	+j 50.00
1.50	1.75	6.240	-j 6.738	74.00	+j 79.90
1.60	1.85	4.447	-j 5.450	89.88	+j110.15
1.70	1.95	3.437	-j 4.421	109.60	+j140.98
1.80	2.05	2.817	-j 3.611	134.20	+j172.40
1.90	2.15	2.440	-j 2.953	166.37	+j200.64
2.00	2.25	2.105	-j 2.416	205.00	+j235.30
2.10	2.35	1.936	-j 1.956	255.55	+j258.20
2.20	2.45	1.733	-j 1.548	320.90	+j286.70
2.30	2.55	1.649	-j 1.195	397.69	+j288.08
2.40	2.65	1.515	-j 0.852	501.30	+j281.90
2.50	2.75	1.476	-j 0.556	593.16	+j223.50
2.60	2.85	1.384	-j 0.243	700.90	+j123.00
2.70	2.95	1.341	+j 0.047	744.70	-j258.50
2.80	3.05	1.311	+j 0.334	716.30	-j182.20
2.90	3.15	1.294	+j 0.623	627.20	-j302.20
3.00	3.25	1.290	+j 0.922	513.20	-j366.70
3.10	3.35	1.301	+j 1.235	404.40	-j383.70
3.20	3.45	1.332	+j 1.570	314.30	-j370.40
3.30	3.55	1.387	+j 1.936	244.60	-j341.30
3.40	3.65				
3.50	3.75	1.623	+j 2.807	154.40	-j267.00
3.60	3.85				
3.70	3.95	2.210	+j 3.971	107.00	-j192.30
3.80	4.05	2.732	+j 4.573	96.28	-j161.17
3.90	4.15	3.796	+j 5.497	85.06	-j123.00

Table A-4 Theoretical data for the input admittance of modified dipole;

$\beta_0 h$	$\beta_0 a$	Y_0	Z_0
0.60	0.91	0.221 +j 4.274	12.06 -j233.40
0.70	1.01	0.452 +j 5.352	15.68 -j185.80
0.80	1.11	0.972 +j 6.878	20.14 -j142.50
0.90	1.21	2.149 +j 8.970	25.25 -j105.40
1.00	1.31	5.365 +j11.910	31.46 -j 69.82
1.10	1.41	12.940 +j13.100	38.17 -j 38.63
1.20	1.51	20.930 +j 3.925	46.15 -j 8.65
1.30	1.61	15.780 -j 5.855	55.70 +j 20.66
1.40	1.71	9.613 -j 7.116	67.20 +j 49.70
1.50	1.81	6.331 -j 6.158	81.17 +j 78.94
1.60	1.91	4.586 -j 5.065	98.24 +j108.48
1.70	2.01	3.570 -j 4.142	119.40 +j138.50
1.80	2.11	2.928 -j 3.393	145.79 +j168.90
1.90	2.21		
2.00	2.31	2.189 -j 2.258	221.30 +j228.30
2.10	2.41		
2.20	2.51	1.791 -j 1.417	343.40 +j271.65
2.30	2.61		
2.40	2.71	1.554 -j 0.733	526.48 +j248.16
2.50	2.81	1.528 -j 0.438	604.80 +j173.58
2.60	2.91	1.407 -j 0.128	704.89 +j 64.01
2.70	3.01	1.357 +j 0.161	726.47 -j 86.37
2.80	3.11	1.321 +j 0.449	678.50 -j230.67
2.90	3.21	1.298 +j 0.741	581.06 -j331.63
3.00	3.31	1.289 +j 1.042	469.09 -j379.29
3.10	3.41	1.296 +j 1.360	367.32 -j385.36
3.20	3.51	1.323 +j 1.700	285.01 -j366.34
3.30	3.61	1.377 +j 2.074	222.17 -j334.72
3.40	3.71	1.468 +j 2.491	175.56 -j297.95
3.50	3.81	1.629 +j 2.865	149.94 -j263.79
3.60	3.91	1.849 +j 3.398	123.56 -j227.10
3.70	4.01	2.237 +j 4.161	100.22 -j186.45
3.80	4.11	2.790 +j 4.736	92.33 -j156.75
3.90	4.21	3.934 +j 5.681	82.38 -j118.97

Table A-5 Theoretical data for the input admittance of modified dipole;

$\beta_0 h$	$\beta_0 a$	Y_0	Z_0
0.60	1.01	0.299 +j 4.507	14.64 -j220.90
0.70	1.11	0.603 +j 5.602	18.99 -j176.45
0.80	1.21	1.274 +j 7.122	24.34 -j136.50
0.90	1.31	2.730 +j 9.073	30.41 -j101.10
1.00	1.41	6.088 +j11.192	37.50 -j 68.95
1.10	1.51	12.710 +j10.770	45.81 -j 38.80
1.20	1.61	17.430 +j 3.117	55.60 -j 9.94
1.30	1.71	14.070 -j 4.232	65.14 +j 19.61
1.40	1.81	9.375 -j 5.675	78.06 +j 47.25
1.50	1.91	6.508 -j 5.209	93.65 +j 74.97
1.60	2.01	4.840 -j 4.421	112.64 +j102.90
1.70	2.11	3.814 -j 3.671	136.10 +j131.00
1.80	2.21	3.143 -j 3.024	165.24 +j158.98
1.90	2.31	2.745 -j 2.524	196.26 +j181.60
2.00	2.41	2.343 -j 1.992	247.74 +j210.61
2.10	2.51	2.217 -j 1.535	304.96 +j211.13
2.20	2.61	2.019 -j 1.173	370.39 +j215.18
2.30	2.71	1.747 -j 0.850	462.75 +j225.26
2.40	2.81	1.737 -j 0.533	526.13 +j161.51
2.50	2.91	1.528 -j 0.226	640.36 +j 94.48
2.60	3.01	1.450 +j 0.069	688.10 -j 32.50
2.70	3.11	1.388 +j 0.358	675.60 -j174.20
2.80	3.21	1.340 +j 0.648	604.84 -j292.29
2.90	3.31	1.307 +j 0.944	502.97 -j363.10
3.00	3.41	1.289 +j 1.251	399.48 -j387.73
3.10	3.51	1.288 +j 1.577	310.70 -j380.28
3.20	3.61	1.310 +j 1.929	240.95 -j354.80
3.30	3.71	1.361 +j 2.316	188.56 -j320.92
3.40	3.81	1.506 +j 2.610	165.84 -j287.48
3.50	3.91	1.613 +j 3.248	122.66 -j246.98
3.60	4.01	1.878 +j 3.629	112.46 -j217.34
3.70	4.11	2.263 +j 4.263	97.16 -j183.02
3.80	4.21	2.905 +j 4.976	87.50 -j149.89

Table A-6 Theoretical data for the input admittance of modified dipole;

β_0^h	β_0^a	y_0	z_0
0.60	1.11	0.385 +j 4.698	17.32 -j211.43
0.70	1.21	0.764 +j 5.784	22.43 -j169.94
0.80	1.31	1.575 +j 7.235	28.72 -j131.97
0.90	1.41	3.225 +j 8.926	35.81 -j 99.10
1.00	1.51	6.581 +j10.306	44.01 -j 68.93
1.10	1.61	11.845 +j 8.992	53.56 -j 40.66
1.20	1.71	14.788 +j 3.139	64.71 -j 13.74
1.30	1.81	12.550 -j 1.970	77.79 +j 12.22
1.40	1.91	9.238 -j 3.709	93.22 +j 37.42
1.50	2.01	7.060 -j 3.960	107.74 +j 60.43
1.60	2.11	5.131 -j 3.769	126.58 +j 92.97
1.70	2.21	4.095 -j 3.192	151.89 +j118.42
1.80	2.31	3.390 -j 2.649	183.14 +j143.12
1.90	2.41	2.940 -j 2.182	219.33 +j162.78
2.00	2.51	2.522 -j 1.723	270.30 +j184.70
2.10	2.61	2.273 -j 1.320	328.99 +j191.06
2.20	2.71	2.023 -j 0.971	401.83 +j192.85
2.30	2.81	1.847 -j 0.617	487.00 +j162.79
2.40	2.91	1.707 -j 0.324	565.37 +j107.14
2.50	3.01	1.601 -j 0.045	624.02 +j 17.46
2.60	3.11	1.498 +j 0.271	646.41 -j116.94
2.70	3.21	1.421 +j 0.562	608.32 -j240.63
2.80	3.31	1.361 +j 0.855	526.76 -j331.00
2.90	3.41	1.316 +j 1.157	428.46 -j376.74
3.00	3.51	1.288 +j 1.474	336.22 -j384.63
3.10	3.61	1.280 +j 1.811	260.28 -j368.27
3.20	3.71	1.296 +j 2.177	201.93 -j339.14
3.30	3.81	1.346 +j 2.582	158.80 -j304.55
3.40	3.91	1.532 +j 3.120	126.82 -j258.23
3.50	4.01	1.618 +j 3.557	105.98 -j232.94
3.60	4.11	1.920 +j 4.144	92.05 -j198.67
3.70	4.21	2.390 +j 4.831	82.28 -j166.29
3.80	4.31	3.310 +j 5.499	80.35 -j133.49
3.90	4.41	4.470 +j 6.180	76.84 -j106.24

Table A-7 Theoretical data for the input admittance of modified dipole;

β_0^h	β_0^a	Y_0	Z_0
0.60	1.31	0.534 +j 4.946	21.59 -j199.85
0.70	1.41	1.006 +j 5.923	27.88 -j164.10
0.80	1.51	1.924 +j 7.099	35.56 -j131.23
0.90	1.61	3.498 +j 8.199	44.02 -j103.18
1.00	1.71	6.005 +j 8.710	53.66 -j 77.82
1.10	1.81	9.044 +j 7.630	64.59 -j 54.50
1.20	1.91	10.986 +j 4.681	77.04 -j 32.82
1.30	2.01	10.760 +j 1.485	91.22 -j 12.59
1.40	2.11	9.278 -j 0.542	107.41 +j 6.28
1.50	2.21	7.669 -j 1.446	125.91 +j 23.73
1.60	2.31	6.341 -j 1.706	147.06 +j 39.56
1.70	2.41	5.324 -j 1.655	171.27 +j 53.25
1.80	2.51	4.553 -j 1.470	198.89 +j 64.22
1.90	2.61	3.962 -j 1.230	230.20 +j 71.43
2.00	2.71	3.500 -j 0.970	265.30 +j 73.50
2.10	2.81	3.106 -j 0.726	305.26 +j 71.40
2.20	2.91	2.782 -j 0.445	350.47 +j 56.11
2.30	3.01	2.360 -j 0.178	493.38 +j 43.77
2.40	3.11	1.940 +j 0.089	514.39 -j 23.52
2.50	3.21	1.742 +j 0.395	545.98 -j123.80
2.60	3.31	1.591 +j 0.700	526.68 -j231.77
2.70	3.41	1.476 +j 1.010	461.37 -j315.77
2.80	3.51	1.382 +j 1.330	375.80 -j361.47
2.90	3.61	1.309 +j 1.663	292.20 -j371.30
3.00	3.71	1.258 +j 2.018	222.49 -j356.91
3.10	3.81	1.233 +j 2.401	169.30 -j329.60
3.20	3.91	1.242 +j 2.821	130.76 -j296.94
3.30	4.01	1.298 +j 3.289	103.92 -j263.23
3.40	4.11	1.469 +j 3.790	88.91 -j229.40
3.50	4.21	1.642 +j 4.410	74.13 -j199.15
3.60	4.31	2.129 +j 5.110	69.47 -j166.75
3.70	4.41	2.617 +j 5.821	64.25 -j142.90
3.80	4.51	3.690 +j 6.710	62.93 -j114.43
3.90	4.61	4.871 +j 7.392	62.16 -j 94.32

Table A-8 Theoretical data for the input admittance of modified dipole;

$\beta_0 h$	$\beta_0 a$	Y_0		Z_0	
0.6	1.51	0.529	+j 5.053	20.507	-j195.74
0.7	1.61	0.985	+j 5.977	26.840	-j162.88
0.8	1.71	1.713	+j 6.922	33.690	-j136.12
0.9	1.81	2.861	+j 7.814	41.310	-j112.85
1.0	1.91	4.537	+j 8.402	49.760	-j 92.16
1.1	2.01	6.640	+j 8.258	59.137	-j 73.54
1.2	2.11	8.851	+j 7.046	69.490	-j 56.60
1.3	2.21	9.820	+j 4.988	80.950	-j 41.12
1.4	2.31	9.860	+j 2.839	93.660	-j 26.97
1.5	2.41	9.126	+j 1.197	107.726	-j 14.13
1.6	2.51	8.103	+j 0.173	123.360	-j 2.64
1.7	2.61	7.087	-j 0.366	140.720	+j 7.27
1.8	2.71	6.190	-j 0.597	160.050	+j 15.42
1.9	2.81	5.484	-j 0.638	179.920	+j 20.94
2.0	2.91	4.803	-j 0.564	205.370	+j 24.13
2.1	3.01	4.314	-j 0.440	229.449	+j 23.39
2.2	3.11	3.832	-j 0.250	259.860	+j 16.92
2.3	3.21	3.484	-j 0.068	286.960	+j 5.58
2.4	3.31	3.128	+j 0.172	318.740	-j 17.56
2.5	3.41	2.868	+j 0.386	342.462	-j 46.02
2.6	3.51	2.596	+j 0.657	362.030	-j 91.70
2.7	3.61	2.377	+j 0.919	365.950	-j141.49
2.8	3.71	2.185	+j 1.202	351.300	-j193.29
2.9	3.81	2.019	+j 1.502	318.780	-j237.26
3.0	3.91	1.880	+j 1.830	272.900	-j265.94
3.1	4.01	1.780	+j 2.148	228.750	-j275.84
3.2	4.11	1.702	+j 2.587	177.460	-j269.80
3.3	4.21	1.633	+j 2.966	144.699	-j255.10
3.4	4.31	1.737	+j 3.508	113.400	-j228.90
3.5	4.41	1.939	+j 4.005	97.930	-j202.28
3.6	4.51	2.142	+j 4.496	86.356	-j181.28
3.7	4.61	2.731	+j 5.041	83.080	-j153.36
3.8	4.71	3.273	+j 5.576	78.290	-j133.37
3.9	4.81	4.050	+j 6.271	72.670	-j122.50

Table A-9 Theoretical data for the input admittance of modified dipole;

$\beta_0 h$	$\beta_0 a$	Y_0	Z_0
0.6	1.61	0.477 +j 5.138	17.93 -j192.98
0.7	1.71	0.853 +j 6.006	23.19 -j163.22
0.8	1.81	1.457 +j 6.933	29.04 -j138.14
0.9	1.91	2.397 +j 7.857	35.53 -j116.44
1.0	2.01	3.785 +j 8.626	42.65 -j 97.22
1.1	2.11	5.650 +j 8.941	50.51 -j 79.93
1.2	2.21	7.764 +j 8.429	59.12 -j 64.18
1.3	2.31	9.559 +j 6.928	68.59 -j 49.71
1.4	2.41	10.442 +j 4.804	79.04 -j 36.36
1.5	2.51	10.315 +j 2.738	90.57 -j 24.04
1.6	2.61	9.530 +j 1.172	103.37 -j 12.71
1.7	2.71	8.500 +j 0.176	117.65 -j 24.41
1.8	2.81	7.470 -j 0.370	133.60 +j 6.61
1.9	2.91	6.540 -j 0.612	151.55 +j 14.19
2.0	3.01	5.744 -j 0.665	171.79 +j 19.90
2.1	3.11	5.067 -j 0.596	194.64 +j 22.91
2.2	3.21	4.494 -j 0.454	220.27 +j 22.25
2.3	3.31	4.004 -j 0.264	248.70 +j 16.41
2.4	3.41	3.581 -j 0.039	279.18 +j 3.01
2.5	3.51	3.215 +j 0.213	309.65 -j 20.47
2.6	3.61	2.897 +j 0.480	335.95 -j 55.68
2.7	3.71	2.618 +j 0.773	351.38 -j103.76
2.8	3.81	2.375 +j 1.083	348.62 -j158.93
2.9	3.91	2.166 +j 1.416	323.42 -j211.44
3.0	4.01	1.992 +j 1.777	279.60 -j249.31
3.1	4.11	1.857 +j 2.169	227.84 -j265.99
3.2	4.21	1.769 +j 2.592	179.66 -j263.25
3.3	4.31	1.738 +j 3.042	141.57 -j247.83
3.4	4.41	1.784 +j 3.528	114.12 -j225.73
3.5	4.51	1.901 +j 4.093	93.34 -j200.97
3.6	4.61	2.194 +j 4.657	82.79 -j175.73
3.7	4.71	2.624 +j 5.248	76.21 -j152.44
3.8	4.81	3.240 +j 5.723	74.91 -j132.32
3.9	4.91	4.040 +j 6.035	76.60 -j114.41

Table A-10 Theoretical data for the input admittance of modified dipole;

$\beta_0 h$	$\beta_0 a$	Y_0		Z_0	
0.6	1.71	0.411	+j 5.248	14.84	-j189.38
0.7	1.81	0.729	+j 6.122	19.18	-j161.07
0.8	1.91	1.237	+j 7.071	24.00	-j137.22
0.9	2.01	2.031	+j 8.068	29.34	-j120.20
1.0	2.11	3.234	+j 9.024	35.19	-j104.32
1.1	2.21	4.958	+j 9.721	41.64	-j 81.64
1.2	2.31	7.180	+j 9.791	48.71	-j 66.42
1.3	2.41	9.534	+j 8.831	56.51	-j 52.29
1.4	2.51	11.298	+j 6.772	65.12	-j 39.03
1.5	2.61	11.889	+j 4.223	74.69	-j 26.53
1.6	2.71	11.374	+j 1.953	85.40	-j 14.67
1.7	2.81	10.249	+j 0.364	97.45	-j 3.46
1.8	2.91	8.960	-j 0.571	111.16	+j 7.09
1.9	3.01	7.746	-j 1.024	126.88	+j 16.77
2.0	3.11	6.688	-j 1.166	145.10	+j 25.29
2.1	3.21	5.795	-j 1.120	166.36	+j 32.15
2.2	3.31	5.046	-j 0.956	191.32	+j 36.25
2.3	3.41	4.416	-j 0.724	220.49	+j 36.16
2.4	3.51	3.886	-j 0.446	253.97	+j 29.12
2.5	3.61	3.435	-j 0.138	290.65	+j 11.67
2.6	3.71	3.049	+j 0.194	326.62	-j 20.81
2.7	3.81	2.720	+j 0.545	353.40	-j 70.81
2.8	3.91	2.441	+j 0.917	359.05	-j134.82
2.9	4.01	2.207	+j 1.309	335.26	-j198.80
3.0	4.11	2.019	+j 1.722	286.79	-j244.50
3.1	4.21	1.880	+j 2.157	229.69	-j263.51
3.2	4.31	1.795	+j 2.613	178.60	-j260.00
3.3	4.41	1.780	+j 3.091	139.91	-j242.95
3.4	4.51	1.829	+j 3.625	110.95	-j219.91
3.5	4.61	1.978	+j 4.263	89.59	-j193.02
3.6	4.71	2.245	+j 4.849	78.62	-j169.84
3.7	4.81	2.651	+j 5.399	73.28	-j149.25
3.8	4.91	3.216	+j 5.889	71.43	-j130.81
3.9	5.01	3.944	+j 6.258	72.08	-j114.38

Table A-11 Theoretical data for the input admittance of modified dipole;

$\beta_0 h$	$\beta_0 a$	Y_0		Z_0	
0.6	1.91	0.291	+j 5.534	9.49	-j180.20
0.7	2.01	0.513	+j 6.469	12.31	-j154.08
0.8	2.11	0.889	+j 7.525	15.48	-j131.06
0.9	2.21	1.490	+j 8.730	19.01	-j111.31
1.0	2.31	2.471	+j10.082	22.94	-j 93.56
1.1	2.41	4.069	+j11.507	27.31	-j 77.24
1.2	2.51	6.607	+j12.712	32.19	-j 61.93
1.3	2.61	10.292	+j12.932	37.68	-j 47.34
1.4	2.71	14.496	+j10.967	43.88	-j 33.19
1.5	2.81	17.159	+j 6.499	50.97	-j 19.30
1.6	2.91	16.761	+j 1.554	59.15	-j 5.49
1.7	3.01	14.334	-j 1.753	68.74	+j 8.41
1.8	3.11	11.569	-j 3.246	80.13	+j 22.48
1.9	3.21	9.233	-j 3.611	93.94	+j 36.74
2.0	3.31	7.434	-j 3.427	110.95	+j 51.14
2.1	3.41	6.078	-j 3.000	132.29	+j 65.31
2.2	3.51	5.050	-j 2.478	159.59	+j 78.32
2.3	3.61	4.260	-j 1.929	194.82	+j 88.21
2.4	3.71	3.642	-j 1.382	240.01	+j 91.06
2.5	3.81	3.156	-j 0.849	295.51	+j 79.53
2.6	3.91	2.766	-j 0.329	356.55	+j 42.41
2.7	4.01	2.455	+j 0.209	404.41	-j 34.46
2.8	4.11	2.206	+j 0.661	415.89	-j124.69
2.9	4.21	2.049	+j 1.160	369.60	-j209.21
3.0	4.31	1.910	+j 1.622	304.09	-j258.19
3.1	4.41	1.823	+j 2.242	218.26	-j268.55
3.2	4.51	1.792	+j 2.824	160.21	-j252.48
3.3	4.61	1.820	+j 3.391	122.85	-j228.96
3.4	4.71	1.914	+j 3.957	99.09	-j204.80
3.5	4.81	2.086	+j 4.533	83.79	-j182.04
3.6	4.91	2.351	+j 5.117	74.14	-j161.36
3.7	5.01	2.727	+j 5.697	68.35	-j142.80
3.8	5.11	3.236	+j 6.254	65.26	-j126.12
3.9	5.21	3.901	+j 6.754	64.13	-j111.02

Table A-12 Theoretical data for the input admittance of modified dipole;

$\beta_0 h$	$\beta_0 a$	Y_0		Z_0	
0.6	2.11	0.217	+j 5.254	6.319	-j170.58
0.7	2.21	0.393	+j 6.881	8.268	-j144.86
0.8	2.31	0.691	+j 8.084	10.492	-j122.80
0.9	2.41	1.202	+j 9.530	13.032	-j103.29
1.0	2.51	2.107	+j11.308	15.926	-j 85.46
1.1	2.61	3.771	+j13.488	19.230	-j 68.78
1.2	2.71	6.939	+j15.911	23.030	-j 52.81
1.3	2.81	12.828	+j17.406	27.440	-j 37.23
1.4	2.91	21.226	+j14.161	32.600	-j 21.75
1.5	3.01	25.196	+j 3.962	38.730	-j 6.09
1.6	3.11	20.705	-j 4.484	46.134	+j 9.99
1.7	3.21	14.673	-j 7.108	55.200	+j 26.74
1.8	3.31	10.401	-j 6.938	66.540	+j 44.38
1.9	3.41	7.682	-j 5.981	81.047	+j 63.10
2.0	3.51	5.926	-j 4.961	99.960	+j 82.92
2.1	3.61	4.745	-j 3.922	125.220	+j103.50
2.2	3.71	3.962	-j 3.029	159.768	+j123.58
2.3	3.81	3.315	-j 2.239	207.175	+j139.93
2.4	3.91	2.864	-j 1.497	274.258	+j143.32
2.5	4.01	2.515	-j 0.948	348.190	+j131.19
2.6	4.11	2.347	-j 0.35	416.81	+j 62.16
2.7	4.21	2.105	+j 0.248	468.453	-j 55.25
2.8	4.31	1.958	+j 0.870	426.473	-j189.59
2.9	4.41	1.858	+j 1.461	332.539	-j261.61
3.0	4.51	1.799	+j 2.015	246.564	-j276.09
3.1	4.61	1.782	+j 2.554	183.727	-j263.33
3.2	4.71	1.807	+j 3.090	141.020	-j241.18
3.3	4.81	1.877	+j 3.634	112.202	-j217.20
3.4	4.91	2.001	+j 4.191	92.781	-j194.31
3.5	5.01	2.189	+j 4.767	79.555	-j173.25
3.6	5.11	2.456	+j 5.361	70.621	-j154.17
3.7	5.21	2.823	+j 5.973	64.688	-j136.85
3.8	5.31	3.320	+j 6.594	60.914	-j120.98
3.9	5.41	3.984	+j 7.205	58.772	-j106.29

FORTRAN IV C LEVEL 12 MAIN DATE = 71110 12/13/39

```

0029      SX=SIN(1AR)
C
C
C      SOLVE CHARACTERISTIC EQUATION  $L\sqrt{(\theta)} = 0$ 
C      RT=ROOTS OF  $L\sqrt{(\theta)} = 0$ 
C      CNT=CM:
C      20 1000
0030      CALL RTNKA(1AR,KMA,F,DEAF,FOI,0.2,1.E-06,17,1EP,I,PI,CNT)
0031      NMA=(1EP-PI)/2
0032      DO 301 KMA=1,NMA
0033      CPD=PI(KMA)
0034      CALL LEGFITAR,CDF,CPD,DP,BAP,DPNP,PNX,DENH,PNL,DPNL)
0035      RLTA(KMA)=PDL(KMA)
0036      301 CONTINUE
C
C
C      READ INPUT DATA
C      HT= ANTENNA HEIGHTS IN ELECTRICAL LENGTH
C      RS= CENTRAL SPHERE RADIUS IN ELECTRICAL LENGTH
C      KMN= NUMBER OF EQUAL SEGMENTS ALONG THE ANTENNA AND THE SPHERE
C      FOR WHICH CURRENT DISTRIBUTIONS ARE COMPUTED.
C
0037      3 READ(5,4)HT,RS,KMN
0038      HT=HT*RS
0039      WRITE(6,4)HT,RS,KMN
0040      4 FORMAT(2F10.4,15)
0041      CT=-2.*TAN(HT-RS)/RLTA
0042      CALL SPHNA(CT,HT,SH,DSH,SDS)
0043      DO 500 KL=1,NMA
0044      GLD=RT(KL)
0045      CALL LEGF(ITA,DF,GLD,C,PNP,DPNP,PNX,DPNM,PNL,GNL)
0046      CALL GTJAM(GLD,HT,RS,KMN,CNOMP,GMXJP,GMXJ,GMXJPI,GMXJL,GCJF,GY1
0047      2ST1,GY1S12,GM1QH,GM1CMP,GJ1CJ,IDX,1)
0047      500 CONTINUE
C
C
C      GENERATES MATRIX ELEMENTS
C
0048      DO 102 KR=1,MAX,2
0049      IR=(KR+1)/2
0050      ASB(1,IR)=0.
0051      DO 102 KK=KR,MAX,2
0052      KK2=KK+4
0053      IK=(KK+1)/2
0054      ITEST(IR,IK)=0
0055      FSI(IR,IK)=0.
0056      IDX=0
0057      DO 10 IN=1,NMA
0058      ITEST(IR,IK)=ITEST(IR,IK)+1
0059      ORD=RT(IN)
0060      P(IN)=(2.*ORD+1.)/(CPD+(CPD+1.))
0061      PR(IN)=P(IN)*RLTA(IN)*CNT(IN)/(SX*SX*DPNL(IN))
0062      FSP=P(IN)*CNT(IN)/(GLD*P(IN)*KMN(KR,CPD)*FAN(KR,ORD))
0063      FSI(IR,IK)=FSI(IR,IK)+FSP
0064      RATI=ABS(FSP/FSI(IR,IK))
0065      IF(KR.NE.KK)GO TO 17
0066      IDX=1
0067      ASPB=PR(IN)/(FAN(KR,ORD)*GMXJPI(IN))

```

```

0068      ASB(IK)=ASB(IR)+ASP8
0069      RATA=ABS(ASP8/ASB(IR))
0070      17 IF(CKD-KK2)10,10,21
0071      21 IF(IDX.LT.1)GO TO 25
0072      IF(RATF.LT.1.E-04.AND.RATA.LT.1.E-04)GO TO 19
0073      GO TO 10
0074      25 IF(RATF.LT.1.E-04)GO TO 19
0075      10 CONTINUE
0076      19 FI(IR,IK)=-2.*PI(KR+1)*PI(KK+1)*FS(IR,IK)
0077      FI(KI,IR)=FI(IR,IK)
0078      IF(IR.EQ.KK)GO TO 51
0079      V(IR,IK)=CT*PI(KR+1)*PI(KK+1)/(KR*KK*(KR+1)*(KK+1))
0080      V(KI,IR)=V(IR,IK)
0081      GO TO 101
0082      51 V(IR,IR)=CT*PI(KR+1)**2/(KR*(KR+1))**2-2.*(1./HT+DSOS(KR+1))/((2.*
      1KR+1)*KR*(KR+1))
0083      101 A(IF,IR)=FI(IR,IK)+V(IR,IK)
0084      A(KI,IR)=A(IR,IK)
0085      102 CONTINUE
0086      DTIB(IR)=PI(KR+1)*(-2/(ZC*COS(HT-RS)*KR*(KR+1))+ASB(IR)/(60*RLTAB)
      1)
0087      DTR(IR)=CMPLX(0.,-DTIB(IR))
0088      A(IR,M1)=DTR(IR)
0089      103 CONTINUE
0090      CALL CSIMEC(A,50,MAXX,1)
0091      WRITE(6,7)HT,RS
0092      7 FORMAT(//////46H *** ANSWER FOR COEFFICIENTS OF FIELD FOR HT=F10.4
      1,1X7H AND RS=F10.4/5H 1,10X,5H REAL,20X,5H IMAG)
0093      DO 8 I=1,MAXX
0094      WRITE(6,9)I,A(I,M1)
0095      9 FORMAT(15,2(10X,E15.3))
0096      8 CONTINUE
0097      RIMG=(0.,1.)
0098      ADM1=RIMG*TAN(HT-RS)/ZC
0099      ADM2=(0.,0.)
0100      DO 700 K1=1,MAXX
0101      ADM2=ADM2+PI(2*K1)*A(K1,M1)/(2*K1*(2*K1-1))
0102      700 CONTINUE
0103      ADM2=120*ADM2/(ZC*COS(HT-RS))
0104      ADM3=(0.,0.)
0105      DO 701 K2=1,NMA
0106      AD3=PK(K2)*GY1ST1(K2,1)
0107      ADM3=ADM3+AD3
0108      RAT=CABS(AD3/ADM3)
0109      IF(RAT.LT.1.E-03)GO TO 901
0110      701 CONTINUE
0111      901 ADM3=-RIMG*ADM3/(120.*RLTAB)
0112      ADM4=(0.,0.)
0113      DO 703 K3=1,MAXX
0114      K32=2*K3
0115      AD4=(0.,0.)
0116      DO 704 K4=1,NMA
0117      CKD=RT(K4)
0118      AD3=P(K4)*GM1CM(K4,1)*DNE(K4)/FKN((K32-1),CKD)
0119      AD4=AD4+AD3
0120      IF(CKD.EQ.1.)LT.K32)GO TO 704
0121      RAT=ABS(AD3/AD4)
0122      IF(RAT.LT.1.E-03)GO TO 902

```

```

0123      704 CONTINUE
0124      902 ADM4=ADM4-A(K3,M1)*PI(2*K3)*AC4
0125      RAT1=CABS(AC4*A(K3,M1)*PI(2*K3)/ADM4)
0126      IF(RAT1.LT.1.E-02)GO TO 903
0127      703 CONTINUE
0128      903 ADM=2*(ADM1+ADM2+ADM3+ADM4)
0129      RIM=1./ADM
0130      AADM=CABS(ADM)
0131      ARIM=1./AADM
0132      TADM=47.252(AIMAG(ADM),REAL(ADM))*180/PI
0133      TRIM=-TADM
0134      WRITE(6,18)
0135      16 FORMAT(//////41H ***** INPUT ADMITTANCE AND IMPEDANCE *****/11H ADMIT
          TANCE,50X,11H IMPEDANCE )
0136      WRITE(6,18)
0137      WRITE(6,904)ADM,AADM,TADM,RIM,ARIM,TRIM
0138      WRITE(6,27)ADM1,ADM2,ADM3,ADM4
0139      27 FORMAT(2X,E15.8,2X,E15.8/)
0140      18 FORMAT(2(2X,6H REAL ,10X,6H IMAG ,10X,11H MAGNITUDE ,8X,6H PHASE))
0141      904 FORMAT(2(2X,E15.8),2X,E15.8,2X,F6.1,2(2X,E15.8),2X,E15.8,2X,F6.1)
0142      WRITE(6,20)
C
0143      20  COMPUTES CURRENT DISTRIBUTIONS ALONG ANTENNA
0144      20  FORMAT(//////49H ** CURRENT DISTRIBUTION ALONG CONICAL SURFACE **)
0145      DIV=(HT-RS)/KMN
0146      KMN1=KMN+1
0147      CUNC(1)=0.5*ADM
0148      CUND(1)=CUNC(1)/(2*PI*RS*SX)
0149      ACUNC=CABS(CUNC(1))
0150      ACUND=CABS(CUND(1))
0151      TCUNC=ATAN2(AIMAG(CUNC(1)),REAL(CUNC(1)))*180/PI
0152      TCUND=TCUNC
0153      WRITE(6,904)CUNC(1),ACUNC,TCUNC,CUND(1),ACUND,TCUND
0154      DO 905 K5=2,KMN1
0155      HTC=RS+DIV*(K5-1)
0156      CUNC1=-RING*(SIN(HTC-RS)-COS(HTC-RS)*TAN(HT-RS))/ZC
0157      CUNC2=(0.,0.)
0158      DO 800 K6=1,MAXX
0159      CUNC2=CUNC2+PI(2*K6)*A(K6,M1)/(2*K6*(2*K6-1))
0160      800 CONTINUE
0161      CUNC2=CUNC2+COS(HTC-RS)/(COS(HT-RS)*RLTAB)
0162      CUNC3=(0.,0.)
0163      IF(K5.EQ.KMN1)GO TO 866
0164      DO 801 K7=1,NYA
0165      AD3=PK(K7)*GY1ST1(K7,K5)
0166      CUNC3=CUNC3+AD3
0167      RAT=CABS(AD3/CUNC3)
0168      IF(RAT.LT.1.E-02)GO TO 1001
0169      801 CONTINUE
0170      1001 CUNC3=-RING*CUNC3/(120*RLTAB)
0171      866 CUNC4=(0.,0.)
0172      DO 803 K8=1,MAXX
0173      K82=2*K8
0174      CUN4=(0.,0.)
0175      DO 804 K9=1,NYA
0176      CKD=RT(K9)
0177      AD4=P(K9)*GM1CN(K9,K5)*CNT(K9)/FKN((K82-1),CKD)
0178      CUN4=CUN4+AD4
0179      IF((CKD-4.).LT.K82)GO TO 804

```

```

0179      RAT=CABS(AD3/CUN4)
0180      IF(RAT.LT.1.E-03)GO TO 1002
0181      804 CONTINUE
0182      1002 CUNC4=CUNC4-A(K5,M1)*PI(2*KB)/CUN4
0183      RAT1=CABS(CUN4*A(K5,M1)*PI(2*KB)/CUN4)
0184      IF(RAT1.LT.1.E-03)GO TO 1003
0185      803 CONTINUE
0186      1003 CUNC(K5)=CUNC1+CUNC2+CUNC3+CUNC4
0187      CUNC(K5)=CUNC(K5)/(2*PI*HT*SA)
0188      ACUNC=CABS(CUNC(K5))
0189      ACUNC=CABS(CUNC(K5))
0190      TCUNC=ATAN2(AIMAG(CUNC(K5)),REAL(CUNC(K5)))*180/PI
0191      TCUNC=TCUNC
0192      WRITE(6,18)
0193      WRITE(6,904)CUNC(K5),ACUNC,TCUNC,CUNC(K5),ACUNC,TCUNC
0194      WRITE(6,22)K5,CUNC1,CUNC2,CUNC3,CUNC4
0195      22 FORMAT(2X,15/12X,E15.8,2X,E15.8/1)
0196      905 CONTINUE
C      COMPUTES CURRENT DISTRIBUTIONS ON THE SPHERE
0197      WRITE(6,23)
0198      23 FORMAT(///51F ** CURRENT DISTRIBUTION ALONG SPHERICAL SURFACE **)
0199      CUNS1=RIMG*TAN(HT-RS)/ZC
0200      CUNS2=(0.,0.)
0201      DO 501 KM1=1,MAXX
0202      CUNS2=CUNS2+PI(2*KM1)-A(KM1,N1)/(2*KM1*(2*KM1-1))
0203      501 CONTINUE
0204      CUNS2=CUNS2/(COS(HT-RS)-RLTA)
0205      DO 502 KM2=1,NM1
0206      CUB(KM2)=RK(KM2)*C**1ST*(KM2,1)/(SX*SX*DPNL(KM2))
0207      CU*(KM2)=P(KM2)+GMLDP(KM2,1)*DN1(KM2)/(SX*SX*DPNL(KM2))
0208      502 CONTINUE
0209      DO 503 KM3=1,10
0210      IF(KM3.EQ.10)GO TO 504
0211      ITABS=ITAB+10*(KM3-1)
0212      TAPBS=PI*(ITABS-DFB)/180
0213      DFBS=DFB
0214      GO TO 505
0215      504 ITABS=95
0216      DFBS=DFB
0217      TAPBS=PI*(ITABS-DFBS)/180
0218      505 DO 506 KM4=1,NM4
0219      CKD=RT(KM4)
0220      CALL LEGF(ITABS,DFBS,CKD,C,PBP,DFNP,PNH,DPNR,PNL,DPNL)
0221      506 CONTINUE
0222      CUNS3=(0.,0.)
0223      DO 507 KM5=1,NM4
0224      AUB=CUB(KM5)*SIN(TAPBS)**2*DPNL(KM5)
0225      CUNS3=CUNS3+AUB
0226      RAT=CABS(AUB/CUNS3)
0227      IF(RAT.LT.1.E-03)GO TO 508
0228      507 CONTINUE
0229      503 CUNS3=-RIMG*CUNS3/(180*RLTA)
0230      CUNS4=(0.,0.)
0231      DO 509 KM6=1,MAXX
0232      KHE2=2*KM6
0233      CUS4=(0.,0.)
0234      DO 510 KM7=1,NM4
0235      BPD=RT(KM7)

```

```

0236      ADP=CUN(KM7)-(SIN(TAPB5))*+21*DNPL(KM7)/FKN((KM2-1),OPD)
0237      CUS4=CUS4+ADP
0238      IF((OPB-6).LT.12+KMG)GO TO 510
0239      FAF=ABS(ADB/CUS4)
0240      IF(RAT).LT.1.E-03GO TO 511
0241 510 CONTINUE
0242      CUNS1=CUNS4-CUN4*FAF*(M1+PI*(2+KRF6))
0243      RAT1=CABS(CUNS1+KMB,PI*(PI*(2+KMG)/CUNS4)
0244      IF(RAT1).LT.1.E-03GO TO 512
0245 509 CONTINUE
0246 512 CUNS(KM3)+CUNS1+CUNS2-CUNS3+CUNS4
0247      CUN5(KM3)=CUNS(KM7)/(2.+PI*(KRF5)*SIN(TAPB5))
0248      ACUNS=CABS(CUNS(KM3))
0249      ACUN5=CABS(CUN5(KM3))
0250      TACUS=ATAN2(AIMAG(CUNS(KM3)),REAL(CUNS(KM3)))*180/PI
0251      TACUD=TACUS
0252      WRITE(6,18)
0253      WRITE(6,904)CUNS(KM3),ACUNS,TACUS,CUN5(KM3),ACUN5,TACUD
0254      WRITE(6,24)KMB,TAPB,CUNS1,CUNS2,CUNS3,CUNS4
0255      24 FORMAT(2X,15,2X,E15.8/12X,E15.8,2X,E15.8/)
0256 508 CONTINUE
0257      ITAF=-3
0258      WRITE(6,26)
0259      26 FORMAT(///10H ** FAF FIELD **)
0260      DO 201 KFF=1,12
0261      ITAF=ITAF+5
0262      RITAF=ITAF*PI/180
0263      DFF=0.
0264      CALL LEGF1(ITAF,DFF,100,PI,OP1)
0265      FAF(KF)=(0.,0.)
0266      KT=-1
0267      DO 202 KFF=1,13
0268      KT=-KT
0269      FAF(KF)=FAF(KF)+A(KFF,M1)*DPI(2*KFF)*KT/((2*KFF*(2*KFF-1))*HT*SH
1(2*KFF))
0270 202 CONTINUE
0271      FAF(KF)=SIN(RITAF)*FAF(KF)/(REAL(CUN5(1)))
0272      AFARF=CABS(FAF(KF))
0273      TFARF=ATAN2(AIMAG(FAF(KF)),REAL(FAF(KF)))*180/PI
0274      WRITE(6,203)ITAF,FAF(KF),AFARF,TFARF
0275 201 CONTINUE
0276 203 FORMAT(2X,15,2X,E15.8,2(2X,E15.8),2X,F10.4)
0277      CALL LEGF1(ITA,DF,100,PI,OP1)
0278      RRST=0.
0279      DO 678 IRST=1,13
0280      DOWN=CABS(HT*SH*(3+IRST))+2+12*(IRST-1)**(2*IRST)-(4*(IRST-1)
0281      RRST=RRST+CABS(A(IRST,M1))*2/DOWN
0282 678 CONTINUE
0283      RRST=1./RRST*60.
0284      WRITE(6,575)RRST
0285 679 FORMAT(2X,E15.8)
0286      GO TO 3
0287      DEBUG SUBCHK
0288      AT !
0289      END

```

FORTRAN IV G LEVEL 16

GTJRM

DATE = 71110

13/16/39

```

0001      SUBROUTINE GTJRM(ORD,HT,PS,EMN,GMOMP,GMXJP,GMXJ1,GMXJF1,GMXJF1,GMXJF1,GJC
          1JP,GY1ST1,GY1ST2,GM1CM,GM1CMF,GJ1QJ,DEX,IAMI)
C
C
C      THIS SUBROUTINE GENERATES ALL FRACTIONAL ORDER BESSEL'S FUNCTION FOR
C      MODIFIED CONICAL ANTENNA.
C      IF IAMI=1, THE RADIUS OF CENTRAL SPHERE IS GREATER THAN ZERO.
C      IF IAMI=2, IT IS BICONICAL ANTENNA.
C      ORD= ORDER OF BESSEL'S FUNCTION
C      HT = ANTENNA HEIGHT
C      RS=RADIUS OF CENTRAL SPHERE IN ELECTRICAL LENGTH
C      CMOMP = M(HT)/M'(HT)
C      CMXJP = R(HT)/J'(HT)
C      GPMXJ = R(HT)/J(HT)
C      GMXJF1= M(HT)/J'(RS)
C      GPMXJF1= M(HT)/J(RS)
C      GJQJP = J(HT)/J'(HT)
C      GM1OMP=M(RS)/M'(HT)
C      GJ1QJ=J(RS)/J'(HT)
C      GY1ST1=(J(RS)*R(HT)-M(RS)*J(HT))/R'(HT)*J'(RS)
C      GY1ST2=(R'(HT)*J(RS)-J'(HT)*R(RS))/M'(HT)*J'(RS)
C
0002      DIMENSION GTJ(60),DGTJ(60),GTN(60),DGTN(60),BJ(120),DBJ(120),BY(12
          10),DBY(120),GMOMP(60),GMXJP(60),GPMXJ(60),GTR(60),DGTM(60),UTR(5),
          2UTH(5),VTR(5),VTH(5),GMXJF1(60),GPMXJF1(60),GJQJP(60),GY1ST1(50,20)
          3,GY1ST2(60,20),GM1OM(60,20),GM1OMP(60,20),GTRR(5),VTRR(5),GTN1(60)
          4,GTJ1(60),GTN1(60),DGTN1(60),GJ1QJ(60,20)
0003      C=1.E-05
0004      ITEST=0
0005      DEX=0
0006      K=(IFIX(ORD+C)+1)/2
0007      ORD=ORD+0.5
0008      KB=IFIX(ORD)+1
0009      PIC=3.14159265
0010      STB=SQRT(PIC/(2.*RS))
0011      STBU=SQRT(PIC*PS/2.)
0012      STH=SQRT(PIC/(2.*HT))
0013      STHU=SQRT(PIC*HT/2)
0014      SXR=RS/ORD
0015      SXH=HT/ORD
0016      IF(SXH.GE.1..OR.SXR.GE.1.)GO TO 14
0017      ALPHR=ALOG((1.+SQRT(1.-SXR**2))/SXR)
0018      ALPHH=ALOG((1.+SQRT(1.-SXH**2))/SXH)
0019      TXR=SQRT(1-SXR*ASXR)
0020      TXH=SQRT(1-SXH*ASXH)
0021      CXR=1/TXR
0022      CXH=1/TXH
0023      TEST1=ALPHR
0024      TEST2=ALPHH-ALPHR
0025      TEST3=TEST2/2
0026      AU=60/ORD
0027      IF(TEST3=AU)14,15,15
0028      14 CALL BESJ(RS,ORD,BJ,DBJ,1.E-07,120)
0029      CALL BESY(RS,ORD,BY,DBY,1.E-07)
0030      DO=STH*(0.5*BY(KB)+PS*DBY(KB))
0031      BK=STHU*(0.5*BJ(KB)+PS*DBJ(KB))
0032      GTN1(K)=ORD*STBU*BJ(KB)/ON+STHU*BY(KB)
0033      GTJ1(K)=K*STBU*BJ(KB)

```

FORTRAN IV G LEVEL 19

GTJAM

DATE = 71110

18/18/39

```

0034      CALL PESY(HT,CHC,KY,CBY,1.E-07)
0035      CALL PESJ(HT,CHC,FJ,CBJ,1.E-07,IER)
0036      GTJ(K)=HT*CBJ(KC)
0037      DGTJ(K)=ST*HD*(O,ST*BJ(KB)+HT*CBJ(KB))
0038      GTN(K)=ST*BY(KR)
0039      DGTN(K)=ST*HD*(O,ST*BY(KB)+HT*(LEY(KB))
0040      GTM(K)=-EM*GTJ(K)/BN*GTM(K)
0041      DGTM(K)=-DE*DGTJ(K)/BN*DGTN(K)
0042      GMDMP(K)=-D*GMDJ(K)+EM*GTM(K)/(1-DE*DGTJ(K)+BN*DGTN(K))
0043      GMXJP(K)=GTM(K)+DGTJ(K)
0044      GPMXJ1(K)=DGTM(K)+DGTJ(K)
0045      GMXJP1(K)=GTM(K)+BN
0046      GPMXJ11(K)=DGTM(K)+BN
0047      GJBJ(K)=GTJ(K)/DGTJ(K)
0048      GM1CM(K,1)=GTM1(K)/GTM(K)
0049      GJ10J(K,1)=GTJ1(K)/GTJ(K)
0050      GM10MP(K,1)=GTM1(K)/DGTM(K)
0051      GY1ST1(K,1)=(GTJ1(K)+GTM(K)-GTM1(K)+GTJ(K))/GMXJP1(K)
0052      GY1ST2(K,1)=(DGTM(K)+GTJ1(K)-DGTJ(K)+GTM1(K))/GPMXJ11(K)
0053      GO TO 101
0054      15 CXR2=CXR1*CXR
0055      CXH2=CXH1*CXH
0056      ITET=1
0057      UTR(1)=CXR*(3.-5.*CXR2)/24
0058      UTH(1)=CXH*(3.-5.*CXH2)/24
0059      UTR(2)=CXR2*(81.+4CXR2*(-462+385*CXR2))/1152
0060      UTH(2)=CXH2*(81.+4CXH2*(-462+385*CXH2))/1152
0061      UTR(3)=CXR*CXR2*(30375+CXR2*(-369603+CXR2*(765765-425425*CXR2)))/4
114720
0062      UTH(3)=CXH*CXH2*(30375+CXH2*(-369603+CXH2*(765765-425425*CXH2)))/4
114720
0063      VTR(1)=CXR*(-9+7*CXR2)/24
0064      VTH(1)=CXH*(-9+7*CXH2)/24
0065      VTR(2)=CXR2*(-135+CXR2*(594-455*CXR2))/1152
0066      VTH(2)=CXH2*(-135+CXH2*(594-455*CXH2))/1152
0067      VTR(3)=CXR*CXR2*(-425425+CXR2*(451737+CXR2*(-88375+475475*CXR2)))/414720
0068      VTH(3)=CXH*CXH2*(-425425+CXH2*(451737+CXH2*(-88375+475475*CXH2)))/414720
0069      DEJR=1.
0070      DEYR=1.
0071      DEJPR=1.
0072      DEYPR=1.
0073      DEJH=1.
0074      DEYH=1.
0075      DEJPH=1.
0076      DEYPH=1.
0077      JT=1
0078      DU 19 IP=1,3
0079      JT=-JT
0080      CB=ORC*IP
0081      DEJR=DEJR+UTR(IP)/CB
0082      DEJH=DEJH+UTH(IP)/CB
0083      DEYR=DEYR+JT*UTR(IP)/CB
0084      DEYH=DEYH+JT*UTH(IP)/CB
0085      LEJPR=DEJPR+VTR(IP)/IP
0086      LEYPH=DEYPH+VTH(IP)/IP
0087      DEYPR=DEYPR+JT*VTR(IP)/CB

```

FORTRAN IV G LEVEL 1c

GTJNM

DATE = 71110

12/18/39

```

0088      DEYPH=DEYFH*JI*VTH(IP)/CB
0089      15 CONTINUE
0090      GMDMP(K)=HT*(0.5+HT*SINH(ALPHH)*DEJPH/DEJH)
0091      GJBJP(K)=GMDMP(K)
0092      30 A=(0.5*DEJH+HT*SINH(ALPHH)*DEJPH)
0093      B=(0.5*DEJR+RS*SINH(ALPHR)*DEJPR)
0094      DBR=(0.5-RS*SINH(ALPHR)*DEYPR/DEYR)/(0.5+RS*SINH(ALPHR)*DEJPR/DEJR)
0095      1) DBH=(0.5-HT*SINH(ALPHH)*DEYPH/DEYH)/(0.5+HT*SINH(ALPHH)*DEJPH/DEJH)
0096      EXPNT=(ALPHR-ALPHH)-(TANH(ALPHR)-TANH(ALPHH))
0097      EXPNT=EXPNT*CRD
0098      Y2=SQRT(RS/HT)
0099      Y3=SQRT(TANH(ALPHH)/TANH(ALPHR))
0100      Z1=DEJR*(1.-1./DBR)/DEJH
0101      GM10M(K,1)=Y2*Y3*EXP(-EXPNT)*Z1
0102      GJ10J(K,1)=GM10M(K,1)
0102      GM10MP(K,1)=GM10M(K,1)*HT*DEJH/A
0104      GY1ST1(K,1)=RS/(0.5-RS*SINH(ALPHR)*DEYPR/DEYR)
0105      GY1ST2(K,1)=GY1ST1(K,1)
0106      IF(TEST2.GT.AU)GO TO 32
0107      GMXJP(K)=-DEYR*A*(-DBR*EXP(2.*EXPNT)*DEJH/DEJR+DEYH/DEYR)/(2.*ORD*
1TANH(ALPHH))
0108      GPMXJ(K)=-DEYR*A*(-DBR*EXP(2.*EXPNT)*DEJH/DEJR+DEYH*DBH/DEYR)/(2.*
1ORD*TANH(ALPHH))
0109      GO TO 45
0110      32 IDEX=1
0111      GMXJP(K)=1.E+70
0112      GPMXJ(K)=1.E+70
0113      45 IF(TEST3.GT.AU)GO TO 33
0114      GMXJP1(K)=-DEYR*B*SQRT(HT/(RS*TANH(ALPHH)*TANH(ALPHR)))*(-DBR*EXP(
1EXPNT)*DEJH/DEJR+EXP(-EXPNT)*DEYH/DEYR)/(2.*ORD)
0115      GPMXJ1(K)=-DEYR*B*A*(-DBR*EXP(EXPNT)*DEJH/DEJR+EXP(-EXPNT)*DBH*DEY
1H/DEYR)/(2.*SQRT(HT*RS*TANH(ALPHH)*TANH(ALPHR))*ORD*DEJH)
0116      GO TO 101
0117      22 IDEX=2
0118      GMXJP1(K)=-1.E+70
0119      GPMXJ1(K)=-1.E+70
0120      101 IF(IAMI.EQ.1) GO TO 108
0121      DIV=HT/KMN
0122      RSR=0.
0123      GO TO 109
0124      108 DIV=(HT-RS)/KMN
0125      RSR=RS
0126      109 KMN1=KMN+1
0127      DO 103 KIG=2,KMN1
0128      RSR=RSR+DIV
0129      SRR=SQRT(PIC/(2.*RSR))
0130      STBUR=SQRT(PIC*RSR/2)
0131      SXRR=RSR/CRD
0132      IF(SXH.GE.1..OR.SXRR.GE.1.)GO TO 114
0133      ALPHRR=ALOG(1.+SQRT(1.-SXRR**2))/SXRR)
0134      TXRR=SQRT(1.-SXRR*SXRR)
0135      CXRR=1/TXRR
0136      TEST1=ALPHRR
0137      TEST2=ALPHRR-ALPHH
0138      TEST3=TEST2/2
0139      IF(ORD.GT.30.)GO TO 115

```

```

0140      IF (TEST1-AU)114,115,115
0141      114 CALL BESJ(ASR,ORD,BJ,OBJ,1.E-07,IFR)
0142      CALL BESY(RSP,ORD,BY,DBY,1.E-07)
0143      GTM(K)=-DB*STBR*BJ(KB)/EN+STBR*BY(KB)
0144      GTJ(K)=STBR*BJ(KB)
0145      GTN(K)=STBR*BY(KB)
0146      DGTN(K)=STBR*(0.5-BY(KB)+RSP*DBY(KB))
0147      IF (ITET.NE.1)GO TO 31
0148      CALL BESJ(HT,ORD,BY,DBY,1.E-07)
0149      CALL BESJ(HT,ORD,BJ,OBJ,1.E-07,IFR)
0150      GTJ(K)=STHU*BJ(KB)
0151      DGTJ(K)=STHU*(0.5*BJ(KB)+HT*OBJ(KB))
0152      GTN(K)=STHU*BY(KB)
0153      DGTN(K)=STHU*(0.5*BY(KB)+HT*DBY(KB))
0154      GTM(K)=-DB*GTJ(K)/BN+GTN(K)
0155      DGTM(K)=-DB*DGTJ(K)/BN+DGTN(K)
0156      31 GM1OM(K,KTG)=GTM(K)/GTM(K)
0157      GJ1OJ(K,KTG)=GTJ(K)/GTJ(K)
0158      GM1OMP(K,KTG)=GTM(K)/DGTM(K)
0159      GY1ST1(K,KTG)=-((GTM(K)*GTJ(K))*((1.-(GTM(K)/GTN(K))*(GTJ(K)/GTJ(
0160      1(K)))/GMXJ1(K)
      GY1ST2(K,KTG)=-((GTM(K)*DGTJ(K))*((1.-(DGTJ(K)/GTN(K))*(GTJ(K)/DG
      1TJ(K)))/GPMXJ1(K)
0161      GO TO 103
0162      115 CXRR2=CXRR+CXRR
0163      UTRR(1)=CXRR*(3.-5.*(CXRR2)/24
0164      UTRR(2)=CXRR2*(21.+CXRR2*(-4.52+3.85*CXRR2))/1152
0165      UTRR(3)=CXRR+CXRR2*(30375+CXRR2*(-360603+CXRR2*(765745-425425*CXRR
      12)))/414720
0166      VTRR(1)=CXRR*(1-9.7*CXRR2)/24
0167      VTRR(2)=CXRR2*(-135+CXRR2*(594-455*CXRR2))/1152
0168      VTRR(3)=CXRR+CXRR2*(-425425+CXRR2*(451737+0XRR2*(-863575+475475*CX
      1RR2)))/414720
0169      DEJRR=1.
0170      DEJPRR=1.
0171      DEYRR=1.
0172      DEYPRR=1.
0173      JT=1
0174      DO 119 IPP=1,3
0175      JT=-JT
0176      CB=ORD*IPP
0177      DEJRR=DEJRR+UTRR(IPP)/CB
0178      DEYRR=DEYRR+JT*UTRR(IPP)/CB
0179      DEJPRR=DEJPRR+VTRR(IPP)/CB
0180      DEYPRR=DEYPRR+JT*VTRR(IPP)/CB
0181      119 CONTINUE
0182      BR=(0.5-RS*SINH(ALPHR)*DEYPR/DEYR)
0183      EXPNT=(ALPHR-ALPHH)-(TANH(ALPHR)-TANH(ALPHH))
0184      EXPNT=EXPNT*ORD
0185      EXPNTB=(ALPHR-ALPHRR)-(TANH(ALPHR)-TANH(ALPHRR))
0186      EXPNTB=EXPNTB*GRD
0187      Y2=SQRT(RSR/HT)
0188      Y3=SQRT(TANH(ALPHH)/TANH(ALPHRR))
0189      Z1=(DEJRR/DEJH-DEJRR*DEYRR*EXP(-2.*EXPNTB))/(DEJH*DEYR+CBR)
0190      GM1OM(K,KTG)=Y2*Y3*EXP(-EXPNT)*Z1
0191      GJ1OJ(K,KTG)=GM1OM(K,KTG)
0192      GM1OMP(K,KTG)=GM1OM(K,KTG)*HT*DEJH/A
0193      GY1ST1(K,KTG)=SQRT(RSR*RS)*SQRT(TANH(ALPHR)/TANH(ALPHRR))*DEYRR=EX

```

FORTRAN IV G LEVEL 18

GTJNM

DATE = 71110

10/13/39

```

1P(-EXPNTB)/(DB*LEMR)
0194      GYIST2(K,KTC)=GYIST1(K,KTC)
0195      ! 03 CCNT)MUE
0196      QPD=QPD-Q.5
0197      RETURN
0198      END

```

FORTRAN IV G LEVEL 18

CSIMEQ

DATE = 71110

10/19/39

```

0001      SUBROUTINE CSIMEQ (A,M,N,N1)
      C
      C      THIS SUBROUTINE SOLVES SET OF N LINEAR ALGEBRAIC EQUATIONS.
      C
      C
0002      COMPLEX Z,X,A(M,3)
0003      NPN1 = N+ N1
0004      DO 9 I = 1,N
0005      ZI=0.
0006      DO 2 J = 1,N
0007      XI=CABS(A(J,I))
0008      IF (ZI-XI) 1,2,2
0009      1 ZI= XI
0010      I1 = J
0011      2 CONTINUE
0012      IF (ZI) 3,11,2
0013      3 Z = A(I1,I)
0014      A(I1,I) = A(I,1)
0015      IP1 = I + 1
0016      DO 4 L = IP1,NPN1
0017      X = A(I1,L)
0018      A(I1,L) = A(I,L)
0019      4 A(I,L) = X/Z
0020      DO 8 J = 1,N
0021      IF (J-1) 5, 8, 5
0022      5 IF (REAL(A(J,I)) .EQ. 0. .AND. AIMAG(A(J,I)).EQ. 0.) GO TO 9
0023      Z = -A(J,I)
0024      DO 7 L= IP1, NPN1
0025      7 A(J,L) = A(J,L) + Z * A(I,L)
0026      8 CONTINUE
0027      9 CONTINUE
0028      10 RETURN
0029      11 WRITE (6,12)
0030      12 FORMAT      (31H COEFFICIENT MATRIX IS SINGULAR )
0031      RETURN
0032      END

```

FORTRAN IV G LEVEL 18 RTNI DATE = 71110 18/18/39

0001 SUBROUTINE RTNI(X,TA,NMAX,F,DERF,FCT,AST,EPS,IEND,IER,I,RT,DNT)

C
C
C
C
C
C
C

THIS SUBROUTINE SOLVES THE CHARACTERISTIC EQUATION $L_V(\theta) = 0$ FOR A FIXED CONE ANGLE. IT PROVIDES BOTH ROOTS OF $L_V(\theta) = 0$ AND DERIVATIVE OF L_V WITH RESPECT TO $\cos\theta$

```

0002 DIMENSION RT(50),DNT(50)
0003 TAZ=TA/2
0004 TOLF=100.*EPS RTN03870
0005 GO TO N1=1,NMAX,2
0006 X=XST RTN03540
0007 TOL=X RTN03850
0008 CALL FCT(TA,TOL,N1,F,DERF,FP,I)
0009 DO 6 JJ=1,IEND
0010 IF(F)1,7,1 RTN03920
0011 1 IF(DERF)2,8,2 RTN03950
0012 2 DX=F/DERF RTN03980
0013 X=X-DX RTN03990
0014 TOL=X RTN04000
0015 CALL FCT(TA,TOL,N1,F,DERF,FP,I)
0016 TOL=EPS RTN04040
0017 A=ABS(X) RTN04050
0018 IF(A-1.)4,4,3 RTN04000
0019 3 TOL=TOL*A RTN04070
0020 4 IF(ABS(DX)-TOL)5,5,6 RTN04080
0021 5 IF(ABS(F)-TOLF)7,7,6 RTN04090
0022 6 CONTINUE RTN04100
0023 7 K=(N1+1)/2
0024 RT(K)=X+N1
0025 DNT(K)=-2.*COS(TAZ)*COS(TAZ)*FP/DERF
0026 IF((2.-X).LT.0.001)GO TO 12
0027 IF(X.GT.1.8)GO TO 11
0028 XST=IFIX(X*10000.)/10000.
0029 GO TO 10
0030 11 XST=1.999000
0031 10 CONTINUE
0032 IER=NMAX
0033 RETURN
0034 12 IER=N1
0035 RETURN
0036 8 IER=N1
0037 RETURN
0038 END

```

FORTRAN IV G LEVEL 18 FCN DATE = 71110 18/18/39

```

0001 FUNCTION FCN(X,XN)
0002 T=.5*X
0003 Y=1.57079633*XN
0004 FCN=.62661978*(PSIG(XN+1.)*ALOG(SIN(T))+.5772156649)-TAN(Y)
0005 FCN=-FCN
0006 RETURN
0007 END

```


FORTRAN IV G LEVEL 18

LEGF

DATE = 71110

18/18/39

```

0044      KK1=KK-1
0045      KK2=KK-2
0046      KK3=KK-3
0047      XX=XO+FLOAT(KK3)
0048      XXD=XO+KK2
0049      PNP(KK)={(2.*XX+1.)*CXP*PNP(KK1)-XX*PNP(KK2)}/(XX+1)
0050      PNM(KK)={(2.*XX+1.)*CXM*PNM(KK1)-XX*PNM(KK2)}/(XX+1)
0051      DPNP(KK)=XXD*(CXP*PNP(KK)-PNP(KK1))/CXP2
0052      DPNM(KK)=XXD*(CXM*PNM(KK)-PNM(KK1))/CXM2
0053      40 CONTINUE
0054      100 PNL(K)=PNP(NN1)-PNM(NN1)
0055      DPNL(K)=DPNP(NN1)+DPNM(NN1)
0056      PNL(K)=0.5*PNL(K)
0057      DPNL(K)=0.5*DPNL(K)
0058      RETURN
0059      END

```

FORTRAN IV G LEVEL 18

SPYNX

DATE = 71110

18/18/39

```

0001      FUNCTION SPYNX(N,X)
      C
      C
      C      THIS SUBROUTINE GENERATES VALUES FOR SPHERICAL FUNCTIONS OF THE
      C      SECOND KIND.
      C
0002      IF (X .GT. 0.) GO TO 1
0003      SPYNX=0.
0004      WRITE (6,2)
0005      2 FORMAT (78H SIR, SOME THING WRONG WITH YOU ... YOU KNOW THAT THE A
      ARGUMENT SHOULD NOT BE 0)
      RETURN
0006      1 IF (N .EQ. 1) GO TO 3
0007      A=-CCS(X)/X
0008      IF (N .NE. 0) GO TO 3
0009      SPYNX=A
0010      RETURN
0011      3 B=-((COS(X)+X*SIN(X))/X/X
0012      IF (N .NE. 1) GO TO 4
0013      SPYNX=B
0014      RETURN
0015      4 U=1.
0016      DO 5 I=2,N
0017      U=U+2.
0018      C=U*B/X-A
0019      A=B
0020      B=C
0021      5 SPYNX=B
0022      RETURN
0023      END
0024

```

FORTRAN 17 G LEVEL 18

BESY

DATE = 71110

19/18/39

```

0001      SUBROUTINE BESY(X,XN,PY,CBY,D)
      C
      C
      C THIS SUBROUTINE GENERATES FRACTIONAL BESSEL'S FUNCTION OF THE SECOND KIND
      C FOR ARGUMENT LESS THAN 5
      C
0002      DIMENSION BY(50),CBY(50),BYT1(50),BYT2(50),BJT1(50),BJT2(50),BJP(1
0003      10),BJM(10),BYT1(50),BYT2(50)
0004      PI=7.14159265
0005      C=1.E+05
0006      N=FIX(XN+C)
0007      N1=N+1
0008      FN=XN-FLCAT(N)
0009      IF(X.GE.5.0)GO TO 100
0010      CALL BYTERM(X,FN,D,BYT1,BYT2,M)
0011      CALL BJTERM(X,FN,D,BJT1,BJT2,M)
0012      BJP(1)=0.
0013      BJP(2)=0.
0014      BJM(1)=0.
0015      BJM(2)=0.
0016      XTFN=(X/2.)**FN
0017      XTFN1=(X/2.)**(1.+FN)
0018      DO 400 IK=1,M
0019      BJP(1)=BJP(1)+BJT1(IK)
0020      BJP(2)=BJP(2)+BJT2(IK)
0021      400 CONTINUE
0022      BJM(1)=XTFN*BJP(1)
0023      BJM(2)=XTFN1*BJP(2)
0024      DO 401 IH=1,M
0025      BJM(1)=BJM(1)+BYT1(IH)
0026      BJM(2)=BJM(2)+BYT2(IH)
0027      401 CONTINUE
0028      BJM(1)=BJM(1)/XTFN
0029      BJM(2)=BJM(2)/XTFN1
0030      BY(1)=(BJP(1)+COS(FN*PI)-BJM(1))/SIN(FN*PI)
0031      BY(2)=(BJP(2)+COS((1.+FN)*PI)-BJM(2))/SIN((1.+FN)*PI)
0032      CBY(1)=-BY(2)+FN*BY(1)/X
0033      CBY(2)=BY(1)-(1.+FN)*BY(2)/X
0034      IF(M.LE.2) GO TO 101
0035      DO 200 M=3,N1
0036      CRD1=FLCAT(M-1)+FN
0037      CRD2=CRD1-1.
0038      BY(M)=2.*CRD2*BY(M-1)/X-BY(M-2)
0039      CBY(M)=BY(M-1)-CRD1*BY(M)/X
0040      200 CONTINUE
0041      101 RETURN
0042      100 CALL BESYC(X,XN,CBY,D,IER)
0043      RETURN
      END

```

FORTRAN IV G LEVEL 18

BESYG

DATE = 71110

18/18/39

```

0001      SUBROUTINE BESYG(X,XN,BY,DBY,D,IER)
C
C      THIS SUBROUTINE GENERATES VALUES FOR FRACTIONAL ORDER BESSEL S FUNCT-
C      TIONS OF THE SECOND KIND WITH ARGUMENT GREATER THAN 5.
C
0002      DIMENSION BY(50),DBY(50),BYE1(50),BYE2(50)
0003      PI=3.14159265
0004      C=1.E-05
0005      N=IFIX(XN+C)
0006      N1=N+1
0007      FN=XN-FLOAT(N)
0008      CALL BYTERG(X, FN, BYE1, BYE2, MA)
0009      XE1=1./(2*X)
0010      XE12=XE1**2
0011      BY11=1.
0012      BY12=BYE1(2)*XE1
0013      BY21=1.
0014      BY22=BYE2(2)*XE1
0015      JT=1
0016      DO 400 IK=1, MA
0017      JT=-JT
0018      IK2=2*IK
0019      BY11=BY11+JT*BYE1(IK2+1)*XE12**IK
0020      BY12=BY12+JT*BYE1(IK2+2)*XE1*XE12**IK
0021      BY21=BY21+JT*BYE2(IK2+1)*XE12**IK
0022      BY22=BY22+JT*BYE2(IK2+2)*XE1*XE12**IK
0023      400 CONTINUE
0024      AG1=X-C.25*(2*FN+1)*PI
0025      AG2=X-C.25*(2*(1+FN)+1)*PI
0026      BY(1)=(SIN(AG1))*BY11+COS(AG1)*BY12)*SQRT(2./(|PI*X|))
0027      BY(2)=(SIN(AG2)*BY21+COS(AG2)*BY22)*SQRT(2./(|PI*X|))
0028      DBY(1)=-BY(2)+FN*BY(1)/X
0029      DBY(2)=BY(1)-(1.+FN)*BY(2)/X
0030      IF(N1.LE.2) GO TO 101
0031      DO 200 M=3, N1
0032      ORD1=FLOAT(M-1)+FN
0033      ORD2=ORD1-1.
0034      BY(M)=2.*ORD2*BY(M-1)/X-BY(M-2)
0035      DBY(M)=BY(M-1)-ORD1*BY(M)/X
0036      200 CONTINUE
0037      101 RETURN
0038      END

```

FORTRAN IV G LEVEL 18

DPSI

DATE = 71110

18/18/39

```

0001      FUNCTION DPSI(Z)
0002      X=Z-1.5
0003      DPSI=0.93480200*X**1-C.82878804*X**10.70450294*X**(-0.57956094*X*(0.4
16426845+X*(-0.35206372+X*(0.26484460+X*(-0.27630530+C.21785378*X)
1))))))
0004      RETURN
0005      END

```

FORTRAN IV G LEVEL 18

PSI

DATE = 71110

18/18/39

```

0001      FUNCTION PSI(Z)
0002      X=Z-1.5
0003      PSI=0.36489924E-01*X*(0.93480092+X*(-0.41439837+X*(0.23492277+X*(-
10.14479804+X*(0.91158802E-01+X*(-0.59422362E-01+X*(0.49350996E-01-
10.32681592E-01*X))))))
0004      RETURN
0005      END

```

FORTTRAN IV G LEVEL 18 BESJG DATE = 71110 18/18/39

```

0001      SUBROUTINE BESJG(X,XN,BJT)
      C
      C
      C      THIS SUBROUTINE GENERATES VALUES FOR FRACTIONAL ORDER BESSEL'S FUNC-
      C      TIONS OF THE FIRST KIND WITH ARGUMENT GREATER THAN 5.
      C
      C
0002      DIMENSION BJE1(50)
0003      PI=3.14159265
0004      C=1.E-05
0005      N=IFIX(XN+C)
0006      NI=N+1
0007      FN=XN-FLCAT(N)
0008      CALL BJTERG(X,FN,BJE1,NA)
0009      XE1=1./(2*X)
0010      XE2=XE1**2
0011      BJ11=1.
0012      BJ12=BJE1(2)*XE1
0013      JT=1
0014      DO 400 IK=1,NA
0015      JT=-JT
0016      IK2=2*IK
0017      BJ11=BJ11+JT*BJE1(IK2+1)*XE2**IK
0018      BJ12=BJ12+JT*BJE1(IK2+2)*XE1*XE2**IK
0019      400 CONTINUE
0020      AG=X-C.25*(2.*FN+1)*PI
0021      BJT=(COS(AG)*BJ11-SIN(AG)*BJ12)*SQRT(2./(PI*X))
0022      RETURN

```

FORTTRAN IV G LEVEL 18 PSIG DATE = 71110 18/18/39

```

0001      FUNCTION PSIG(X)
0002      IF (X-2.) 10,11,12
0003      10 PSIG=PSI(X)
0004      RETURN
0005      11 PSIG=-0.4227843351
0006      RETURN
0007      12 I=IFIX(X)-1
0008      Z=X-FLCAT(I)
0009      PSIG=PSI(Z)+SUMP(Z-1.,I)
0010      RETURN
0011      END

```

FORTTRAN IV G LEVEL 18 DPSIG DATE = 71110 18/18/39

```

0001      FUNCTION DPSIG(X)
0002      IF (X-2.) 10,11,12
0003      10 DPSIG=DPSI(X)
0004      RETURN
0005      11 DPSIG=0.6449240668
0006      RETURN
0007      12 I=IFIX(X)-1
0008      Z=X-FLCAT(I)
0009      DPSIG=DPSI(Z)-SUMPP(Z-1.,I)
0010      RETURN
0011      END

```

FORTRAN IV G LEVEL 18 BYTERG DATE = 71110 18/18/39

```

0001      SUBROUTINE BYTERG(X,FA,BYE1,BYE2,MA)
0002      DIMENSION BYE1(50),BYE2(50)
0003      MA=1+10/ALOG(X)
0004      BYE1(1)=1.
0005      BYE2(1)=1.
0006      MA2=MA*2+2
0007      DO 100 I=2,MA2
0008      I1=I-1
0009      I2=I-2
0010      XI1=FLCAT(I1)
0011      XI2=FLCAT(I2)
0012      BYE1(I)=BYE1(I1)*(0.5+FN-XI1)*(0.5+FN+XI2)/XI1
0013      BYE2(I)=BYE2(I1)*(1.5+FN-XI1)*(1.5+FN+XI2)/XI1
0014      100 CONTINUE
0015      RETURN
0016      END

```

FORTRAN IV G LEVEL 18 BJTERM DATE = 71110 18/18/39

```

0001      SUBROUTINE BJTERM(X,FA,U,PI,MN)
0002      DIMENSION BT(50)
0003      MJ=FIX(1.6*X+10.)
0004      CALL CMPMA(1.,FA,GX,IER)
0005      XE2=(X/2.)**2
0006      JT=1
0007      BT(1)=1./GX
0008      DO 20 MN=2,MJ
0009      JT=-JT
0010      MN1=MN-1
0011      XMN=FLCAT(MN)
0012      XMN1=FLCAT(MN1)
0013      BT(MN)=JT*ABS(BT(MN1))*XE2/(XMN1*(XMN1+FN))
0014      IF(ABS(BT(MN)).LE.0) GO TO 10
0015      20 CONTINUE
0016      10 RETURN
0017      END

```

FORTRAN IV G LEVEL 18 BJTERG DATE = 71110 18/18/39

```

0001      SUBROUTINE BJTERG(X,FA,BJE1,MA)
0002      DIMENSION BJE1(50)
0003      MA=1+10/ALOG(X)
0004      BJE1(1)=1.
0005      MA2=MA*2+2
0006      DO 100 I=2,MA2
0007      I1=I-1
0008      I2=I-2
0009      XI1=FLCAT(I1)
0010      XI2=FLCAT(I2)
0011      BJE1(I)=BJE1(I1)*(0.5+FN-XI1)*(0.5+FN+XI2)/XI1
0012      100 CONTINUE
0013      RETURN
0014      END

```

```
FORTRAN IV G LEVEL 18          FACK          DATE = 71110          18/18/39

0001          FUNCTION FACK(K)
0002          FACK=1.
0003          DO 13 J=1,K
0004          XJ=J
0005          13 FACK=FACK*XJ
0006          RETURN
0007          END
```

```
FORTRAN IV G LEVEL 18          FACKP          DATE = 71110          18/18/39

0001          FUNCTION FACKP(X,K)
0002          FACKP=1.
0003          IF(K.LE.1) GO TO 12
0004          K1=K-1
0005          DO 11 I=1,K1
0006          X1=I
0007          FACKP=FACKP*(X**2-X1**2)
0008          11 CONTINUE
0009          12 FACKP=FACKP*X*(X+K)
0010          RETURN
0011          END
```

```
FORTRAN IV G LEVEL 18          FCTO          DATE = 71110          18/18/39

0001          FUNCTION FCTO(TA,X,N1)
0002          Y=X+1.
0003          Y=1.57079633*(Y+1.)
0004          A=TA/2
0005          FCTO=YAN(Y)-0.63661978*(ALOG(SIN(A))+0.577215665+PSIG(XN+1.))
0006          RETURN
0007          END
```

```
FORTRAN IV G LEVEL 18          DFCTO          DATE = 71110          18/18/39

0001          FUNCTION DFCTO(TA,X,N1)
0002          XN=X+N1
0003          Y=1.57079633*(X+1.)
0004          A=TA/2
0005          DFCTO=-0.63661978*DPSIG(XN+1.)+1.57079633/COS(Y)**2
0006          RETURN
0007          END
```

```
FORTRAN IV G LEVEL 18          SUMP          DATE = 71110          18/18/39

0001          FUNCTION SUMP(X,K)
0002          SUMP=C.
0003          DO 13 J=1,K
0004          X1=J
0005          13 SUMP=SUMP+1./(X+X1)
0006          RETURN
0007          END
```

FORTRAN IV G LEVEL 15 SUMS DATE = 71110 18/18/39

```

0001      SUBROUTINE SUMS(FN,I,SUM1,SUM2)
0002      DIMENSION SUM1(50),SUM2(50)
0003      XO=1.+FN
0004      XI=XO+1.
0005      SUM1(1)=0.
0006      SUM2(1)=0.
0007      DO 20 J=2,I
0008          J1=J-1
0009          J2=J-2
0010          FJ1=FLOAT(J1)
0011          FJ2=FLOAT(J2)
0012          SUM1(J)=SUM1(FJ1)-2./FJ1+1./(XO+FJ1)-1./(XO-FJ2)
0013          SUM2(J)=SUM2(FJ1)-2./FJ1+1./(X1+FJ1)-1./(X1-FJ2)
0014      20 CONTINUE
0015      RETURN
0016      END

```

FORTRAN IV G LEVEL 13 SUMM DATE = 71110 18/18/39

```

0001      FUNCTION SUMM(X,K)
0002      SUMM=0.
0003      K1=K+1
0004      DO 13 J=1,K1
0005          J1=J-1
0006          XJ1=XJ1
0007      13 SUMM=SUMM+1./X-XJ1
0008      RETURN
0009      END

```

FORTRAN IV G LEVEL 15 SUMNS DATE = 71110 18/18/39

```

0001      SUBROUTINE SUMNS(TA,X,N1,I,SUMN,SUMND)
0002      DIMENSION SUMN(50),SUMND(50)
0003      PIC=3.14159265
0004      XN=X+N1
0005      FC=FCFC(TA,X,N1)
0006      DFC=DFCFC(TA,X,N1)
0007      DO 20 M=1,I
0008          M1=M-1
0009          SUMN(M)=(FC*PIC+2*SUM(M)-SUMP(XN,M)+SUMX(XN,M1))
0010          SUMND(M)=(SUMN(XN,M1)+SUMP(XN,M))*SUMN(M)+(DFC*PIC+SUMFP(XN,M)-SUM
0011      1XX(XN,M1))
0012      20 CONTINUE
0013      RETURN
0014      END

```

FORTRAN IV G LEVEL 13 SUM DATE = 71110 18/18/39

```

0001      FUNCTION SUM(K)
0002      SUM=0.
0003      DO 13 J=1,K
0004          XJ=J
0005      13 SUM=SUM+1./XJ
0006      RETURN
0007      END

```

```

FORTRAN IV G LEVEL 18                                BFO                                DATE = 71110                                18/18/39

0001          FUNCTION BFO(X)
0002          IF (X=3.) 1,1,2
0003          1 Y=X*X/9.
0004          BFO=1.+Y*(-2.2459997+Y*(1.2656208+Y*(-.3163866+Y*(.0444479+Y*(-.00
139444+.00021*Y))))))
0005          RETURN
0006          2 Z=3./X
0007          FO=.79788456+Z*(-.0000077+Z*(-.0056274+Z*(-.00009512+Z*(.00157237
1+Z*(-.00072809+.00014476))))))
0008          TO=X-.78539816+Z*(-.0+166397+Z*(-.00003954+Z*(.00262573+Z*(-.00054
11291+Z*(-.00027030+.00013558*Z))))))
0009          BFO=FO*CCS(TO)/SQRT(X)
0010          RETURN
0011          END

```

```

FORTRAN IV G LEVEL 18                                BFI                                DATE = 71110                                18/18/39

0001          FUNCTION BFI(X)
0002          IF (X=3.) 1,1,2
0003          1 Y=X*X/9.
0004          BFI=X*(.5+Y*(-.56249985+Y*(.21093573+Y*(-.03954289+Y*(.00443319+Y*
1(-.00031761+Y*.00001109))))))
0005          RETURN
0006          2 Z=3./X
0007          F1=.79788456+Z*(.00000156+Z*(.01659667+Z*(.00017105+Z*(-.00249511+
1Z*(.00112452-.00020033*Z))))))
0008          T1=X-.78539816+Z*(-.00000120+Z*(.00005050+Z*(.00262573+Z*(.0007434
18+Z*(.00079824-.00029166))))))
0009          BFI=F1*CCS(T1)/SQRT(X)
0010          RETURN
0011          END

```

```

FORTRAN IV G LEVEL 18                                SUMMM                                DATE = 71110                                18/18/39

0001          FUNCTION SUMMM(X,K)
0002          SUMMM=0.
0003          N1=K+1
0004          DO 13 J=1,K1
0005          J1=J-1
0006          XJ=XJ1
0007          13 SUMMM=SUMMM+1./(X-XJ1)**2
0008          RETURN
0009          END

```

```

FORTRAN IV G LEVEL 18                                SUMPP                                DATE = 71110                                18/18/39

0001          FUNCTION SUMPP(X,K)
0002          SUMPP=0
0003          DO 10 J=1,K
0004          XI=J
0005          10 SUMPP=SUMPP+1./(X+XI)**2
0006          RETURN
0007          END

```

FORTRAN IV G LEVEL 18

GAMMA

DATE = 71110

18/18/39

```

0001      SUBROUTINE GAMMA (XX,CY,IER)
0002      IF (XX-57.16,6,4
0003      4 IER=?
0004      GX=1.E+75
0005      RETURN
0006      6 X=XX
0007      ERR=1.0E-06
0008      IEP=0
0009      GX=1.
0010      IF (X-2.0)50,50,15
0011      10 IF (X-2.0)110,110,15
0012      15 X=X-1.0
0013      GX=GX*X
0014      GO TO 10
0015      50 IF (X-1.0)60,120,110
0016      60 IF (X-ERR)62,62,80
0017      62 Y=FLCAT (INT (X))-X
0018      IF (ABS (Y)-ERR)70,100,64
0019      64 IF (1.0-Y-ERR)70,120,70
0020      70 IF (X-1.0)80,80,110
0021      80 GX=GX/X
0022      X=X+1.
0023      GO TO 70
0024      110 Y=X-1.0
0025      GY=1.04Y*(-0.57730176+Y*(0.98585399+Y*(-0.87642182+Y*(0.83282124+Y*
1(-0.5684729+Y*(0.25482045+Y*(-0.0514993))))))
0026      GX=GX*GY
0027      120 RETURN
0028      120 IER=1
0029      RETURN
0030      END

```

FORTRAN IV G LEVEL 18

FCT

DATE = 71110

18/18/39

```

0001      SUBROUTINE FCT (TA,X,N1,F,DERF,FP,I)
0002      DIMENSION TERMN(50),SUMN(50),SUMND(50)
0003      PI=3.14159265
0004      FP=0.
0005      CALL TERMNS (TA,X,N1,TERMN,I)
0006      CALL SUMNS (TA,X,N1,I,SUMN,SUMND)
0007      F=FCTC (TA,X,N1)
0008      DERF=DFCTC (TA,X,N1)
0009      DO 40 M=1,I
0010      F=F+TERMN(M)*SUMN(M)/PI
0011      DERF=DERF+TERMN(M)*SUMND(M)/PI
0012      FP=FP-(TERMN(M)*(N*SUMN(M)-1))
0013      40 CONTINUE
0014      FP=(1.+FP)/PI
0015      50 RETURN
0016      END

```

```
FORTRAN IV G LEVEL 18          TERMS          DATE = 71110          18/18/39

0001      SUBROUTINE TERMS(X, FN, D, TERM1, TERM2, I)
0002      DIMENSION TERM1(50), TERM2(50)
0003      T=.5*X
0004      S=SIN(T)**2
0005      X0=1.+FN
0006      X1=X0+1.
0007      TERM1(1)=1.
0008      TERM2(1)=1.
0009      JT=1
0010      DO 10 I=2,50
0011      JT=-JT
0012      I1=I-1
0013      TERM1(I)=JT*S**I1*FACKP(X0, I1)/FACK(I1)**2
0014      TERM2(I)=JT*S**I1*FACKP(X1, I1)/FACK(I1)**2
0015      IF (ABS(TERM2(I))-D) 9, 10, 10
0016      10 CONTINUE
0017      I=50
0018      RETURN
0019      9 I=I
0020      RETURN
0021      END
```

```
FORTRAN IV G LEVEL 18          TERMNS          DATE = 71110          18/18/39

0001      SUBROUTINE TERMNS(TA, X, N1, TERMN, I)
0002      DIMENSION TERMN(50)
0003      XN=X+N1
0004      T=0.5*TA
0005      S=SIN(T)**2
0006      JT=1
0007      DO 10 I=1,50
0008      JT=-JT
0009      TERMN(I)=JT*S**I*FACKP(XN, I)/FACK(I)**2
0010      IF (ABS(TERMN(I))-1.E-07) 9, 10, 10
0011      10 CONTINUE
0012      I=50
0013      RETURN
0014      9 I=I
0015      RETURN
0016      END
```

```
FORTRAN IV G LEVEL 18          FCN          DATE = 71110          18/18/39

0001      FUNCTION FCN(X, XN)
0002      T=.5*X
0003      Y=1.57079633*XN
0004      FCN=-.63661978*(PSIG(XN+1.)+ALOG(SIN(T))+.5772156649)-TAN(Y)
0005      FCN=-FCN
0006      RETURN
0007      END
```

FORTRAN IV G LEVEL 18

BESJ

DATE = 71110

18/18/39

```

0001      SUBROUTINE BESJ(X,XN,BJ,OBJ,C,IER)
      C
      C
      C      THIS SUBROUTINE GENERATES VALUES FOR FRACTIONAL ORDER BESSEL'S FUNCT-
      C      TIONS OF THE FIRST KIND.
      C
0002      DIMENSION BJ(100),OBJ(100),OT(50),BJE1(50)
0003      PI=3.14159265
0004      C=5.E-05
0005      N=IFIX(XN/C)
0006      N1=N+1
0007      N2=N+2
0008      FN=XN-FLOAT(N)
0009      20 IF(X)20,30,25
0010      30 IER=2
0011      RETURN
0012      29 IF(X<15.)32,32,34
0013      32 NTEST=40.+10.*X-X** 2/3
0014      GO TO 26
0015      34 NTEST=90.+X/2.
0016      35 IF(N1-NTEST)40,36,25
0017      38 IER=4
0018      RETURN
0019      40 IF(X.GE.6.C) GO TO 405
0020      CALL BJTFRM(X,FN,C,BT,MN)
0021      BJT=0.
0022      DO 400 IK=1,MN
0023      BJT=BJE1(1+IK)
0024      400 CONTINUE
0025      BJT=(X/2.)*FN*BJT
0026      GO TO 35
0027      405 CALL BESJG(X,FN,BJT)
0028      35 BPREV=0.
0029      70 MMAX=NTEST
0030      NZERC=N+10
0031      100 DO 190 K=NZERC,MMAX,5
0032      FM=1.0E-70
0033      FM=.0
0034      130 M2=M-2
0035      M1=M-1
0036      210 DO 180 K=1,M2
0037      MK=M-K
0038      MK1=MK-1
0039      XMK=FLOAT(MK)+FN
0040      BJ(MK)=2.*XMK*FM1/X-FM
0041      FM=FM1
0042      160 FM1=BJ(MK)
0043      BJ(1)=2.*(1.+FN)*FM1/X-FM
0044      ALPHAT=BJ(1)/BJT
0045      DO 301 J=1,N2
0046      BJ(J)=BJ(J)/ALPHAT
0047      301 CONTINUE
0048      IF(ABS(BJ(MN))-BPREV)-ABS(C*BJ(N1))201,201,190
0049      BPREV=BJ(MN)
0050      IER=0
0051      GO TO 200
0052      201 IER=0

```

BESC0670
BESC0480

BESC0500

BESC0520

BESC0540
BESC0550

BESC0770
BESC0630

BESC0850

BESC0870

FORTRAN IV G LEVEL 18

BESJ

DATE = 71110

19/18/39

```

0053      200 BRJ(1)=-BJ(2)+FN*BJ(1)/X
0054      IF(N1-2)GOO,401,401
0055      401 DC 420 LL=2,M2
0056          LL1=LL-1
0057          CRD1=FLCAT(LL1)+FN
0058      BRJ(LL1)=BJ(LL1)-CRD1*BJ(LL1)/X
0059      420 CONTINUE
0060      500 RETURN
0061      END

```

FORTRAN IV G LEVEL 18

TDSUM

DATE = 71110

18/18/39

```

0001      SUBROUTINE TDSUM(ITA,CF,M,ZDSU)
      C
      C
      C      THIS SUBROUTINE GENERATES VALUES FOR CPK
      C      HALF CONE ANGLE=IFIX(CPK+1)-DF
      C
      C
0002      DIMENSION PI(100),DPI(100)
0003      DOUBLE PRECISION TER(200),DS(200),TA,TA2,SX2,DSU,PIC
0004      PIC=0.3141592653589793
0005      TA=(IYA-DF)*PIC/180
0006      TA2=TA/2
0007      M1=M+1
0008      M2=M+2
0009      M3=M+3
0010      SX2=DSIN(TA2)**2
0011      TER(1)=C.10+01
0012      JT=1
0013      DO 20 I=2,M1
0014          JT=-JT
0015          TER(I)=JT*DABS(TER(I-1))*(M-I+2)*(M+I-1)*SX2/((I-1)*(I-1))
0016      20 CONTINUE
0017      DO 40 I1=M1,M2
0018          TER(I1)=C.0+01
0019      40 CONTINUE
0020      DS(1)=C.10+01
0021      DO 10 I1=2,M2
0022          DS(I1)=C.0+01
0023      DO 11 I2=1,I1
0024          DS(I1)=DS(I1)+TER(I2)*TER(I1-I2+1)/I1
0025      11 CONTINUE
0026      10 CONTINUE
0027      DSU=C.0+01
0028      DO 30 KK=1,M2
0029          DSU=DSU+DS(KK)
0030      30 CONTINUE
0031      CALL LEGFI(ITA,CF,M1,PI,DPI)
0032      ZDSU=2*(-DSIN(TA)**2+PI(M1)*DPI(M1)+2.*M*(M+1)*SX2*DSU)
0033      RETURN
0034      END

```

FORTRAN IV C LEVEL 13

SPJNX

DATE = 71110

18/18/39

```

0001      SUBROUTINE SPJNX(L,X,SB)
      C
      C      THIS SUBROUTINE GENERATES SPHERICAL BESSEL'S FUNCTIONS OF THE FIRST
      C      KIND.
      C
0002      DIMENSION SB(L)
0003      DO 20 NN=1,L
0004      N=NN-1
0005      IPX=0
0006      PIC=3.14159265
0007      TEST1=X-PIC
0008      TEST2=X-2+PIC
0009      30 IF (X.NE.0.)GO TO 1
0010      IF (X.EQ.0) GO TO 2
0011      SB(NN)=0.
0012      GO TO 20
0013      2 SB(NN)=1.
0014      GO TO 20
0015      1 IF (N.GE.2.AND.X.LT.1.) GO TO 10
0016      IF (N.EQ.1) GO TO 3
0017      A=SYN(X)/X
0018      IF (N.NE.0) GO TO 4
0019      SB(NN)=A
0020      GO TO 20
0021      4 IF (X.GE.FLOAT(N)) GO TO 3
0022      IF (ABS(TEST1).LE.1.E-05.OR.ABS(TEST2).LE.1.E-05)GO TO 45
0023      GO TO 11
0024      45 A=(SIN(X)-X*COS(X))/X/X
0025      IPX=1
0026      46 N1= 3.+(0.5+EXP(-FLOAT(N-2)/4.))*X
0027      M=N-N1
0028      U=2**M+5
0029      FN=1.E-30
0030      FN1=0.
0031      N1=N1+1
0032      DO 5 I=1,N1
0033      U=U-2.
0034      FN=U*FN/X-FN1
0035      FN1=FN
0036      5 FN=FN
0037      SB(NN)=FN
0038      IF (IPX.NE.1)GO TO 55
0039      N=N-1
0040      55 DO 6 I=1,N
0041      U=U-2.
0042      FN=U*FN/X-FN1
0043      FN1=FN
0044      6 FN=FN
0045      SB(NN)=SB(NN)**2/FN
0046      GO TO 20
0047      3 B=(SIN(X)-X*COS(X))/X/X
0048      IF (N.NE.1) GO TO 7
0049      SB(NN)=B
0050      GO TO 20
0051      7 U=1.
0052      DO 8 I=2,N

```

FORTRAN IV G LEVEL 10

SPJNX

DATE = 71110

18/18/39

```

0053      U=U+2.
0054      FN1=U*B/X-A
0055      A=B
0056      B=FN1
0057      SB(MN)=B
0058      GO TO C 20
0059 10  A=1.
0060      B=1.
0061      X2=-X*X/2.
0062      P1=0.
0063      P2=P1+1
0064 11  B1=B1+1.
0065      P2=P2+2.
0066      B=B*X2/P1/P2
0067      A=A+B
0068      IF (ABS(B/A) .GE. 1.E-6) GO TO 11
0069      B=1.
0070      DO 12 1=1,N
0071      B=B+2.
0072 12  A=A/B
0073      SB(MN)=A*X**N
0074 20  CONTINUE
0075      RETURN
0076      END

```

FOPTRAN IV G LEVEL 10

BJTERY

DATE 71110

18/18/39

```

0001      SUBROUTINE BJTERY(X,FN,G,BJT1,BJT2,MN)
0002      DIMENSION BJT1(50),BJT2(50)
0003      MJ=IFIX(1.6*X+10.)
0004      CALL GMPXA(1.,FN,GX,IER)
0005      XE2=(X/2.)**2
0006      JT=1
0007      BJT1(1)=1./GX
0008      BJT2(1)=1./(GX*(1.+FN))
0009      DO 20 MN=2,MJ
0010      JT=-JT
0011      MN1=MN-1
0012      MN2=MN-2
0013      XMN=FLOAT(MN)
0014      XMN1=FLOAT(MN1)
0015      XMN2=FLOAT(MN2)
0016      BJT1(MN)=JT*ABS(BJT1(MN1))*XE2/(XMN1*(XMN1+FN))
0017      BJT2(MN)=JT*ABS(BJT2(MN1))*XE2/(XMN1*(XMN1+FN))
0018      IF (ABS(BJT1(MN)).LE.C.AND.ABS(BJT2(MN)).LE.C) GO TO 10
0019 20  CONTINUE
0020 10  RETURN
0021      END

```

FORTRAN IV G LEVEL 18

LEGFI

DATE = 71110

18/18/39

```

0001      SUBROUTINE LEGFI(NX,DF,N,PI,DPI)
0002      DIMENSION SB(6),PI(50),DPI(50)
0003      PIC=3.14159265
0004      G=PIC/180
0005      IDX=0
0006      IF(NX.EQ.180.OR.NX.GE.0)GO TO 305
0007      IF(NX-90)2,2,1
0008      1  IDX=1
0009      NX=180-NX
0010      X=(1X+DF)*G
0011      GO TO 3
0012      2  X=(1X-DF)*G
0013      IF(ABS(X).LE.1.E-02)GO TO 305
0014      3  CX=COS(X)
0015      X2=X*X
0016      PI(1)=1.
0017      DPI(1)=0.
0018      PI(2)=CX
0019      DPI(2)=1.
0020      DO 30 L=3,6
0021      L1=L-1
0022      L2=L-2
0023      FL1=FLOAT(L1)
0024      FL2=FLOAT(L2)
0025      PI(L)=(2.*FL2+1.)*CX*PI(L1)-FL2*PI(L2))/(FL2+1.)
0026      DPI(L)=L1*(CX*PI(L)-PI(L1))/(CX**2-1.)
0027      30  CONTINUE
0028      IF(N.LE.6)GO TO 103
0029      CALL SPJNX(4,X,SB)
0030      PH2=SB(2)/(24.*SB(1))
0031      PH3=SB(3)/(24.*SB(1))
0032      PH4=SB(4)/(192.*SB(1))
0033      IF(ABS(X)-0.02)13,13,14
0034      13  A0=SQRT(1.+X2*(1./5.+7.*X2/360.))
0035      GO TO 15
0036      14  A0=SQRT(X/SIN(X))
0037      15  A1=-.5*A0*PH2
0038      A2=A0*3.*(-.5*PH2+.375*PH2**2)
0039      A3=A0*15.*(-.5*PH4+.75*PH2*PH2-.3125*PH2**3)
0040      DO 40 M=7,N
0041      M1=M-1
0042      M2=M-2
0043      FM1=FLOAT(M1)
0044      FM2=FLOAT(M2)
0045      XM=FLOAT(M-1)
0046      XN=XN+.5
0047      XX=XN*X
0048      PI(M)=DPI(XX)*(A0-A2/XN**2-4.*A2/(X*XN**4))+DPI(XX)*(A1/XN**2.*A2/(
0049      1X*XN**4)+A3*(8./XN**2-1.)/XN**3)
0050      DPI(M)=M1*(CX*PI(M)-PI(M1))/(CX**2-1.)
0051      40  CONTINUE
0052      101 IF(IDX.NE.1)GO TO 103
0053      JT=1
0054      KT=-1
0055      NX=180-NX
0056      DO 102 K=1,N
0057      JT=-JT
0058      KT=-KT

```

FORTRAN IV G LEVEL 18

LECFI

DATE = 71110

18/18/39

```

0058      PI(K)=KT*PI(K)
0059      DPI(K)=JT*DPI(K)
0060      102 CONTINUE
0061      GO TO 103
0062      305 DO 304 IL=1,N
0063      PI(IL)=1.
0064      304 CONTINUE
0065      DPI(1)=0.
0066      DPI(2)=1.
0067      DPI(3)=2.
0068      DO 303 IO=1,N
0069      DPI(IO)=(IO-1)*(DPI(IO-1)-PI(IO))/(IO-2)
0070      303 CONTINUE
0071      IF(IIX.NE.180)GO TO 103
0072      JS=1
0073      KS=-1
0074      DO 306 KP=1,N
0075      JS=-JS
0076      KS=-KS
0077      PI(KP)=KS*PI(KP)
0078      DPI(KP)=JS*DPI(KP)
0079      306 CONTINUE
0080      103 RETURN
0081      END

```

FORTRAN IV G LEVEL 18

BYTERM

DATE = 71110

18/18/39

```

0001      SUBROUTINE BYTERM(X,FN,D,BYT1,BYT2,MM)
0002      DIMENSION BYT1(50),BYT2(50)
0003      MJ=1FIX(10.+SQRT(1.+3.*X*X))
0004      CALL GMMMA(1,-FN,GX,IER)
0005      XE2=(X/2.)**2
0006      JT=1
0007      BYT1(1)=1./GX
0008      BYT2(1)=-FN/GX
0009      DO 20 MM=2,MM
0010      JT=-JT
0011      MM1=MM-1
0012      MM2=MM-2
0013      XMM=FLOCAT(MM)
0014      XMM1=FLOCAT(MM1)
0015      XMM2=FLOCAT(MM2)
0016      BYT1(MM)=JT*ABS(BYT1(MM1))*XE2/(XMM1*(XMM1-FN))
0017      BYT2(MM)=JT*ABS(BYT2(MM1))*XE2/(XMM1*ABS(XMM2-FN))
0018      IF(ABS(BYT1(MM)).LE.C.AND.ABS(BYT2(MM)).LE.D) GO TO 10
0019      20 CONTINUE
0020      10 RETURN
0021      END

```

FORTRAN IV G LEVEL 18

SPHNX

DATE = 71110

18/18/79

```

0001      SUBROUTINE SPHNX(L,X,SH,DSH,DSOS)
C          THIS SUBROUTINE GENERATES VALUES FOR HANKEL'S FUNCTIONS.
0002      COMPLEX SH(50),DSH(50),DSOS(50)
0003      DIMENSION SB(50),SY(50),VTS(5),UTS(5)
0004      CALL SPJAX(L,X,SB)
0005      CALL SPYAX(L,X,SY)
0006      DO 20 NN=1,L
0007          SH(NN)=CMPLX(SB(NN),-SY(NN))
0008      20 CONTINUE
0009          DSH(1)=-SH(2)
0010          DO 30 LL=2,L
0011              DSH(LL)=SH(LL-1)-FLOAT(LL)*SH(LL)/X
0012      30 CONTINUE
0013          IF(L.LE.27)GO TO 31
0014          DO 100 KP=20,L
0015              ORD=KP-0.5
0016              HS=X
0017              SXS=HS/ORD
0018              ALPHS=ALOG((1.+SQRT(1.-SXS**2))/SXS)
0019              TXS=SQRT(1.-SXS*SXS)
0020              CXS=1./TXS
0021              CXS2=CXS*CXS
0022              EXPN=ORD*(ALPHS-TANH(ALPHS))
0023              UTS(1)=CXS*(3.-5.*CXS2)/24
0024              UTS(2)=CXS2*(81.+CXS2*(-462+385*CXS2))/1152
0025              UTS(3)=CXS*CXS2*(30375+CXS2*(-369603+CXS2*(765765-425425*CXS2)))/4
114720
0026              VTS(1)=CXS*(-9+7*CXS2)/24
0027              VTS(2)=CXS2*(-15+CXS2*(544-455*CXS2))/1152
0028              VTS(3)=CXS*CXS2*(-425425+CXS2*(451737+CXS2*(-283575+475475*CXS2)))/4
11414720
0029              DEJS=1.
0030              DEYS=1.
0031              DEJPS=1.
0032              DEYPS=1.
0033              JT=1
0034              DO 19 IP=1,3
0035                  JT=-JT
0036                  CB=ORD**IP
0037                  DEJS=DEJS+UTS(IP)/CB
0038                  DEYS=DEYS+JT*UTS(IP)/CB
0039                  DEJPS=DEJPS+VTS(IP)/CB
0040                  DEYPS=DEYPS+JT*VTS(IP)/CB
0041      19 CONTINUE
0042              RIM=0.5*EXP(-2.*EXPN)*(DEJPS/DEYPS+DEJS/DEYS)
0043              DSOS(KP)=CMPLX(1.,RIM)
0044              DSOS(KP)=0.5/HS+SINH(ALPHS)*DEYPS*DSOS(KP)/DEYS
0045              DSOS(KP)=-DSOS(KP)
0046      100 CONTINUE
0047      31 DO 40 IK=1,L
0048          DSOS(IK)=DSH(IK)/SH(IK)
0049      40 CONTINUE
0050      RETURN
0051      END

```

REFERENCES

1. A. Ralston, "A First Course in Numerical Analysis", Chapter 9, McGraw-Hill Book Company, New York, 1965.
2. F. B. Hilderbrand, "Introduction to Numerical Analysis", Chapter 10, McGraw-Hill Book Company, New York, 1956.
3. E. W. Hobson, "The Theory of Spherical and Ellipsoidal Harmonics", pp. 223-224, Chelsea Publishing Company, New York, 1955.
4. R. W. P. King, "The Theory of Linear Antenna", Harvard University Press, pp. 833-834 and p. 153, Cambridge, Mass., 1956.
5. G. Szego, "Uber einige asymptotische Entwicklungen der Legendreschen Funktionen", Proc. London Math. Soc.
6. S. A. Schelkunoff, "Theory of Antenna of Arbitrary Size and Shape", Proc. IRE, Vol. 29, pp. 493-521, 1941.
7. G. N. Waston, "A Treatise on the Theory of Bessel Functions", Chapter IX, Cambridge University Press, 1948.
8. K. Iizuka, "An Experimental Study of a Monopole over a Grounded Hemisphere", IEEE Trans. Antenna and Propagation, Vol. Ap-16, pp. 764-766, Nov. 1968.
9. M. I. Zhurina and L. N. Karmazina, "Tables and Formulas for the Spherical Functions", Pergamon Press.

DOCUMENT CONTROL DATA - R&D

(Security classification of title, body of abstract and indexing annotation must be entered when the overall report is classified)

ORIGINATING ACTIVITY (Corporate author)

Harvard University under Purchase Order No. C782
to M. I. T. Lincoln Laboratory

2a. REPORT SECURITY CLASSIFICATION

Unclassified

2b. GROUP

None

REPORT TITLE

Modified Dipoles: II. Numerical Solutions

DESCRIPTIVE NOTES (Type of report and inclusive dates)

Final Summary Report

AUTHOR(S) (Last name, first name, initial)

Kao, Peter S.

REPORT DATE

July 1971

7a. TOTAL NO. OF PAGES

99

7b. NO. OF REFS

9

a. CONTRACT OR GRANT NO.

F19628-70-C-0230

b. PROJECT NO.

627A

c.

Purchase Order No. C782

d.

9a. ORIGINATOR'S REPORT NUMBER(S)

Scientific Report No. 13 (Vol. II)

9b. OTHER REPORT NO(S) (Any other numbers that may be assigned this report)

ESD-TR 72-181

AVAILABILITY/LIMITATION NOTICES

Approved for public release; distribution unlimited.

SUPPLEMENTARY NOTES

Vol I is ESD-TR-71-246

12. SPONSORING MILITARY ACTIVITY

Air Force Systems Command, USAF

1. ABSTRACT

The 'modified dipole' has its origin in the consideration of the general properties of a satellite antenna which bears great resemblance to a dipole modified to incorporate at the center a conducting volume which is used to radiate electromagnetic waves and to house a power supply and radio frequency generators, etc. The object of this research is to pursue a theoretical and experimental exploration of the effects induced by the presence of the conducting volume on the antenna performance, i. e., input characteristics, current distribution along the surfaces of the entire radiating structure and radiation properties.

In Volume I a mathematical model consisting of a perfectly conducting sphere from which project the ends of a thin biconical antenna is chosen to simulate the actual sphere-centered thin dipole. The conical antenna is driven at its junction with the sphere by a rotationally symmetric electric field maintained across the gap by a biconical transmission line excited by the TEM mode. The attractive features of this model include the fact that it has surfaces that permit a simple specification of boundary conditions and, hence, a rigorous formulation for the electromagnetic fields and a shape such that its properties should come reasonably close to those of a modified cylindrical antenna as the cone angle becomes quite small.

The measurements of both input admittances and current distributions on modified dipoles (with either conical or cylindrical antenna projecting from the sphere) are also presented in Volume I. Comparisons were also made between modified conical and cylindrical antennas with the same sphere radii and antenna heights. The radius of the cylindrical antenna is the same as the smaller end of the cone. The fact that the admittance curves for modified cylindrical and conical antennas involve only slight shifts suggests that by introducing an equivalent antenna length that is a little longer than the actual physical length of the conical antenna a good approximation is obtained for the cylindrical antenna.

An infinite set of algebraic equations was solved numerically in Volume II for small cone angles. Comparisons were made between the modified conical antenna and its limiting biconical antenna which provides both an extrapolatory numerical check for the modified conical antenna with shrinking central sphere and an understanding of the underlying physical phenomena. Theoretical and experimental results are in very good agreement.

4. KEY WORDS

Modified dipoles
Conical antennas
Cylindrical antennas

Input admittances
Current distributions

UNCLASSIFIED

Security Classification